



Haji, Esraa (2017) *Functional characterisation of the Endoplasmic Reticulum protein (ERp27)*. PhD thesis.

<https://theses.gla.ac.uk/8793/>

Copyright and moral rights for this work are retained by the author

A copy can be downloaded for personal non-commercial research or study, without prior permission or charge

This work cannot be reproduced or quoted extensively from without first obtaining permission in writing from the author

The content must not be changed in any way or sold commercially in any format or medium without the formal permission of the author

When referring to this work, full bibliographic details including the author, title, awarding institution and date of the thesis must be given

Enlighten: Theses

<https://theses.gla.ac.uk/>
research-enlighten@glasgow.ac.uk

Functional Characterisation of the Endoplasmic Reticulum Protein (ERp27)

Esraa M Haji

Supervisor: Professor Neil Bulleid

**Submitted in fulfilment of the requirements for the Degree of
Doctor of Philosophy**

Institute of Molecular, Cell and System Biology

College of Medical, Veterinary and life Sciences

University of Glasgow

2017

Acknowledgment

I am sincerely and heartily grateful to my supervisor, Professor Neil Bulleid for the tremendous effort, support and guidance he showed during my entire PhD journey especially during the writing of my thesis; I am sure that it would not have been possible without his help and advice. I am also thankful to all my colleagues, past and present members, Dr Zhenbo Cao, Dr Marcel Van Lith, Dr Ojore Oka, Dr Philip Robinson, Dr Rachel Martin, Dr Gregory Poet, Dr Chloe Stoye, Dr Fiona Chalmers, Tomasz Szmaja, Xiaofei Cao, Marie Anne Pringle, Lorna Mitchell for their advice, support, and friendship. I am especially grateful to Dr Zhenbo Cao for his patience and I am appreciative of his care, support, encouragement and close friendship. Also, special thanks to Marie Anne Pringle for practically teaching me Molecular Biology techniques. I owe my sincere and earnest thanks to my marvellous father, who has always believed in my abilities, supported me morally and financially throughout my life. I would also like to express my gratitude to my precious mother for her patience, prayers, love and encouragement. It is also a great pleasure to thank my wonderful siblings; Anas, Albaraa, Elaf, Ethar, Leanah, and Bodoor for their unlimited love, support and care and all my friends who have helped me throughout my PhD especially while writing my thesis, they were always beside me and have boosted me morally and supported me in my weakest, madness and loneliest moments. In the memory of King Abdullah Al-Saud I also want to express my sincere thanks to the King Abdullah Scholarships Programme (KASP) represented in the Ministry of Education in Saudi Arabia for funding.

Author's declaration

I declare that this thesis presented for the degree of doctor of philosophy is composed solely by myself, that the work included herein is my own except where explicitly stated otherwise in the text by reference or acknowledgment and this work has not been submitted for any other degree or professional qualification except as specified.

List of figures

Figure 1.1, The mechanism of mammalian ER stress response.....	8
Figure 1.2, The IRE1 pathway for ER stress and quality control.	11
Figure 1.3, The PERK pathway of ER quality control.....	13
Figure 1.4, The ATF6 pathway for ER quality control.	15
Figure 1.5, PDI family members exchange disulphides with substrate protein.	17
Figure 1.6, Schematic showing the interaction between Ero1-L α and human PDI.	19
Figure 1.7, Other alternative pathways for the oxidation of PDI involving members of the peroxidase family; Gpx7/8 or PrxIV.	22
Figure 1.8, VKOR oxidation pathway for PDI.	24
Figure 1.9, The domain structure of the PDI protein.....	26
Figure 1.10, The human PDI family members.....	28
Figure 1.11, A crystal structure of the lectin calnexin (CNX).	30
Figure 1.12, The crystal structure of the full length calreticulin (CRT).	30
Figure 1.13, A schematic representation of the N-linked core oligosaccharide.....	33
Figure 1.14, The calnexin (CNX) and calreticulin (CRT) cycle of glycoprotein folding.	34
Figure 1.15, A, schematic showing the domain structure of ERp57. B, A model of the full length ERp57.	36
Figure 1.16, A model for the interaction of the folding glycoprotein with calnexin or calreticulin.	37
Figure 1.17, A, The domain structure of ERp27. B, The overall crystal structure of ERp27.	40
Figure 2.1, Protein purification steps.....	50
Figure 3.1, ERp27-WT expression and purification.....	66
Figure 3.2, ERp27-I196W expression and purification.....	68
Figure 3.3, ERp27-E231K expression and purification.	70
Figure 3.4, ERp57-WT expression and purification.....	72
Figure 3.5, ERp27 anti body testing on ERp27-E231K cell line.	74
Figure 3.6, Calreticulin-WT (CRT) expression and purification.	76
Figure 3.7, ERp57-R282A expression and purification.....	77
Figure 3.8, Isothermal titration calorimetry (ITC).	80
Figure 4.1, schematic diagram showing the domain structure of V5-tagged ERp57, single point mutant ERp57-R282, double mutant ERp57-cys 2,7, and triple mutant ERp57-cys 2,7-R282.	86
Figure 4.2, Schematic diagram showing the domain structure of Myc-tagged ERp27, ERp27-I196W, and ERp27-E231K.	87
Figure 4.3, The chemical structure of the disuccinimidyl glutarate (DSG) cross-linking agent.	88
Figure 4.4, The interactions between ERp57 and ERp27 or ERp57 and CRT assessed by <i>in vitro</i> cross linking.....	90
Figure 4.5, The interaction between ERp57 and CRT by <i>in vitro</i> cross linking.....	92
Figure 4.6, The interactions between ERp57 and CRT by <i>in vitro</i> cross linking.	93
Figure 4.7, The chemical structure of the Bismaleimidohexane (BMH) cross-linking agent.	94
Figure 4.8, The interaction between ERp57 and CRT by <i>in-cellular</i> cross-linking and the R282A mutation in ERp57 abolishes the interaction with CRT.	95
Figure 4.9, The interaction between ERp57 and ERp27 by <i>in-cellular</i> cross-linking.....	96
Figure 4.10, The interaction between ERp57 and ERp27 by <i>in cellular</i> cross-linking.	97
Figure 4.11, The interaction between ERp57 and ERp27 by <i>in cellular</i> cross-linking.....	98

Figure 4.12, The interaction between ERp57 and ERp27 by <i>in cellular</i> cross-linking.	99
Figure 4.13, The chemical structure of the Dithiobis succinimidyl propionate (DSP) cross-linking agent.	99
Figure 4.14, The interaction between ERp57 and ERp27 by <i>in cellular</i> cross-linking.	100
Figure 4.15, The interaction between ERp57 and ERp27 by <i>in cellular</i> cross-linking.	101
Figure 4.16, The interaction between ERp27 and CRT.	102
Figure 4.17, The interaction between ERp27 and CNX.	103
Figure 4.18, The calnexin and calreticulin cycle for glycoprotein folding.	107
Figure 4.19, The different fates for ERp57. CNX and CRT bring glycoproteins to ERp57 to fold while ERp27 could bring non-glycosylated proteins to ERp57 to fold.	107
Figure 5.1, <i>In cellulo</i> cross-linking of ERp27.	111
Figure 5.2, <i>in cellulo</i> cross-linking of ERp27.	112
Figure 5.3, <i>In cellulo</i> cross-linking of ERp27.	113
Figure 5.4, <i>In cellulo</i> cross-linking of ERp27.	114
Figure 5.5, <i>in cellulo</i> cross-linking of ERp27.	115
Figure 5.6, <i>in cellulo</i> cross-linking of ERp27.	116
Figure 5.7, A schematic showing the approach of preparing protein samples for mass spectrometry.	117
Figure 5.8, <i>In cellulo</i> cross-linking of ERp27.	119
Figure 5.9, <i>In cellulo</i> cross-linking of ERp27.	120
Figure 5.10, <i>In cellulo</i> cross-linking of ERp27.	121
Figure 5.11, The expression of ERp27 in pancreatic islet cells.	122
Figure 5.12, The expression of ERp27 in the pancreatic acinar cells.	123

List of tables

Table 5.1,The protein hits obtained from Mass spectrometry analysis.	118
---	-----

List of abbreviations

AI: Auto Induction.

ATF6: Activating Transcription Factor 6.

ATF4: Activating Transcription Factor 4.

BIP: Immunoglobulin Heavy-Chain Binding protein.

BMH: Bismaleimidohexane.

CF: Cystic Fibrosis.

CFTR: Cystic Fibrosis Transmembrane Regulator.

CHOP: C-EBP-homologous protein.

CNX: Calnexin.

COPII: Coat Protein Complex II.

CRT: Calreticulin.

DSG: Disuccinimidyl glutarate.

DSP: Dithiobis succinimidyl propionate.

DTT: Dithiothreitol.

eIF2 α : Eukaryotic Translation Initiation Factor 2.

ER: The Endoplasmic Reticulum.

ERAD: The Endoplasmic Reticulum Associated Degradation.

ERO1: ER Oxidase 1.

ERSE: ER Stress-Response Element.

FAD: Flavin Adenine Dinucleotide.

GI: Glucosidase I.

GII: Glucosidase II.

Gpx7: Glutathione Peroxidase 7.

Gpx8: Glutathione Peroxidase 8.

HA: Hemagglutinin.

HSQC: Heteronuclear Single-Quantum Coherence.

IPTG: Isopropyl-1-thio- β -D-galactopyranoside.

IRE1: Inositol Requiring Enzyme 1.

ITC: Isothermal Titration Calorimetry.

KO: Knockout.

LB: Lysogeny Broth.

MALDI-MS: Matrix-Assisted Laser Desorption/Ionization.

MHC: Major Histocompatibility Complex.

NMR: Nuclear Magnetic Resonance Spectrometry.

PDI: Protein Disulphide Isomerase.

PERK: Double-Stranded RNA-Activated Protein Kinase.

Prx4: Peroxiredoxin 4.

QSOX: Quiescin Sulphydryl Oxidase.

RER: The Rough Endoplasmic Reticulum.

RIDD: IRE1-Dependent Decay of mRNA.

RIP: Regulated Intramembrane Proteolysis.

RNase: Ribonuclease.

SER: The Smooth Endoplasmic Reticulum.

SRP: The Single Recognition Particle.

SV40: Simian Virus 40.

TB: Terrific Broth.

TCEP: TCEP (tris(2-carboxyethyl) phosphine).

UGGT: UDP glucose: glycoprotein glycosyl transferase.

UPR: The Unfolded Protein Response.

UPRE: Unfolded Protein Response Elements.

VKOR: Vitamin K Epoxide Reductase.

VP1: Virus Protein1.

XBP1: X-Box Binding Protein 1.

Table of Contents

Acknowledgment	i
Author's declaration	ii
List of figures	iii
List of tables.....	v
List of abbreviations.....	vi
Abstract	1
1 Main introduction	2
1.1 The endoplasmic reticulum (ER).....	3
1.2 Protein folding and synthesis in the ER.....	5
1.3 ER stress and quality control.....	7
1.3.1 Inositol requiring enzyme (IRE1).....	9
1.3.2 Double-stranded RNA-activated protein kinase (PERK)	12
1.3.3 Activating transcription factor 6 (ATF6)	14
1.4 Protein disulphide isomerase (PDI) family of enzymes and disulphide bond formation 16	
1.5 Disulphide bond formation pathways.....	18
1.5.1 ER oxidase 1 (Ero1) pathway.....	18
1.5.2 Peroxiredoxin IV pathway.....	20
1.5.3 Glutathione peroxidases 7 and 8 (Gpx7 and Gpx8).....	21
1.5.4 Vitamin K epoxide reductase (VKOR)	23
1.5.5 QSOX	25
1.6 Protein disulphide isomerase (PDI) protein	26
1.6.1 The interaction of lectins and glycoproteins	31
1.6.2 The misfolded glycoprotein sensor (UGGT).....	32
1.6.3 The N-linked glycoprotein folding cycle	32
1.7 Endoplasmic reticulum protein 57 (ERp57).....	35
1.8 Endoplasmic reticulum protein 29 (ERp29).....	38
1.9 Endoplasmic reticulum protein 27 (ERp27).....	39
2 Materials and methods	45
2.1 List of chemicals	46
2.2 List of antibodies	48

2.3	Protein expression and purification	49
2.4	Colloidal Coomassie blue stain	51
2.5	Gel filtration (Superdex 200).....	51
2.6	Ion-exchange chromatography.....	51
2.7	Silver staining	52
2.8	Gel electrophoresis and western blot	52
2.9	Transformation.....	53
2.10	Mini prep purification of DNA by alkaline lysis.....	53
2.11	Sub cloning of DNA fragments into vectors by PCR or restriction digestion	54
2.12	Site Directed Mutagenesis	54
2.13	<i>In vitro</i> protein cross-linking	54
2.14	Immunoprecipitation technique.....	55
2.15	Transient and stable transfections	55
2.16	<i>In cellulo</i> protein cross-linking	56
2.17	Mass spectrometry following DTT elution of substrate-trapped mixed disulphide.....	56
3	Protein expression and purification, <i>In vitro</i> protein interaction by isothermal titration calorimetry (ITC).....	58
3.1	Introduction	59
3.2	Results.....	63
3.3	Protein expression and purification	63
3.3.1	ERp27-WT expression and purification	63
3.3.2	ERp27-I196W expression and purification	67
3.3.3	ERp27-E231K expression and purification.....	69
3.3.4	ERp57-WT expression and purification	71
3.3.5	ERp27-antibody testing.....	73
3.3.6	Calreticulin WT expression and purification	75
3.3.7	ERp57-R282A expression and purification	77
3.4	Isothermal titration calorimetry ITC.....	78
3.5	Discussion	81
4	<i>In vitro</i> and <i>in cellulo</i> protein-protein interaction by cross-linking assay.....	84
4.1	Introduction.....	85
4.2	Results.....	88
4.2.1	<i>In vitro</i> cross-linking	88
4.2.2	<i>In cellular</i> cross-linking.....	94
4.3	Discussion	104
5	<i>In cellulo</i> protein-protein interaction by cross-linking assay and mass spectrometry	108

5.1	Introduction	109
5.2	Results	111
5.2.1	Protein sample preparation for Mass Spectrometry	111
5.2.2	The effect of ERp27 on pancreatic digestive enzymes	122
5.3	Discussion	124
6	Main discussion	127
7	Future perspectives	133
8	References	135

Abstract

ERp27 is a 27.7 kDa redox-inactive member of the protein disulphide isomerase (PDI) family. It was found to interact with another PDI member, the well-known thiol-oxidoreductase ERp57 (58 kDa) *in vitro*. Although it is known that ERp57 interacts with ERp27 *in vitro* this interaction was not investigated in living cells. In this research project we applied *in vitro* and *in cellulo* approaches to investigate the same interaction of ERp57 and ERp27 then to compare it to the interaction of ERp57/calnexin (CNX)/calreticulin (CRT) complex to determine if the ERp57 interaction with ERp27 competes with the ERp57/CNX/CRT complex. Additionally, we investigated the physiological role of ERp27. Protein expressions and purifications were carried out by the Nickel agarose affinity chromatography to obtain sufficient amount of proteins for analysis. Additionally, proteins were purified by gel filtration-chromatography. The interaction between purified ERp27 and ERp57 was determined using isothermal titration calorimetry (ITC) and by chemical cross-linking. The ITC results confirmed the interaction between ERp57 and the lectin CRT. However, we could not detect an interaction between ERp57 and ERp27 possibly due to low protein concentrations. Moreover, the *in vitro* cross-linking results were in agreement with the previous research and verified the binding of ERp57 with ERp27. However, *in cellulo* chemical cross-linking suggested that the same interaction does not occur in living cells. Nevertheless, this investigation revealed that ERp27 binds to other proteins *in cellulo*. Mass spectrometry results have identified protein candidates that interact with ERp27 in living cells which are the PDI homologous P5 and the ER oxidoreductin Ero1. These results provide new insights of the role of ERp27 and provide suggestions for further research.

1 Main introduction

1.1 The endoplasmic reticulum (ER)

The endoplasmic reticulum (ER) is an organelle that consists of various domains which have distinct functions. However, it is a continuous membrane that includes; the nuclear envelope (NE) (Watson, 1955), the rough ER (RER), and the smooth ER (SER) (Dallner et al., 1963, Palade and Siekevitz, 1956). There are morphological differences between the two types of ER which can be visually distinguished (Baumann and Walz, 2001, Voeltz et al., 2002). The RER is more granulated in texture because of the ribosomes that covers its surface compared to the SER which is more convoluted or coiled. This variation in their manifestation is directly related to their functions as the ribosomes that covers the RER are responsible for protein synthesis (Prinz et al., 2000, Rolls et al., 2002, Simon and Blobel, 1991).

Consequently, the abundance of either the SER or the RER varies among different cells depending on their functions. Accordingly, cells that secrete synthesised proteins will mostly contain the RER (Dallner et al., 1963). However, one type of the SER that is abundant in cells is transitional ER which is involved in protein packaging and transportation to the Golgi apparatus (Palade, 1975, Hobman et al., 1998). The ER proteins have different functions which include; protein integration into the membrane, calcium ion storage in the ER lumen and their regulated release in the cytosol (Meldolesi and Pozzan, 1998), protein folding (Braakman and Hebert, 2013), synthesis, and modification in the ER lumen, synthesis of phospholipids in the cytosolic leaflet of the ER membrane (Voeltz et al., 2002, Fagone and Jackowski, 2009).

The SER is particularly found in specific cells and the activities it plays in each cell type varies. It is the site for steroid synthesis in steroid-synthesising cells (Black et al., 2005) whereas it is significant for detoxification of substances within the liver cells (Ishizuki et al., 1983). Furthermore, in muscles and neurons it is known as the sarcoplasmic reticulum membrane and mostly involved in the calcium uptake and release for muscle contractions such as the heart (Gao et al., 2017, Voeltz et al., 2002).

In this research project the ER is very significant as it is the place where almost one third of both secretory and membrane proteins are synthesised and folded (Kaufman, 1999). Unfolded proteins will be corrected by ER chaperones as only correctly folded protein will

be exported out of the ER to the Golgi apparatus and will be able to function either as secretory or membrane proteins (Ariyasu et al., 2017, Ron and Walter, 2007).

The permanently misfolded proteins will be targeted for Endoplasmic Reticulum Associated Degradation (ERAD) (Ellgaard and Helenius, 2003), which is a machinery that can cope with a certain number of misfolded proteins which are produced under normal cellular conditions but not under ER stress (Kaneko et al., 2017). However, under ER stress when more misfolded proteins are produced in an overwhelming way, exceeding capacities of both the ER and ERAD, then cells will enter apoptosis (Hacker, 2000). The cells have a defence system that can protect them in such circumstances called the Unfolded Protein Response (UPR) or also known as ER stress response (Ariyasu et al., 2017, Yoshida, 2007).

1.2 Protein folding and synthesis in the ER

Protein folding is the initial step for proteins entering the secretory pathway. These proteins are initially targeted to the endoplasmic reticulum (ER) which is the entry point for the secretory pathway (Vitale and Denecke, 1999, Jin et al., 2017). In mammalian cells, typically but not exclusively, proteins are translocated into the ER by the recognition of a single sequence in the N-terminus of the protein (Braakman and Bulleid, 2011, High, 1995). The single recognition particle (SRP) will recognise the signal sequence then the resulting complex of the nascent peptide chain/ribosome/SRP will be delivered to the ER membrane through the SRP receptor then directed to the proteinaceous pore within the membrane called the Sec61 translocon (Alder et al., 2005) which allows the growing polypeptide chain across the membrane and into the ER (Sitia and Braakman, 2003, Braakman and Bulleid, 2011, Helenius et al., 1992, Dejgaard et al., 2010).

The folding commences co-translationally/translocationally with the aid of folding factors and continues posttranslationally until proteins reach their native protein structure (Sitia and Braakman, 2003, Rutkevich et al., 2010, Braakman and Bulleid, 2011). As proteins fold they form disulphide bonds (Feige and Hendershot, 2011), the formation, isomerisation, and reduction of which is catalysed by thiol oxidoreductases of the protein disulphide isomerase (PDI) family (Rutkevich et al., 2010, Poet et al., 2017). Protein folding can be interrupted by some dysfunctions such as cystic fibrosis (CF) in humans which is caused by inherited mutations (Kim and Skach, 2012).

Despite the aid of the folding factors in the ER, proteins occasionally fail to achieve their correctly folded state and end up misfolded (Credle et al., 2005). To ensure these toxic particles are eliminated, cells adopt a protein quality control system that is able to control diseases such as systemic amyloid disease (Chen et al., 2015). The best characterised pathway is ERAD (Vembar and Brodsky, 2008, Ellgaard and Helenius, 2003). ERAD plays a key role in ER homeostasis as the inactivation of ERAD would result in accumulation of misfolded proteins in the membrane and the lumen of the ER (Hebert and Molinari, 2007). The misfolded proteins amount varies considerably caused by different reasons; mutations, shortage of chaperone availability, or sub stoichiometric amounts of binding partners (Ruggiano et al., 2014).

In most cases, the misfolded proteins become substrates for ERAD which clears the ER of harmful species. The inactivation of ERAD will result in accumulation of misfolded proteins which cause a situation known as ER stress which is a common status for disorders such as prion accumulation; Alzheimer's (Honjo et al., 2017) and Parkinson's diseases (Hartl and Hayer-Hartl, 2009, Ruggiano et al., 2014, Ron and Walter, 2007, Walter and Ron, 2011).

1.3 ER stress and quality control

Protein quality control is a unique mechanism for adaptation to ER stress. The ER is essential for synthesising proteins and the lipid membrane as it is the first organelle that the newly synthesised protein passed through (Jin et al., 2017, Alder et al., 2005). It is found that ER stress, inflammatory responses, and oxidative stress triggers a major defence system that helps cells survive any stress circumstances caused by either physiological, pathological, or biochemical stimuli and possibly adapt to it (Harding et al., 2003). A highly specific signalling pathway has evolved in the ER named the unfolded protein response (UPR) (Merksamer and Papa, 2010).

The UPR works by increasing the capacity of protein folding and decreasing the rate of protein translation. There are three branches which operate in parallel. Each of these branches are categorised by a number of ER-signalling components and classified as a distinct arm of the UPR. The ER membrane bound transducers are; Inositol Requiring Enzyme 1 (IRE1) (Karagoz et al., 2017), Activating Transcription Factor 6 (ATF6) (Adachi et al., 2008), and Double-stranded RNA-Activated Protein Kinase (PERK) (Jin et al., 2017, Walter and Ron, 2011).

This way the UPR helps cells to adapt to stress situations and survive conditions of abnormalities. However, when homeostasis of protein folding cannot be achieved then the UPR will adopt a programme for cell death (Dandekar et al., 2015, Ron and Walter, 2007).

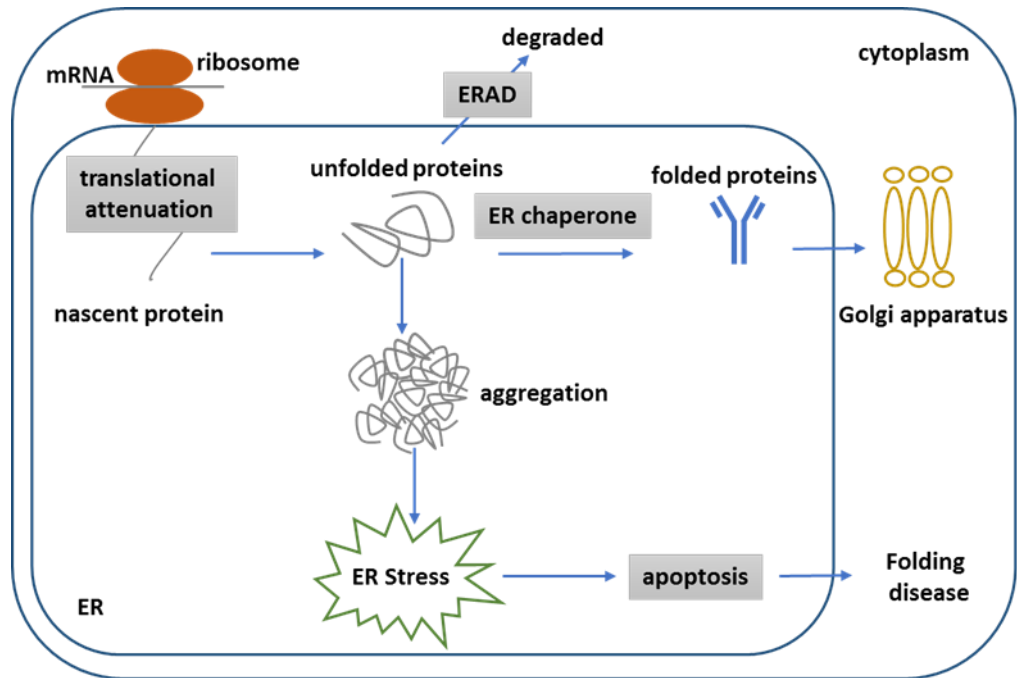


Figure 1.1, The mechanism of mammalian ER stress response.

This pathway consists of four steps; (1) translational attenuation, (2) expression of ER chaperones, (3) ERAD, and (4) apoptosis. The accumulation of unfolded proteins induces ER stress. Accordingly, cells will induce ER stress to cope (Yoshida, 2007).

1.3.1 Inositol requiring enzyme (IRE1)

IRE1 is the most conserved transducer in the ER as it contains both endoribonuclease and Ser/Thr kinase activities. It is known as one of the unfolded proteins sensors in the ER membrane. Two IRE1 genes exist in the mammalian genome; IRE1 α and IRE1 β . IRE1 α is expressed in almost all types of cells while IRE1 β is restricted to the intestinal epithelial cells (Tirasophon et al., 2000). IRE1 binds to the ER chaperone Bip which adjusts homeostasis of the UPR (Pincus et al., 2010). IRE1 can detect unfolded protein in the ER via its luminal domain. However, it has another domain, the cytoplasmic domain that contains ribonuclease (RNase) and kinase activities (Dandekar et al., 2015, Yoshida, 2007).

Under ER stress conditions, IRE1 α was found to be homo dimerised and auto-phosphorylated to activate its RNase activity (Sha et al., 2009). The non-conventional splicing of the mRNA encoding X-box binding protein 1 (XBP1) is catalysed by the activation of IRE1 α . XBP1 protein activation is encoded by the spliced XBP1 mRNA. It functions as a powerful transcriptional factor to activate various ER chaperones and enzymes to be able to promote protein folding, secretion of correctly folded proteins as well as degradation of misfolded proteins (Dandekar et al., 2015, Yoshida et al., 2001, Ariyasu et al., 2017, Credle et al., 2005).

IRE1 activation will convert XBP1 pre-mRNA (XBP1 (U) mRNA) into the mature mRNA (XBP1 (S) mRNA) in an unconventional splicing reaction. This mature form codes for a protein that possesses a DNA binding domain and a transcriptional activation domain. The unconventional splicing of XBP1 (U) mRNA removes 26 bp, to allow translation of the active XBP1 (S) (Sha et al., 2009). XBP1 (S) translocates to the nucleus to bind unfolded protein response elements (UPRE). Such binding enhances the expression of genes involved in ERAD by forming a heterodimer with ATF6 (Yoshida et al., 2001).

IRE1 recognises the specific stem-loop RNA structure of XBP1 (U) mRNA for splicing which forms a complex with the nascent XBP1 polypeptide chain and ribosome and in turn stabilises XBP1 (U) mRNA on the ER membrane leading to efficient splicing by IRE1. Translational pausing of XBP1 (U) mRNA is mediated by a peptide module at the carboxyl domain which is required for efficient targeting to the membrane of the ER and splicing of XBP1 (U) mRNA by IRE1 (Yanagitani et al., 2011). Additionally, XBP1 is regulated at the

protein level. As an example, XBP1 (U) proteins and XBP1 (S) form a complex then under regular cellular conditions, they undergo rapid proteasome degradation. That in turn inhibits the transcription of target genes of XBP1 (S) during the ER stress recovery phase (Yoshida et al., 2006).

IRE1 RNase activity is involved in a mechanism termed regulated IRE1-dependent decay of mRNA (RIDD). This mechanism is responsible for selectively degrading ER-associated mRNA coding secretory or membrane proteins, leading to unburden the protein load of the ER. mRNA coding ER chaperones which stabilises the ER avoid RIDD by an unknown mechanism. Yet, it remains unknown how Ire1 recognises RIDD targets (Hollien et al., 2009, Hollien and Weissman, 2006).

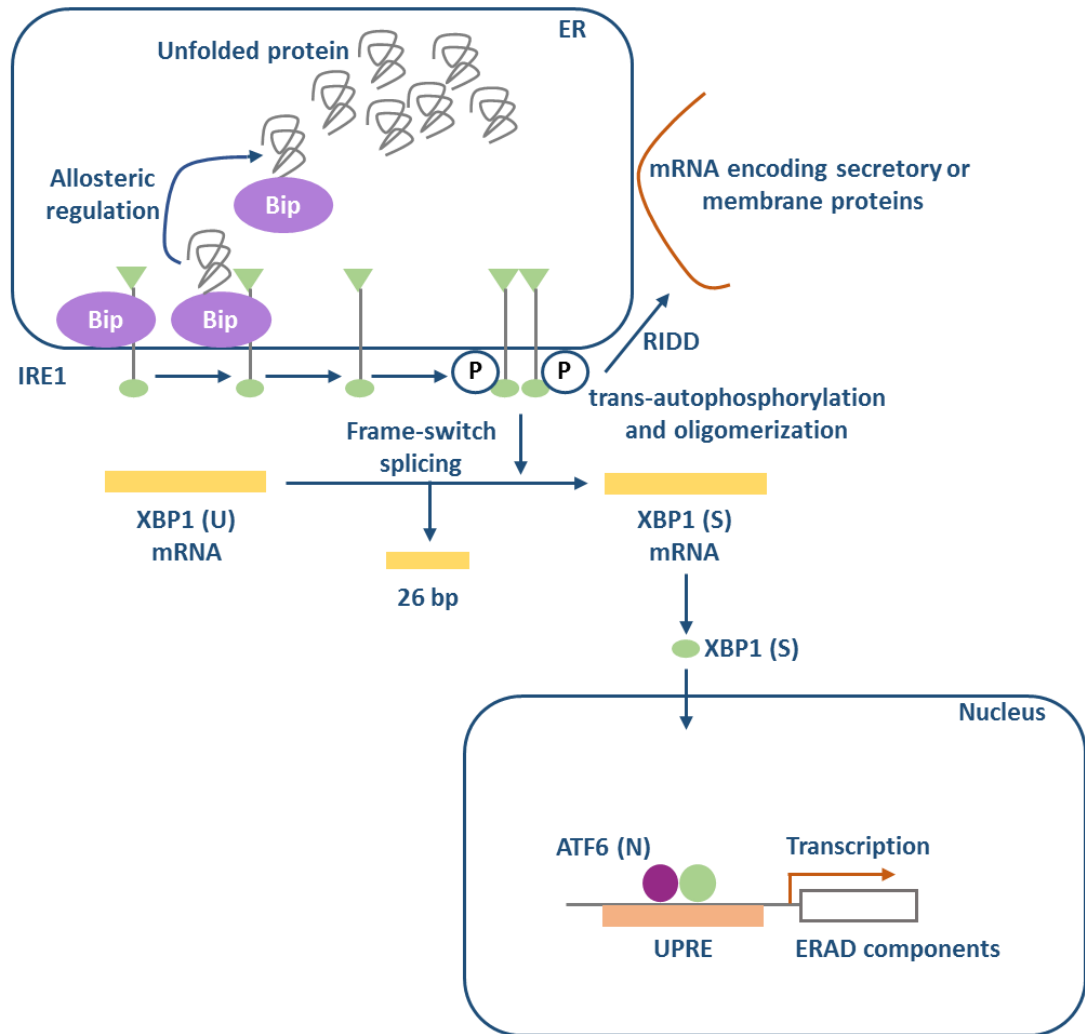


Figure 1.2, The IRE1 pathway for ER stress and quality control.

This model shows UPR induction where the Ire1 luminal domain interacts with the Bip ATPase domain. This interaction is abrogated when unfolded protein binds Bip. Trans-autophosphorylation and oligomerization activates IRE1. After that, Ire1 converts the XBP1 (U) mRNA to XBP1 (S) mRNA by frame-switch splicing resulting in production of XBP1 (S) mRNA. XBP1 (S) mRNA translocates to the nucleus and forms a heterodimer with ATF6 (N) that enhances the gene expression of ERAD (Ariyasu et al., 2017).

1.3.2 Double-stranded RNA-activated protein kinase (PERK)

In the ER lumen, PERK is considered one of the most important ER stress UPR arms. Similar to Ire1, PERK is capable of detecting the accumulation of unfolded proteins using its luminal domain which is vital when in association with Bip (Carrara et al., 2015, Bertolotti et al., 2000). Under ER stress conditions, PERK is activated by *trans*-autophosphorylation and oligomerisation. This activation leads to inactivation of the eukaryotic translation initiation factor 2 (eIF2 α) which leads to general inhibition of protein translation (Cui et al., 2011, Harding et al., 1999).

It remains unknown how PERK detects unfolded proteins in the ER lumen. However, there is a proposed induction of the UPR in which the ER chaperone, Bip, interacts with both PERK and Ire1 luminal domains. This interaction is abrogated when unfolded proteins bind Bip (Bertolotti et al., 2000, Carrara et al., 2015).

There are chemical inhibitors which inhibit dephosphorylation of eIF2 α such as guanabenz (GBZ), a selective inhibitor of eIF2 α in eukaryotes. It blocks dephosphorylation mediated by virus protein as well as viral replication to protect cells from stress generated by protein accumulations (Tsaytler et al., 2011). Salubrinal is another eIF2 α inhibitor that selectively binds to a regulatory subunit of protein phosphatase 1, PPP1R15A/GADD34, to prolong phosphorylation in human cells and accordingly managing protein levels and production rates by available chaperones. Subsequently, allows protein folding and thereby rescue cells from protein misfolding and stress (Boyce et al., 2005). In addition, similar to GBZ, sephin1 also binds and inhibits the stress-induced PPP1R15A, but not PPP1R15B, to prolong the phospho-signalling pathway preventing lethality of protein misfolding stress (Das et al., 2015). These inhibitors suggest that PERK has cytoprotective effects.

It has been established that eIF2 α activates translation of particular genes which have short open reading frames in their 5' region and that increase the translation of other genes such as Activating Transcription Factors 4 (ATF4) (Harding et al., 1999, B'chir et al., 2013) after eIF2 α phosphorylation. This gene is involved in metabolism and is resistant to oxidation stress and provides a cytoprotective effect in the early stages of ER stress (Harding et al., 2000, Harding et al., 2003). The ATF4 activates C-EBP-homologous Protein

(CHOP) (Oyadomari and Mori, 2004) which is a proapoptotic transcription factor in later stages of ER stress. Accordingly, PERK was found to have two different effects on the cell by being both cytoprotective and apoptotic. Moreover, PERK is believed to have a role in determining cell fate under ER stress conditions (Liu et al., 2015).

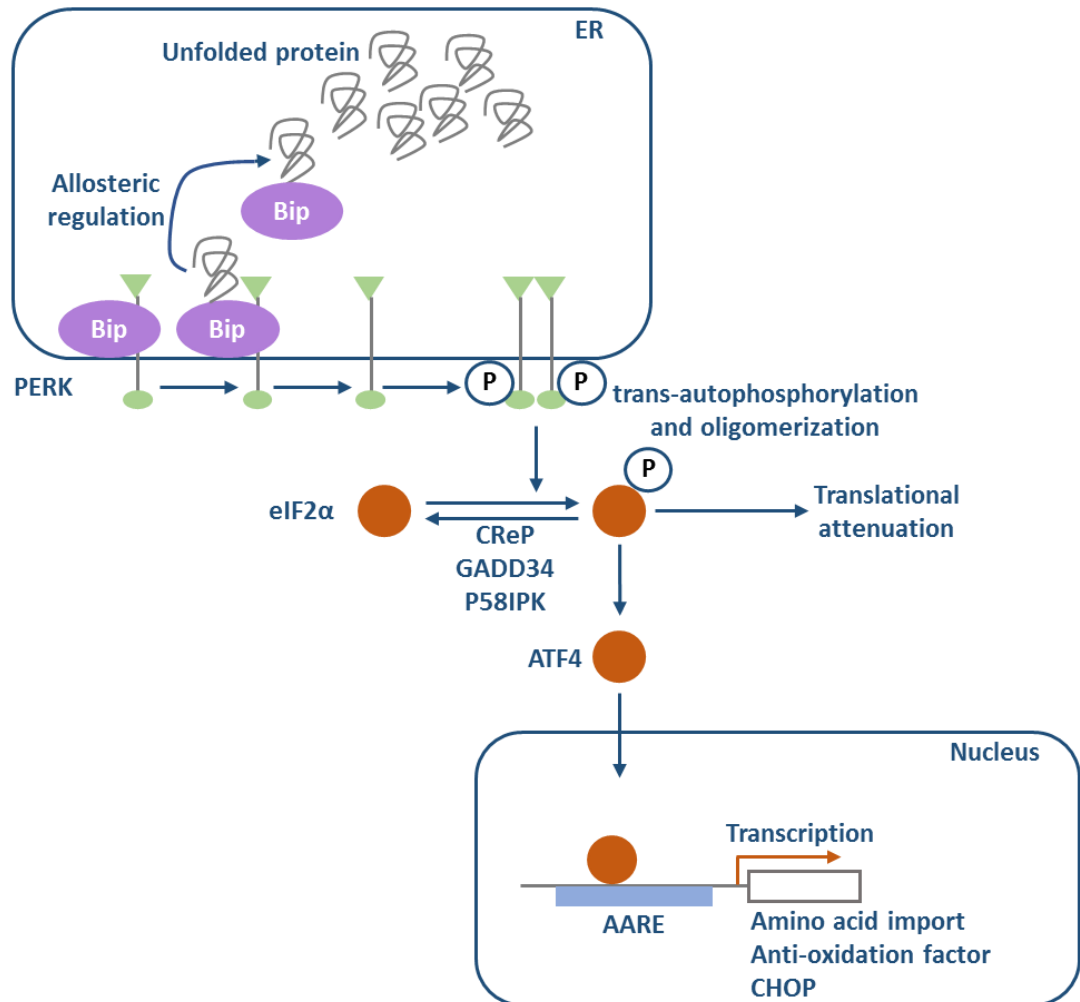


Figure 1.3, The PERK pathway of ER quality control.

The luminal domain of PERK interacts with the ATPase domain of Bip which dissociates upon unfolded protein binding to Bip. ATF4 factor enhances amino acid transport, oxidation and apoptotic genes. Phosphorylated eIF2α will get dephosphorylated by CReP, GADD34, and P58IPK (Ariyasu et al., 2017).

1.3.3 Activating transcription factor 6 (ATF6)

ATF6 is a sensor protein that is localised in the ER membrane. It also functions as a bZip transcription factor that enhances the expression of ER chaperone genes. ATF6 is translocated to the ER through Coat Protein Complex II (COPII) vesicles which transport it from the ER to the Golgi apparatus (Chen et al., 2002), where it undergoes Regulated Intramembrane Proteolysis (RIP) by Site-1 and Site-2 proteases (Ye et al., 2000, Chen et al., 2002). There are two models for ATF6 stress sensing mechanisms; the first model suggests that under ER stress, the ER chaperone Bip will dissociate from ATF6 uncovering the Golgi localisation signal of ATF6 which accordingly leads to the translocation of the ATF6 to the Golgi (Chen et al., 2002, Schindler and Schekman, 2009). In the second model, under normal cellular conditions the ATF6 luminal domain forms either dimers or oligomers by intramolecular disulphide bonds. However, under stress conditions the ATF6 disulphide bonds are cleaved and the monomeric form of the ATF6 translocates to the Golgi (Nadanaka et al., 2007, Sato et al., 2011).

The N-terminal bZip domain of ATF6 (N) is released from the Golgi by RIP and enters the nucleus, then through ER stress-response element (ERSE) it will upregulate the expression of the genes (Yoshida et al., 1998). In the promoter region of the mammalian UPR, a unique sequence was found consisting of 19 nucleotides (CCAAT-N9-CCACG) designated ERSE. A general transcription factor (NF-Y) also known as (CBF) was confirmed to bind to CCAAT part of ERSE. Additionally, the CCACG part was found to be very specific to the mammalian UPR (Roy and Lee, 1999, Yoshida et al., 2000). ER chaperone genes and folding enzyme genes are ATF6 (N) targeted genes involved in the ER quality control (Yoshida et al., 2001, Belmont et al., 2010). There are two isoforms of the ATF6 expressed ubiquitously in mammals; ATF6 α and ATF6 β (Haze et al., 2001, Haze et al., 1999, Thuerauf et al., 2007). It was found that a single knockout in mice (KO) of either isoform sensitises the animals to ER stress, however, does not have any lethal effect. Yet, when a double knockout (KO) of ATF6 α and β was carried out it was embryonic lethal for reasons which are unknown (Ariyasu et al., 2017, Yamamoto et al., 2007).

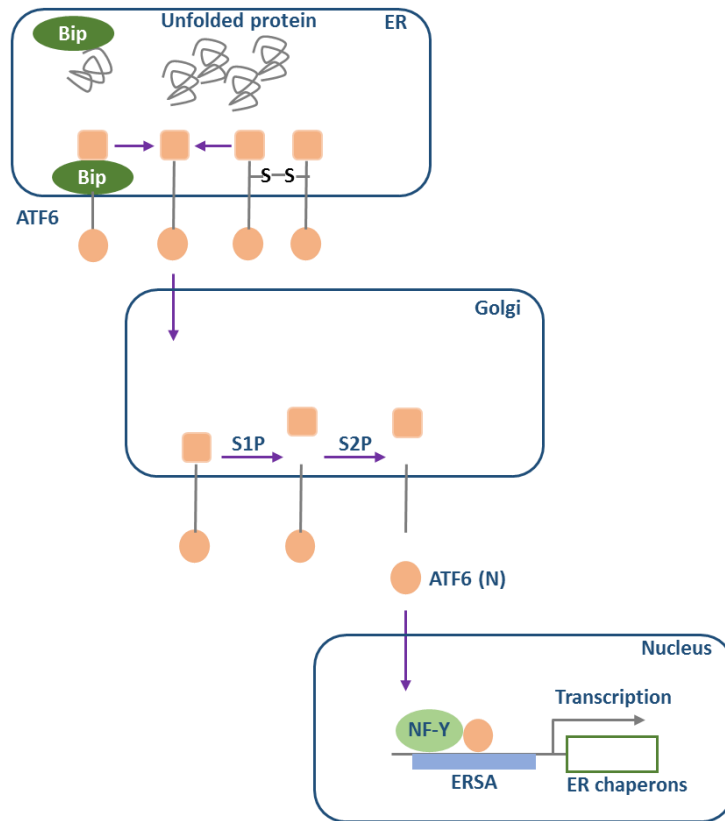


Figure 1.4, The ATF6 pathway for ER quality control.

In this model unfolded proteins are detected by ATF6 and translocated to the Golgi apparatus. When in the Golgi, ATF6 gets cleaved by the proteases (S1P) and (S2P) and ATF6 (N), the N-terminal form gets translocated to the nucleus and binds the ERSE to enhance transcription with ER chaperone genes by forming a heterodimer with NF-Y (Ariyasu et al., 2017).

1.4 Protein disulphide isomerase (PDI) family of enzymes and disulphide bond formation

The protein disulphide isomerase (PDI) family is a group of proteins that comprises about 20 members which can be catalytically active or inactive (Tannous et al., 2015). It includes proteins that have similar sequences, domain structure and localisation in the ER. These proteins localise to the ER lumen or to the luminal side of the ER membrane and share a common domain structure, which is the thioredoxin fold (Atkinson and Babbitt, 2009). The PDI family is critical for the process of disulphide bond formation, isomerisation and reduction (Rutkevich et al., 2010). Although the name of the family suggests that all members have a role in protein disulphide isomerisation, only a subset are able to efficiently catalyse isomerisation (Ellgaard and Ruddock, 2005).

Protein stability is enhanced by disulphide bonds which also regulate redox-dependant functions (Bastolla and Demetrius, 2005). In the ER, PDI family members catalyse the formation of disulphides (Kosuri et al., 2012). Following co-translational translocation into the ER, disulphides can be formed between residues that come within close proximity even if they are not linked in the final native structure. Such non-native disulphides are predominant in the misfolded protein. However, they can still be intermediates in normal folding (Jansens et al., 2002, Hatahet and Ruddock, 2009, Bulleid and Ellgaard, 2011).

Non-native disulphides can prevent correct folding and therefore have to be reduced for the native disulphide to form and this process is also catalysed by a PDI family member (Jansens et al., 2002, Kosuri et al., 2012). Thus, PDI family members are crucial enzymes for the formation and reduction of disulphide bonds for protein correct folding in the ER (Hatahet and Ruddock, 2009, Feige and Hendershot, 2011).

Disulphide bond formation requires PDI to be oxidised (Ellgaard and Ruddock, 2005). There are a number of pathways for disulphide exchange proteins to be oxidised by specific oxidases, including Ero1, peroxiredoxin (Prx4) (Tavender et al., 2010), glutathione peroxidase (Gpx 7 and 8) (Nguyen et al., 2011), and vitamin K epoxide reductase (VKOR) (Schulman et al., 2010). The enzyme quiescin sulphydryl oxidase (QSOX) is an exception as the pathway for disulphide oxidation is not as well characterised. In addition, QSOX is capable of oxidising polypeptides directly and does not require a disulphide exchange

protein such as PDI as the enzyme itself contains thioredoxin domains (Bulleid and Ellgaard, 2011).

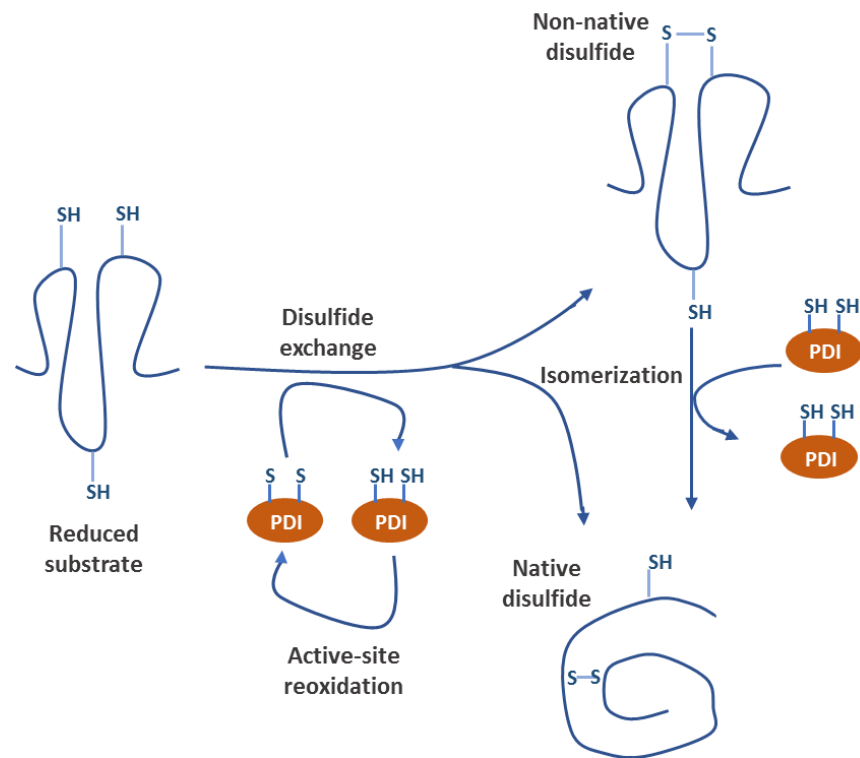


Figure 1.5, PDI family members exchange disulphides with substrate protein.

In newly synthesised proteins entering the ER, cysteine pairs form disulphide bonds following a disulphide exchange reaction with a PDI family member. Native and non-native disulphides can be formed as a result of the exchange with PDI members. Non-native disulphides will be subjected to isomerisation, either directly or through cycles of reduction and oxidation to form the native disulphide (Bulleid and Ellgaard, 2011).

1.5 Disulphide bond formation pathways

1.5.1 ER oxidase 1 (Ero1) pathway

This pathway is the best characterised pathway for disulphide bond formation. The fundamental steps are comparable between yeast and mammals (Appenzeller-Herzog et al., 2008). Here the major contributors to disulphide bond formation are Ero1 and PDI family of oxidoreductases. There is only one isoform, called Ero1p, in yeast (Pollard et al., 1998, Frand and Kaiser, 1998) while there are two isoforms present in mammals; Ero1 α and Ero1 β , which are similar in function but distributed in different tissues (Cabibbo et al., 2000, Pagani et al., 2000). However, the primary enzyme oxidised by both is PDI (Pdi in yeast and PDIA1 in mammals), although, other members of the family might be substrates (Inaba et al., 2010).

The oxidation power of molecular oxygen is used by Ero1 to create a disulphide bond within PDI de novo (Frand and Kaiser, 1999). For disulphide bonds to form, electron flow is necessary and they move from the client to PDI and then to Ero1 (Benham et al., 2013). PDI is also capable of isomerisation of disulphide bonds within a client protein (Hatahet and Ruddock, 2009). To reduce molecular oxygen, producing hydrogen peroxide during the process, Ero1 uses the cofactor flavin adenine dinucleotide (FAD) (Tu and Weissman, 2002, Gross et al., 2006).

In this pathway within mammalian cells, PDI depends on its thioredoxin domains a and a' (Kozlov et al., 2010a). These domains are separated by two thioredoxin-like b domains arranged as abb'xa' (Tian et al., 2006, Tian et al., 2008). The linker region x is significant for modulating client proteins binding to PDI (Nguyen et al., 2008, Wang et al., 2010). The a-type domains of PDI contain CGHC active sites. The high biochemical reduction potential of the active sites (- 180 mV) makes PDI thermodynamically suitable for donating electrons to reduced protein clients (Lundstrom and Holmgren, 1993, Benham et al., 2013).

During disulphide bond formation, the PDI a domain is oxidised by its a' domain which is itself oxidised by Ero1 α (Araki and Nagata, 2011, Baker et al., 2008, Chambers et al., 2010). The transfer of a disulphide bond from Ero1 α to the PDI a' domain of the PDI is affected by the cysteine pair C₉₄XXXXC₉₉ region within a flexible loop of Ero1 α (Masui et

al., 2011). Reversibly, the C₉₄XXXXC₉₉ site of Ero1 α receives a disulphide bond from C₃₉₄XXC₃₉₇ which is close to FAD (Masui et al., 2011, Gross et al., 2004, Benham et al., 2013). A similar mechanism occurs in yeast by Ero1p (Sevier and Kaiser, 2006b). There are other oxidation pathways alongside Ero1 which are explained in the sections below.

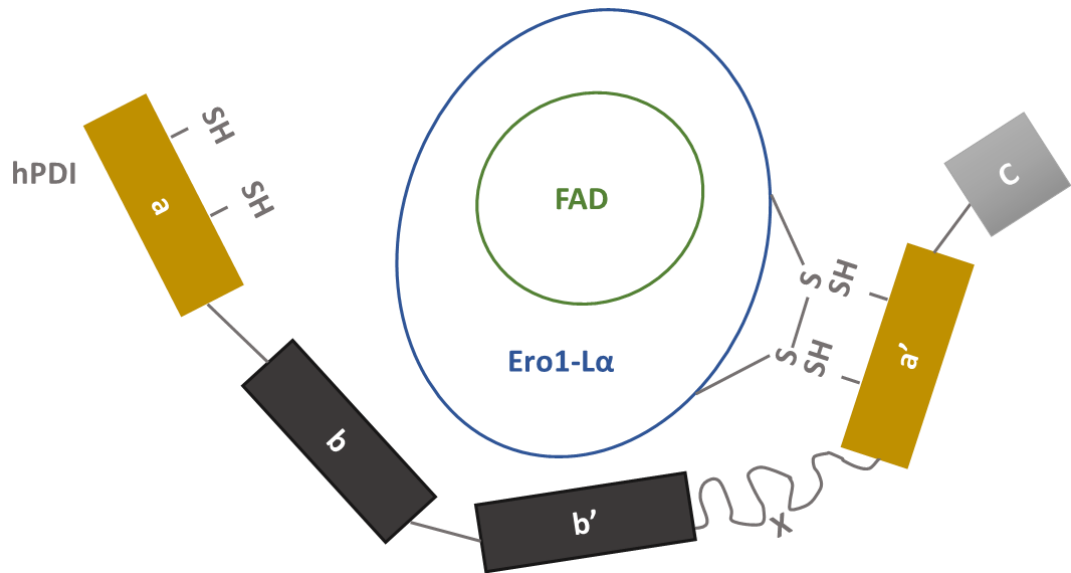


Figure 1.6, Schematic showing the interaction between Ero1-L α and human PDI.

The four thioredoxin domains of human PDI are arranged in a U-shape where the a and a' domains are facing each other. The b' x a' fragment of the human PDI provides the essential Ero1-L α binding site. The cysteine pair Cys⁹⁴-Cys⁹⁹ of Ero1-L α face the active site of the a' domain of the human PDI (Wang et al., 2009).

1.5.2 Peroxiredoxin IV pathway

Peroxiredoxin IV (PrxIV) is an ER localised enzyme that can act as electron acceptor for PDI and in turn uses hydrogen peroxide as a terminal electron acceptor. PrxIV belongs to the family of 2-cysteine peroxiredoxins that share a similar structure and mechanism (Cao et al., 2011, Tavender et al., 2008).

The first step of this pathway is the formation of sulfenylated cysteines at the peroxidatic cysteine active site by reaction with hydrogen peroxide in the ER. PrxIV forms a decamer in a donut-like shape that contains five dimers (Cao et al., 2011). Each polypeptide within the dimeric structure contains a peroxidatic cysteine. There is a conformational change in the dimer on sulfenylation which brings the peroxidatic cysteine into close proximity to the resolving cysteine on an adjacent polypeptide. That will then form a disulphide bond which can easily accept electrons from PDI and oxidise its active site. Consequently, for each oxygen molecule reduced, a disulphide will be formed in PDI by Ero 1 and another one will be formed by PrxIV after the reduction of hydrogen peroxide to water (Tavender et al., 2010, Bulleid, 2012). Under ER stress, PrxIV has a cytoprotective effect which is due to the metabolism of hydrogen peroxide produced by Ero1. Additionally, PrxIV provides a sensor for hyperoxidising conditions within the ER by becoming hyperoxidised after extreme oxidative stress (Tavender and Bulleid, 2010).

1.5.3 Glutathione peroxidases 7 and 8 (Gpx7 and Gpx8)

There are two peroxidases localised to the ER lumen in addition to PrxIV. Gpx 7 is a soluble protein, however, Gpx 8 is a type I membrane protein. Both have an ER retrieval sequence at their carboxyl terminal. They have been shown to drive the oxidation of PDI *in vitro* (Nguyen et al., 2011).

Their proposed mechanism involves the oxidation of the catalytic cysteine by hydrogen peroxide which results in the formation of sulfenylated cysteine. This particular cysteine can then accept electrons from PDI family members and form mixed disulphides between Gpx 7/8 and PDI, which will resolve the second cysteine on the active site of the PDI to form oxidised PDI (Bulleid, 2012, Wang et al., 2014).

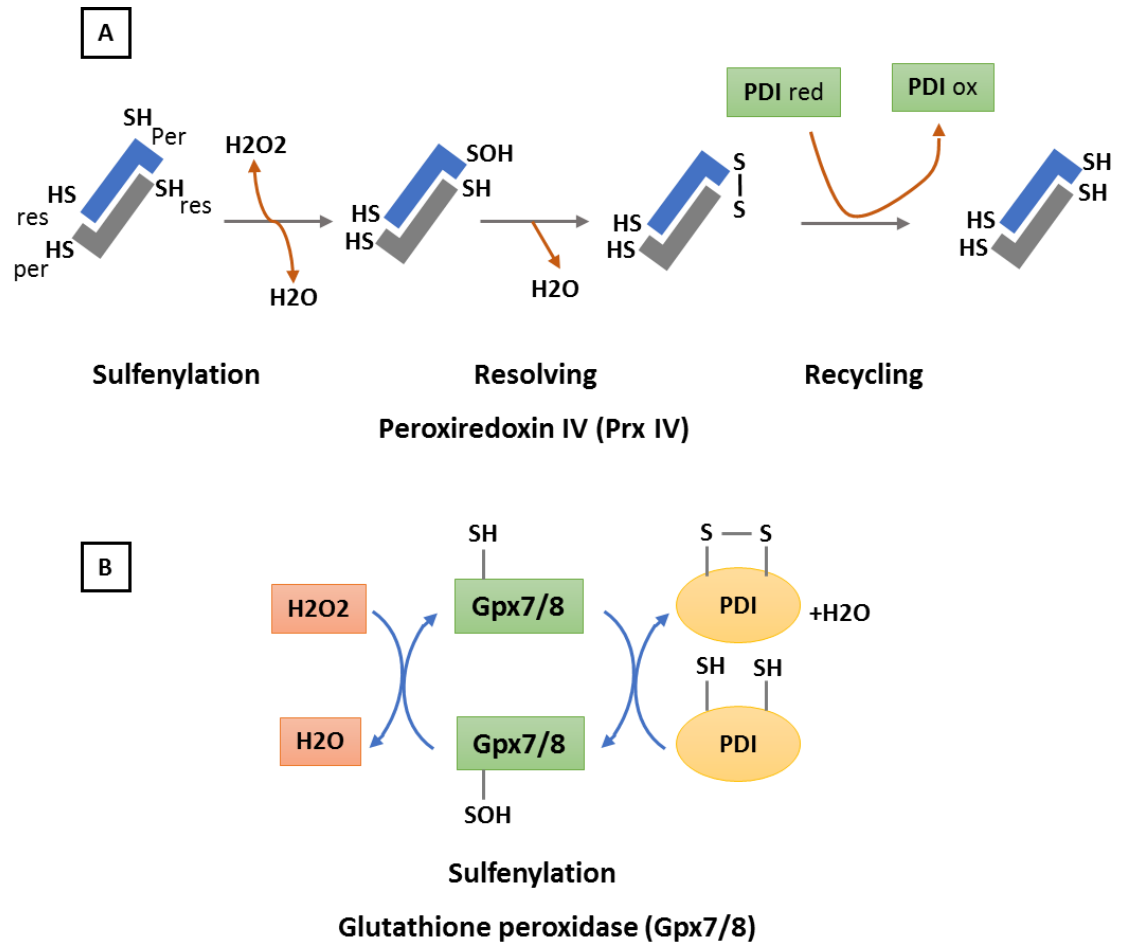


Figure 1.7, Other alternative pathways for the oxidation of PDI involving members of the peroxidase family; Gpx7/8 or PrxIV.

The first step of both cycles is to form sulfenylated cysteine by oxidation of the active site cysteine. This residue will be resolved by the PDI active site in Gpx7/8 or the adjacent cysteine in PrxIV. The reduced PDI will recycle PrxIV to re-generate a free thiol within the active site then PrxIV becomes oxidised. In Gpx7/8 all the mixed disulphide will be resolved to a second cysteine in the active site of PDI in order to form oxidised PDI (Bulleid, 2012).

1.5.4 Vitamin K epoxide reductase (VKOR)

Ero 1 and peroxidase pathways have been known to be the main pathways for electron flow during disulphide bond formation. However, their absence does not prevent disulphide bond formation in mammalian cells. It was proved that in the absence of Ero 1, PrxIV, and Gpx 7/8 there is an alternative oxidative pathway derived from the activity of vitamin K epoxide reductase (VKOR). VKOR is a cofactor for blood coagulation important for γ carboxylation of glutamate residues in proteins (Jin et al., 2007). This enzyme is capable of donating electrons to vitamin K and vitamin K epoxide resulting in the formation of vitamin K hydroquinone (Berkner, 2008, Jin et al., 2007, Rutkevich and Williams, 2012).

Active site cysteines in the transmembrane domain of VKOR will form disulphide bonds within VKOR by donating electrons to vitamin K epoxide. Those electrons are then transferred through an internal disulphide exchange reaction to form a disulphide between two cysteines within the luminal domain of VKOR (Jin et al., 2007, Schulman et al., 2010). PDI members can exchange electrons with VKOR to form a disulphide within the PDI active site (Bulleid, 2012, Braakman and Bulleid, 2011, Rishavy et al., 2011).

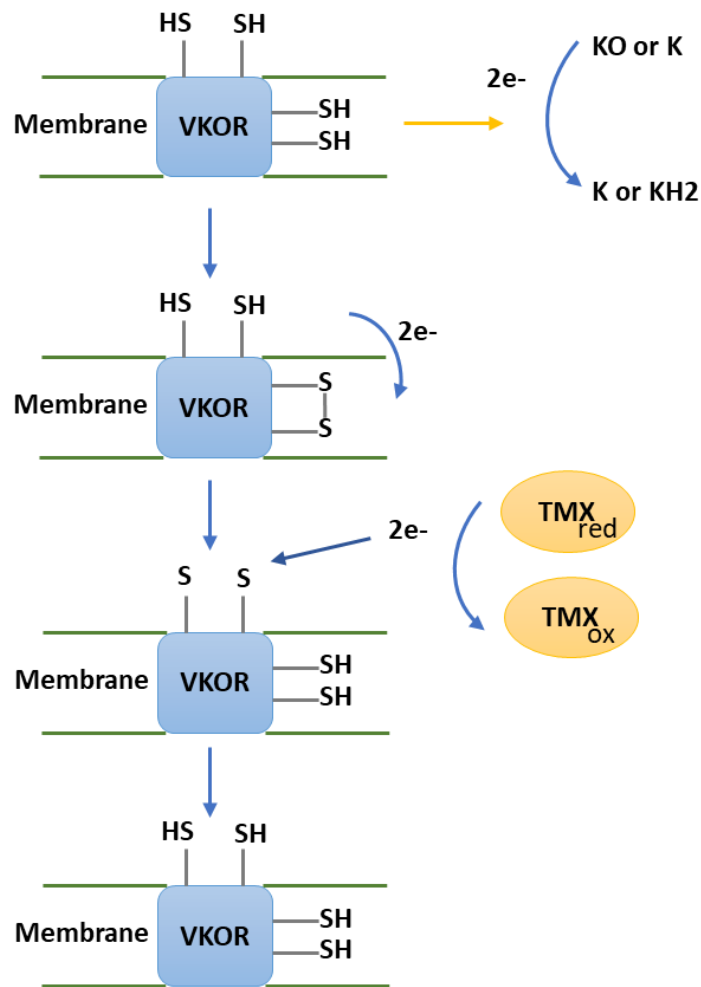


Figure 1.8, VKOR oxidation pathway for PDI.

VKOR, a membrane protein, also has the ability to oxidise PDI family members. It contains two cysteines in the transmembrane domain which can form a disulphide after the donation of electrons to either vitamin K epoxide (KO) or vitamin K (K) and generate vitamin K hydroquinone (KH₂). The formed disulphide can exchange with the cysteines in the VKOR luminal domain. The disulphide can be reduced by the activity of the PDIs TMX1, TMX4, and ERp18 leading to the oxidation of these proteins (Bulleid, 2012).

1.5.5 QSOX

This pathway is quite unique compared to the previous pathways. This enzyme is capable of oxidising polypeptides directly without requiring disulphide exchange protein as it possesses a flavoenzyme domain like Ero1 and a PDI-like thioredoxin domain (Kodali and Thorpe, 2010). The polypeptide donates electrons which will be accepted by the thioredoxin domain and passed directly to the FAD via an internal disulphide exchange reaction (Heckler et al., 2008).

Hence, QSOX is an efficient disulphide catalyst and capable of introducing covalent bonds to a large number of protein substrates. Human QSOX was found to fulfil the function of Ero1p in yeast when overexpressed (Chakravarthi et al., 2007). A couple of aspects may affect the QSOX function. One factor is that the amount of ER localised enzyme maybe limited as most of the intracellular protein is localised to the Golgi apparatus (Chakravarthi et al., 2007). Additionally, QSOX contains transmembrane domain which could restrict the catalysis of soluble substrates (Bulleid, 2012, Rutkevich and Williams, 2012).

1.6 Protein disulphide isomerase (PDI) protein

The PDI protein is the main member of the family and the best characterised ER thiol oxidoreductase in the ER. The domain structure of PDI revealed four thioredoxin-like domains: a, b, b', and a' followed by an acidic carboxyl terminal c-domain (Ellgaard and Frickel, 2003, Appenzeller-Herzog and Ellgaard, 2008, Kozlov et al., 2010a). The a and a' are catalytically active (Ellgaard and Ruddock, 2005) whereas the b and b' domains are non-catalytic. The b' domain contains the substrate binding site. However, the b domain function is still unclear (Appenzeller-Herzog et al., 2008, Feige and Hendershot, 2011).

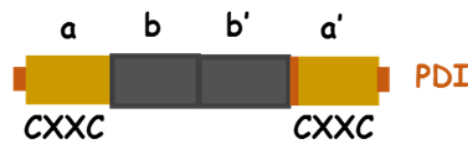


Figure 1.9, The domain structure of the PDI protein.

The diagram shows the catalytic a and a' domains which contain the CXXC active sites and the non-catalytic b and b' domains.

The PDI protein is a multi-functional member of the thioredoxin superfamily. It catalyses the formation of native disulphides of peptide chains either from the reduced form or randomly joined disulphides (Wang and Tsou, 1993, Ellgaard and Ruddock, 2005). In proteins, disulphide bonds are covalent bonds that form between pairs of cysteine side chains and play a crucial role in stabilising the protein structure during protein folding (Oka and Bulleid, 2013, Appenzeller-Herzog et al., 2008).

PDI was considered for a long time to be the only catalytic disulphide forming enzyme in the ER. It donates electrons to its targeted substrates from its active site cysteine residues resulting in oxidation of the substrates. Subsequently, it becomes re-oxidised by one of the oxidoreductases such as Ero1-L α in mammals (Appenzeller-Herzog et al., 2008), or Ero1p in yeast (Frand and Kaiser, 1999, Tu and Weissman, 2002) directing the electrons to an ultimate acceptor such as oxygen molecules. However, for almost two decades, it has been clear that PDI is a member of a super family that contains almost 20 members. Most PDI family members are known for being able to catalyse disulphide formation but whether they all catalyse this reaction under normal cellular conditions is still unclear (Hatahet and Ruddock, 2009).

The identified 20 members of the PDI family are characterised by similarities to the PDI protein (Kozlov et al., 2010a). Some have a similar domain structure and localisation in the ER, but they do not necessarily have a similar physiological function. All of the human PDI members have at least one domain similar to either one of the four domains of the PDI protein (Fig 10). Most members have at least one catalytic domain, however, some of them have non-catalytic domains or have lost the active-site cysteines and therefore are considered non-catalytic such as ERp27 (Alanen et al., 2006) and ERp29 (Hatahet and Ruddock, 2009, Nakao et al., 2017).

The PDI family members that have been reported are; PDI, PDIp, ERp57, ERp72, P5, PDIr (Ferrari and Soling, 1999), ERdj5 (Cunnea et al., 2003, Hosoda et al., 2003), PDILT (Van Lith et al., 2005), thioredoxin-related transmembrane protein 2 (TMX2) (Meng et al., 2003), ERp44 (Anelli et al., 2003), ERp46 (Knoblach et al., 2003, Sullivan et al., 2003), ERp18 (Alanen et al., 2003, Knoblach et al., 2003), TMX (Matsuo et al., 2001), ERp27 (Alanen et al., 2006, Kober et al., 2013), ERp29 (Gao et al., 2016, Sakono et al., 2014), TMX3, TMX4, TMX5, hAG-2, and hAG-3 (Hatahet and Ruddock, 2009). Only a few of these PDIs are tissue specific such as PDIp which is expressed in the pancreatic beta cells (Desilva et al., 1996) and PDILT (Van Lith et al., 2005) which is testis-localised protein.

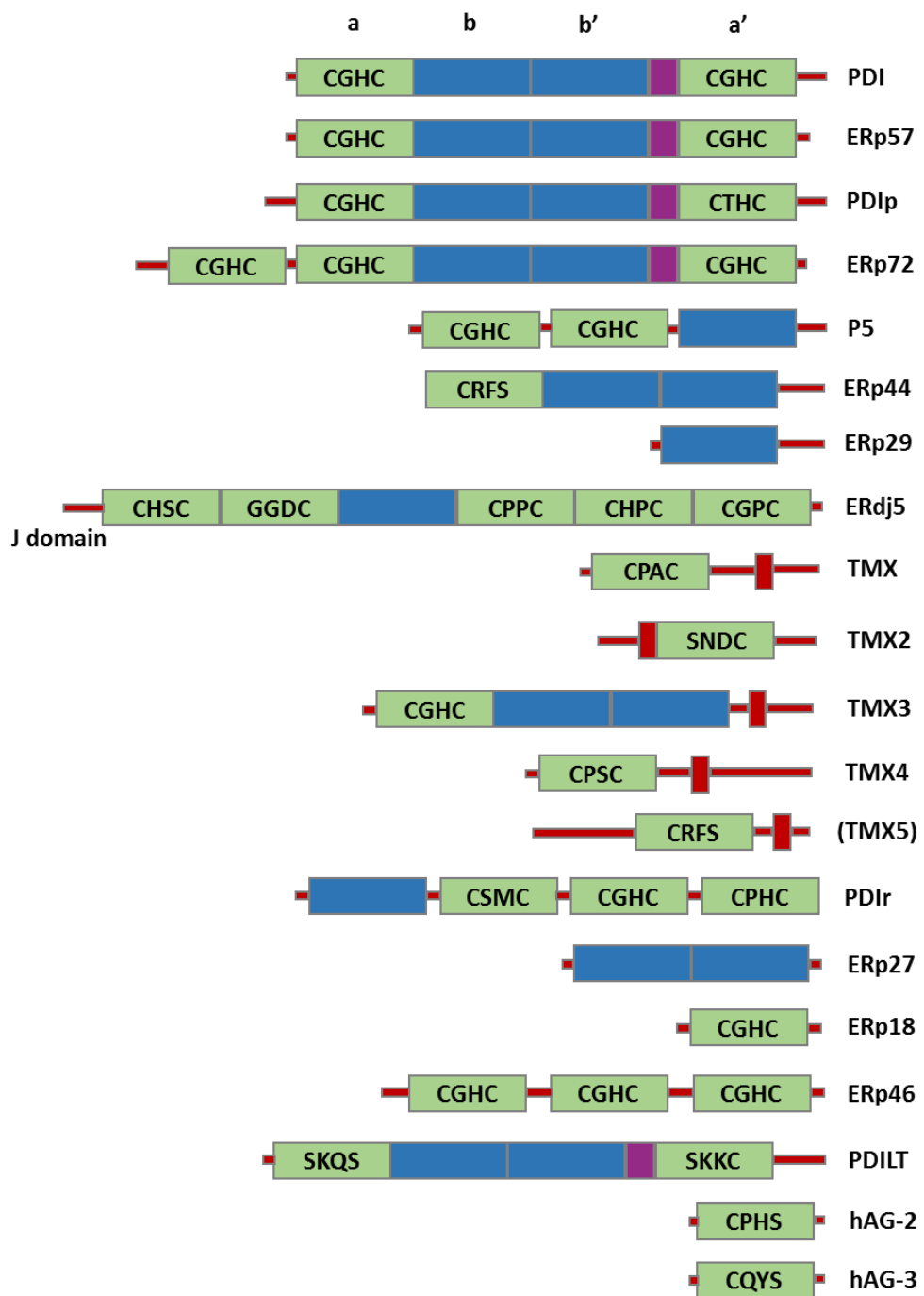


Figure 1.10, The human PDI family members.

The thioredoxin-like domains (catalytic domain) are shown in green. The non-catalytic domains are shown in blue. The transmembrane regions are in red (Ellgaard and Ruddock, 2005).

The endoplasmic reticulum lectins calnexin (CNX) and calreticulin (CRT) and their role in glycoprotein folding and their relation to the oxidoreductase ERp57

Calnexin (CNX, about 572 residues, 65.4 kDa) is a type I ER membrane protein (Tjoelker et al., 1994, Wada et al., 1991). CNX was found to be expressed ubiquitously, regardless the cell type, lineage, or the maturation stage of the cell (Okazaki et al., 2000). Its expression was found to be affected by a various stress types; for example, deprivation of amino acids, calcium mobilising agents, heat shock, and heavy metals (Williams, 2006, Wada et al., 1991, Caramelo and Parodi, 2015).

Calreticulin (CRT), the soluble paralog of CNX (about 400 residues, 46.5 kDa) (Fliegel et al., 1989, Smith and Koch, 1989) is a resident lectin that is localised to the ER lumen by the C-terminal KDEL sequence (Afshar et al., 2005). CRT is also a multifunctional protein that is found in a variety of locations other than the ER lumen such as the nucleus (Roderick et al., 1997), secretory granules (Fraser et al., 2000, Andrin et al., 1998), cytosol (Gold et al., 2010), and the outer side of the plasma membrane (Ghiran et al., 2003, Johnson et al., 2001, Arosa et al., 1999). Furthermore, it is known for its significant role in glycoprotein folding (Williams, 2006, Caramelo and Parodi, 2015) and calcium homeostasis (Li et al., 2002) in addition to suggested roles in mRNA stability, complement activation, angiogenesis, and trafficking of nuclear receptors (Raghavan et al., 2013, Gold et al., 2010).

CNX also works as a molecular chaperone (Ihara et al., 1999). Regardless of its ability to bind Ca^{2+} , it does not have a significant role in Ca^{2+} homeostasis (Li et al., 2002, Ellgaard and Frickel, 2003, Williams, 2006, Caramelo and Parodi, 2015, Gold et al., 2010, Raghavan et al., 2013). CNX and CRT have 45 % homology in terms of their sequence similarity in addition to domain organisation and structure. Both have an N-terminal domain followed by a pro-rich domain (P-domain) and a C-terminal domain (Caramelo and Parodi, 2015, Kapoor et al., 2003).

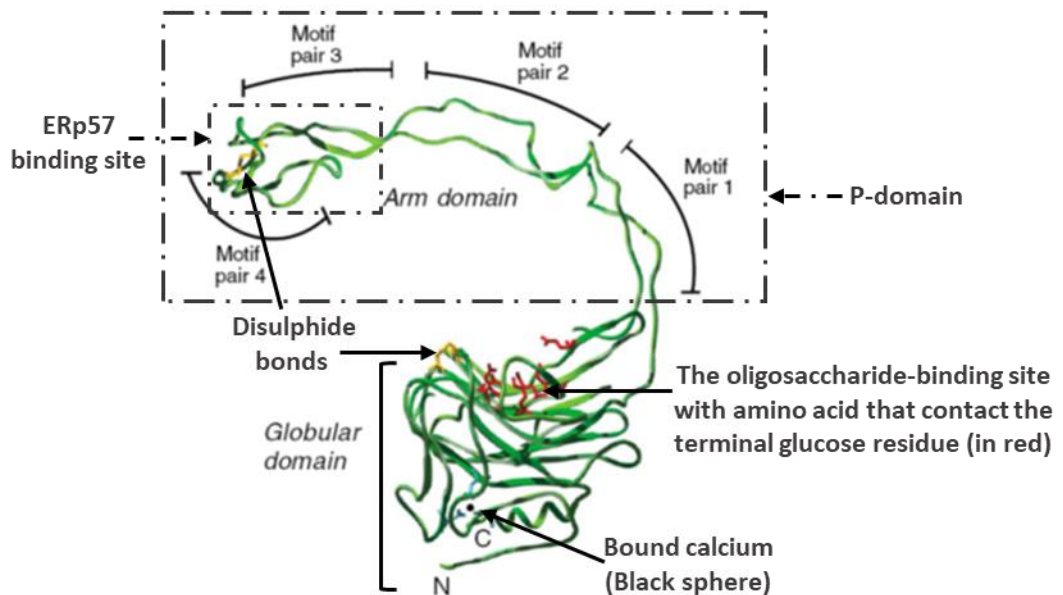


Figure 1.11, A crystal structure of the lectin calnexin (CNX).

The diagram shows the ER globular domain containing a disulphide bond (in yellow) and bound calcium (black sphere). The arm domain (P-domain) has four different motifs and contains the negatively charged tip that can interact with the thiol oxidoreductase, ERp57 (Williams, 2006).

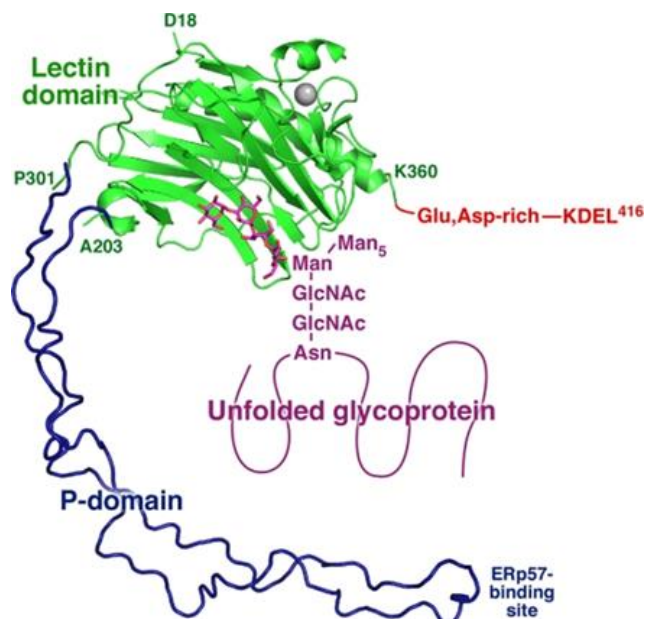


Figure 1.12, The crystal structure of the full length calreticulin (CRT).

The structure shows the lectin domain (in green) and the P-domain (in dark blue) containing the ERp57 binding site. A carbohydrate is shown as part of the N-linked glycan linked to the asparagine residues of unfolded protein. The C-terminal has a Glu, Asp-rich domain that is capable of binding calcium in addition to the ER retention signal (KDEL) (Kozlov et al., 2010b).

1.6.1 The interaction of lectins and glycoproteins

The binding of glycoproteins to CNX/CRT has many advantages; it increases the folding efficiency, decreases aggregation and facilitates disulphide bond isomerisation. The isomerisation of the disulphide bridge is mediated by the oxidoreductase, ERp57, which is a PDI family member that mimics the PDI protein. Both PDI and ERp57 are composed of four domains (a, b, b', and a') in which the b' domain of PDI contains the substrate binding site (Klappa et al., 1998, Pirneskoski et al., 2004). However, the b' domain of ERp57 has a cluster of positively charged residues that can interact with the negatively charged tip of the P-domain of CNX (Jessop et al., 2009a, Maattanen et al., 2006).

There are a number of cellular and viral glycoproteins that are considered to be substrates for the lectins; CNX and CRT such as class I major histocompatibility complex (MHC) (Williams et al., 2002, Sadasivan et al., 1996), the cystic fibrosis transmembrane conductance regulator (CFTR) (Pind et al., 1994, Loo et al., 1998), T-cell receptor subunits (Hochstenbach et al., 1992, Vanleeuwen and Kearse, 1996), HIV gp120 and gp160 (Otteken and Moss, 1996, Li et al., 1996), α_1 -antitrypsin (Ware et al., 1995, Le et al., 1994), and the prion protein (Capellari et al., 1999, Rudd et al., 2001). Although CNX and CRT bind to different glycoproteins they can also bind to the same substrate in different stages of the folding pathway as established with the MHC class I heavy chain and also the influenza hemagglutinin (HA) (Tatu et al., 1995, Ellgaard and Frickel, 2003).

1.6.2 The misfolded glycoprotein sensor (UGGT)

Glycoproteins might be folded at the first attempt. However, many proteins need more than one round of the CNX/CRT cycle to achieve their native conformational structure. In cases where proteins are misfolded, a sensor called UGGT, (about 170 kDa, 1555 residues in human), is responsible for recognising misfolded proteins and directing them back to the CNX/CRT cycle until they fold successfully (Solda et al., 2007, Caramelo and Parodi, 2015).

1.6.3 The N-linked glycoprotein folding cycle

This cycle is very significant for N-linked glycoproteins to be correctly folded and to achieve their native conformation. The process occurs by CNX or CRT, and ERp57 (Helenius et al., 1997, High et al., 2000, Oliver et al., 1997, Elliott et al., 1997). As the nascent polypeptide chain is translocated through the Sec61 complex into the ER lumen, CNX and CRT function as lectins recognising glycoproteins carrying monoglucosylated oligosaccharide side chains. Two enzymes can generate the monoglucosylated oligosaccharides, and hence promote the binding of CNX and CRT. Glucosidase I (GI) and glucosidase II (GII) can remove the two outermost glucose residues of the side chain resulting in the formation of the monoglucosylated (Glc1Man9GlcNAc2) (Hebert et al., 1995, Ware et al., 1995). This glycoform can be recognised by CRT and CNX, which are able to retain glycoproteins in the ER until GII cleaves the last glucose residue. At this stage, correctly folded proteins will be transported out of the ER to their final destination. However, those proteins which are unable to adopt their native conformation or do not achieve their assembled complexes and are recognised by UDP glucose: glycoprotein glucosyl transferase (UGGT). This enzyme can add a single glucose back on the structure and form the monoglucosylated form (Cannon and Helenius, 1999). This process would allow the interaction with the CNX and CRT cycle (Wada et al., 1997). The de-glucosylation cycle continues until glycoproteins are properly folded (Oliver et al., 1999, Benham, 2012, Caramelo and Parodi, 2015). In other cases, the glycoproteins are permanently misfolded and will be targeted for Endoplasmic Reticulum Associated Degradation (ERAD) (Ellgaard and Frickel, 2003, Vitale and Denecke, 1999, Benham, 2012).

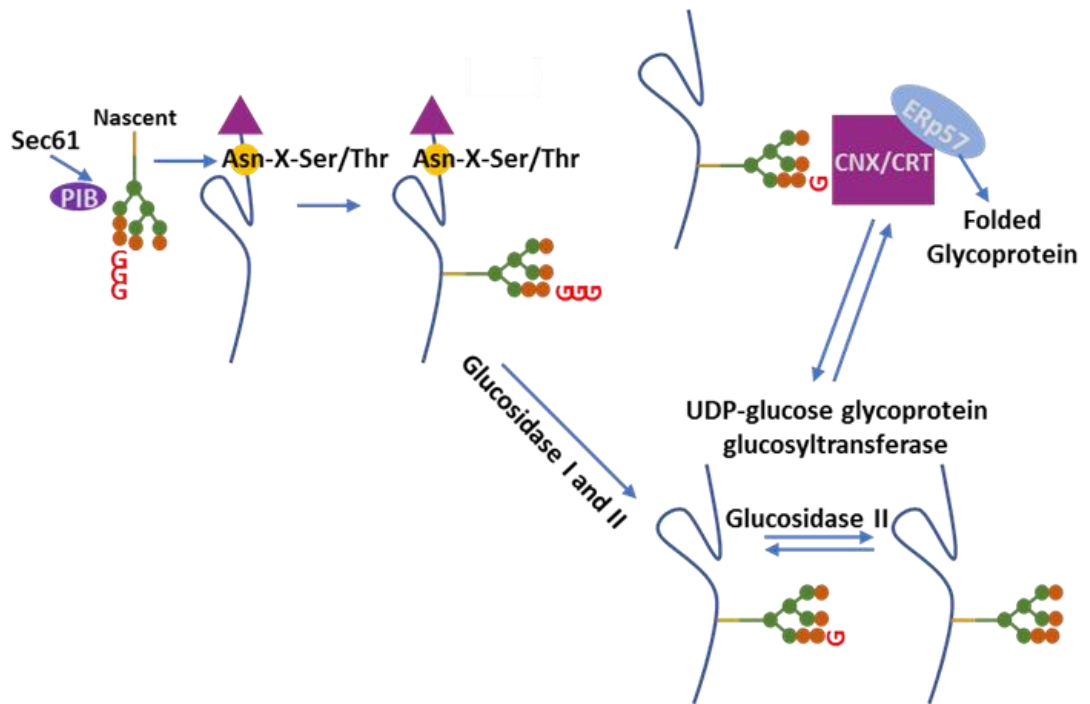


Figure 1.14, The calnexin (CNX) and calreticulin (CRT) cycle of glycoprotein folding.

As proteins are translocated via the Sec61 into the endoplasmic reticulum (ER) lumen, the most outer glucose will be trimmed by glucosidase I and glucosidase II resulting in the monoglucosylated glycoform. The mono glycoform then will enter the cycle of CNX and CRT with ERp57 and correctly folded glycoproteins then exit the ER. Misfolded glycoproteins will be re-glycosylated by UDP-glucose glycoprotein glucosyltransferase which will add a glucose on the glycan and send it back to the CNX/CRT cycle. If the glycoprotein is permanently misfolded it will be targeted for endoplasmic reticulum associated degradation (ERAD).

1.7 Endoplasmic reticulum protein 57 (ERp57)

ERp57 (about 58 kDa, 505 amino acids), which also known as PDIA3, ERp60, and GRP58, (Coe and Michalak, 2010) is a soluble protein, and a well-known PDI family member of the thiol oxidoreductases. The thiol disulphide isomerases are involved in the formation of disulphide bonds in the endoplasmic reticulum in mammalian cells. It is localised to the ER lumen and it is the closest in homology to the PDI protein (Ellgaard and Frickel, 2003). It functions as disulphide isomerase, oxidoreductase, and a chaperone (Erickson et al., 2005) in the ER. However, it is mainly associated with the two ER lectins CNX and CRT for glycoprotein folding (Jessop et al., 2007, Frasconi et al., 2012, Frickel et al., 2004).

ERp57 is highly expressed in a variety of tissues such as liver, kidney, placenta, lungs, and the pancreas, however, low expression was noticed in the brain, skeletal muscles, and the heart (Coe and Michalak, 2010). Despite the great similarity to PDI, it has distinctive functions. It is established that the ERp57 and CRT interaction can be hindered by vancomycin, however, the antibiotic is not able to inhibit the interaction at higher concentration of CRT (Frasconi et al., 2012).

ERp57 is also suggested to function as a cysteine protease (Urade and Kito, 1992), a hormone-induced protein of the brain (Mobbs et al., 1990), and a carnitine palmitoyl transferase (Murthy and Pande, 1994). Besides being a folding factor during the synthesis of glycoproteins (Zapun et al., 1998) it also plays a central role in the quality control of the ER. Moreover, it is essential in regulating gene expression and the assembly of the major histocompatibility complex (MHC) (Chapman and Williams, 2010).

Additionally, studies have revealed that in mice ERp57 is important in embryonic development (Coe and Michalak, 2010). It was also implicated in human pathologies such as prion disorders Alzheimer's (Erickson et al., 2005) and Parkinson's diseases as well as cancer (Coe and Michalak, 2010). These studies have shed light on the importance of ERp57 in human diseases and suggested the possibility of using ERp57 for developing novel cures and early stages of diagnosing such diseases (Coe and Michalak, 2010).

Similar to PDI protein, ERp57 has been shown to adopt an overall U-shape with the two catalytic domains containing the catalytic cysteines, a- and a', facing each other (Coe and Michalak, 2010). The thioredoxin domains b and b' are at the bottom where the tip of the

b' domain contains the CNX binding site (Kozlov et al., 2006). ERp57 b and b' domains are distinct to PDI b and b' domains in which the acidic C-terminus is replaced by a basic C-terminus (Coe and Michalak, 2010, Pirneskoski et al., 2004).

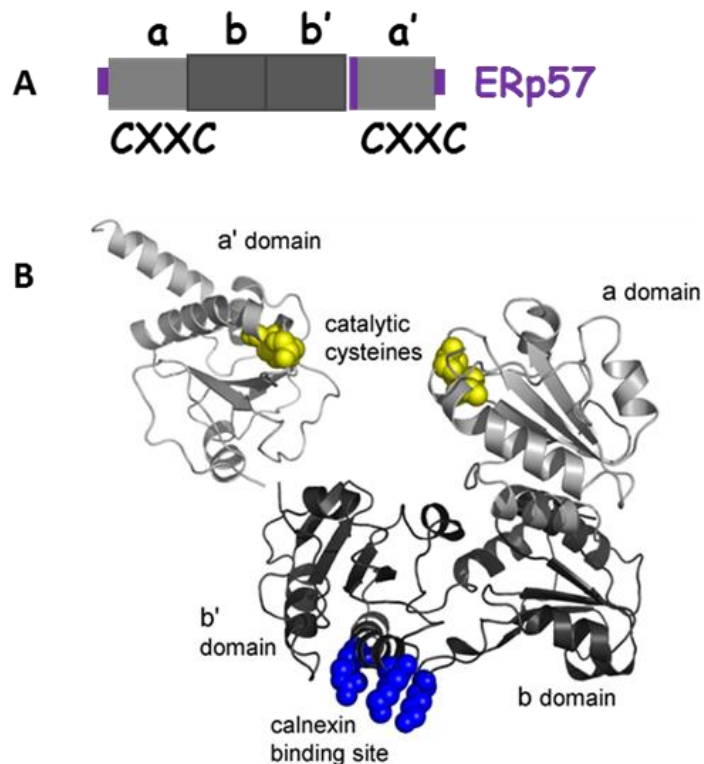


Figure 1.15, A, schematic showing the domain structure of ERp57. B, A model of the full length ERp57.

A, a cartoon detailing the catalytic a and a' domains which contains the CXXC active sites and the non-catalytic b and b' domains. **B**, the structure reveals a U-shape where the catalytic a and a' domains are facing each other. The b and b' domains are at the bottom and the b' domain contain the CNX binding site (Kozlov et al., 2006).

Furthermore, the b' domain of PDI binds to substrate proteins while the b' domain of ERp57 has been shown to be associated with CNX and CRT as it binds the tip of the P-domain of the lectins specifically for glycoprotein folding (Jessop et al., 2007) forming a complex with CNX and CRT as explained earlier (Wada et al., 1991, Williams, 2006).

The interaction of ERp57 with the lectins has been investigated previously (Jessop et al., 2007). Nuclear magnetic resonance spectroscopy (NMR) studies (Frickel et al., 2002) and Isothermal Titration Calorimetry (ITC) experiments (Frickel et al., 2002) have investigated this interaction and revealed that when viral glycoproteins folding is taking place in the ER of living cells, ERp57 forms disulphide bonds with the substrates of those glycoproteins that bind to the lectins (Frasconi et al., 2012). However, inhibition of this association of

the glycoprotein and the lectins prevents the formation of disulphide bonds with the oxidoreductase (Frickel et al., 2002).

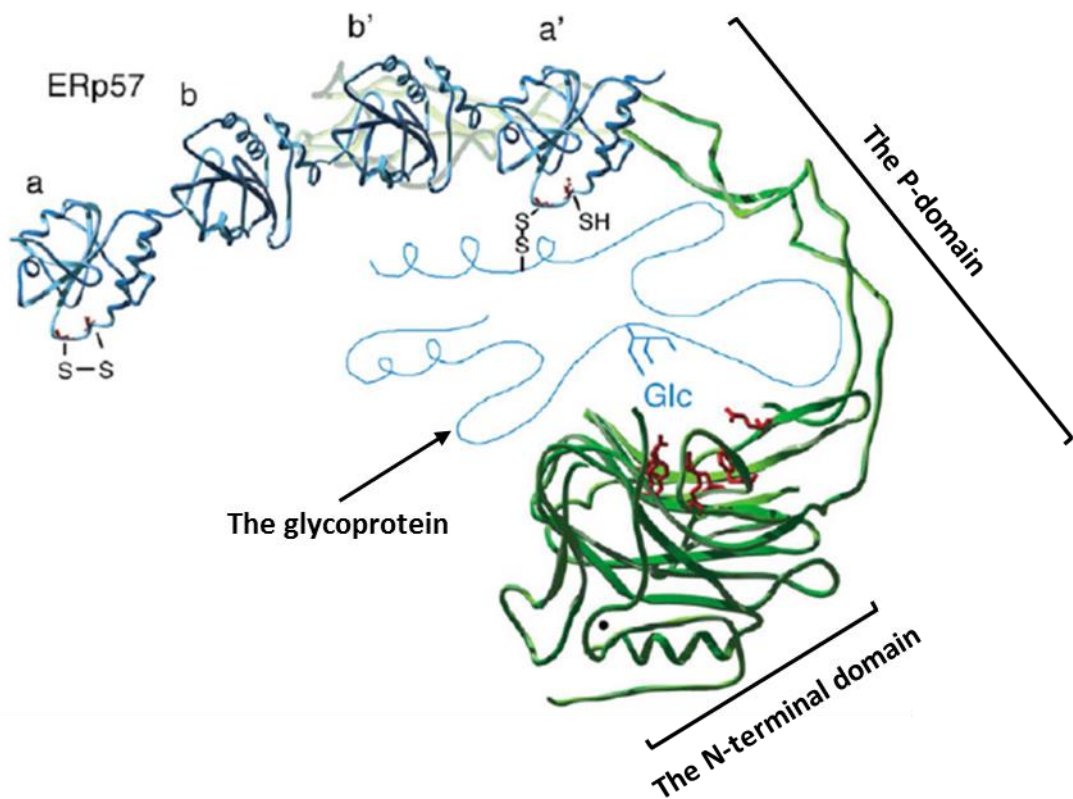


Figure 1.16, A model for the interaction of the folding glycoprotein with calnexin or calreticulin.

The model shows the domain structure of calnexin (in green). The tip of calnexin P-domain binding the b' domain of ERp57 (in dark blue). The glycoprotein (thin light blue) can interact with both calnexin as well as the polypeptide binding site forming disulphide bonds (Williams, 2006).

It was found that in ERp57 the $\alpha 2'$ - helix in the b' domain is positively charged by +4, whereas in PDI it is -4. The positive charges of ERp57 play a central role in binding the negative charged tip of the P-domain of the lectin CNX. When those residues are mutated in ERp57 to negatively charged amino acids, the ERp57/CNX/CRT complex is abrogated (Coe and Michalak, 2010, Kozlov et al., 2010a).

ERp57 was also reported to be able to form a complex with another PDI family member named ERp27 *in vitro*. The interaction between ERp27 and ERp57 has been investigated. NMR and protein cross-linking experiments proved that ERp27 can bind ERp57 *in vitro* (Alanen et al., 2006).

We are particularly interested in this interaction which we have investigated further using both *in vitro* and *in cellulo* assays which will be explained later.

1.8 Endoplasmic reticulum protein 29 (ERp29)

ERp29 (about 28 kDa, 261 amino acids) is another PDI family member which is quite similar to ERp27 (Kober et al., 2013) in terms of domain structure and is a catalytically inactive protein missing the CXXC active site (Barak et al., 2009). The crystal structure of ERp29 has revealed a couple of domains. The first is the thioredoxin like domain and the other one is the D-domain which is of unknown function (Kozlov et al., 2017). Recently, it was established that ERp29 also interacts with the ER lectins CNX and CRT by binding the tip of their P-domain in a similar fashion to the oxidoreductase ERp57 (Nakao et al., 2017, Sakono et al., 2014).

Studies have revealed that the tip of the P-domain of CNX and CRT acts as an adapter binding different chaperones within the ER lumen. ERp29 (Liepinsh et al., 2001) and ERp57 (Oliver et al., 1999) as well as other ER chaperones such as Bip and CypB are capable of binding CNX and CRT. This observation of protein scaffolds binding the same model indicates that there are converging pathways of folding machineries within the ER lumen (Kozlov et al., 2017).

NMR studies that focused on the binding between the ERp29 D-domain and the P-domain of CNX/CRT have determined the binding affinity with CNX which is 20 μ M and 17 μ M with CRT. Furthermore, NMR has shown that the lectin-glycoprotein associations are long-lived in comparison to other chaperones complexes (Kozlov et al., 2017).

Whether this interaction of ERp29 and the lectins is similar to the lectins-ERp57 complex or if they are occurring sequentially or competing is to be investigated.

1.9 Endoplasmic reticulum protein 27 (ERp27)

ERp27 is a PDI family member that found exclusively in vertebrates (Kober et al., 2013). The human ERp27 (about 27.7 kDa, 273 amino acids) (Amin et al., 2013) was found to be expressed in a number of tissues including kidney, bone marrow, spleen, lungs, thymus, and highly expressed in the pancreas (Lash et al., 2000, Alanen et al., 2006). The expression in the pancreas occurs particularly within the acinar cells which secrete hormones. However, the pancreatic islet cells which secrete insulin do not show evidence of expressing ERp27 (personal communication with Professor Kenji Inaba, Tohoku University, Sendai, Japan).

The ERp27 crystal structure has been solved and revealed two thioredoxin-like domains b and b' and therefore it is known to be catalytically inactive (Kober et al., 2013). The sequence of this protein has revealed two cysteines that are localised to different domains and found to be solvent- inaccessible so are unlikely to form a disulphide (Kober et al., 2013). In comparison to other redox-inactive PDI members such as ERp29 which has a single thioredoxin fold domain and the other one is all α -helical domain, ERp27 possesses two thioredoxin fold domains and therefore may form a distinct subfamily under the PDI family (Alanen et al., 2006, Ma et al., 2003, Kober et al., 2013, Liepinsh et al., 2001).

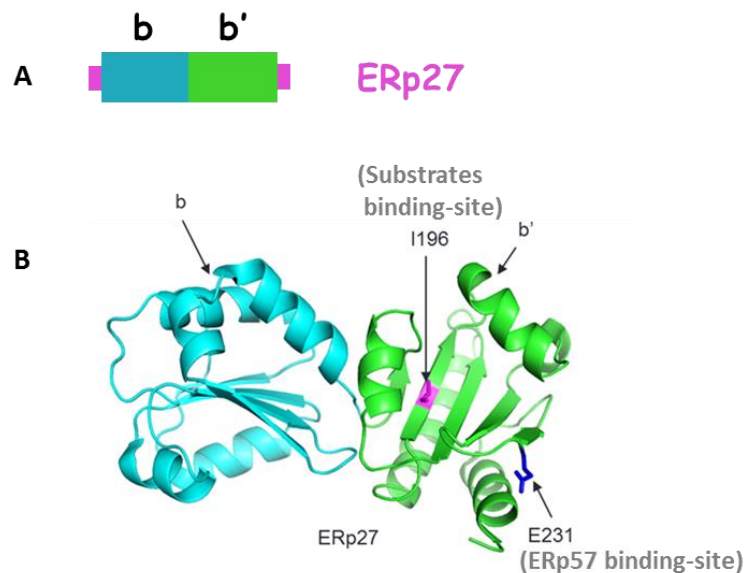


Figure 1.17, A, The domain structure of ERp27. B, The overall crystal structure of ERp27.

A, the domain structure depicts the two thioredoxin-like domains b and b'. ERp27 lacks the CXXC active site and is classified as a non-catalytic member of the PDI family. **B**, ERp27 consists of two thioredoxin domains, b and b'. The b' domain contains a hydrophobic cleft similar to the PDI protein which contains the peptides binding site and the tip of the b' domain contains an ERp57 binding site (Kober et al., 2013).

ERp27 has a degree of homology to PDI protein and because other PDIs also possess the b and b' domains an alignment has been carried out between ERp27 and those members. The percentage identities are as follows: ERp27 homology with PDI (33.5 %), ERp57 (16.5 %), ERp72 (14.7 %), PDlp (28.1 %). However, no homology was found with ERp29 the other non-catalytic member of the family (Alanen et al., 2006).

The C-terminal domain of ERp27 (b' domain) was found to be homologous to the PDI b' domain and has a hydrophobic groove in the middle containing the substrate binding site. It is established that the b' domain of ERp27 can bind the 14-amino acid peptide Δ -somatostatin. Mutating specific residues within this site inactivates the substrate binding site, particularly mutating the (Isoleucine) I196 residue into Tryptophan (W) (Alanen et al., 2006, Pirneskoski et al., 2004). Expanding on that, an ITC experiment has indicated that ERp27 functions as a chaperone in the ER as it binds unfolded full-length proteins. However, when the protein is correctly folded then ERp27 does not show any degree of measurable binding affinity (Kober et al., 2013).

Additionally, the tip of the b' domain was also found to contain an ERp57 binding site. This site was verified by mutating the (Glutamic acid) E231 residue to Lysine (K) which blocked the interaction (Jessop et al., 2009a). This particular site in the ERp27-b' domain was found to contain a motif Asp-Glu-Trp-Asp, which was postulated to fulfil a similar function to the motif Asp-Glu-Trp-Asp, located on the tip of the P-domain of the two ER lectins CNX and CRT (Alanen et al., 2006). This suggested that both ERp27 and the lectins CNX and CRT bind to ERp57 at similar binding sites (Kober et al., 2013, Williams, 2006, Alanen et al., 2006).

In this research project we are not going to shed the light on all PDI members. We are going to emphasise ERp27 (Alanen et al., 2006), which is our protein of interest, and its interaction with another member of the oxidoreductases, ERp57 *in vitro* and *in cellulo* (Jessop et al., 2009a).

From previous research studies, PDI family members were found to be important enzymes that contribute to disulphide bond formation (Sevier and Kaiser, 2006a), isomerisation and reduction (Inaba et al., 2010, Masui et al., 2011, Frand and Kaiser, 1998). Members of this family are similar in some respects, however, have differences in structure which make PDIs functionally very diverse (Kozlov et al., 2010a, Ellgaard and Ruddock, 2005). ERp57 (Maattanen et al., 2006) is as well studied as PDI itself and is required for glycoprotein folding in collaboration with the ER lectins CNX and CRT in addition to a wide range of other functions (Maattanen et al., 2006, Williams, 2006).

The P- domain of CNX and CRT is very important and found to bind other ER chaperones (Nakao et al., 2017, Kozlov et al., 2017) in addition to its involvement in the glycoprotein folding cycle (Ellgaard and Frickel, 2003, 1997). For glycoproteins to fold with the aid of ERp57, CNX and CRT bring N-glycosylated glycoproteins to ERp57 to fold. Furthermore, the CNX and CRT P-domain contains a sequence motif similar to that found on the tip of the b' domain of ERp27 (Alanen et al., 2006). ERp27 has also been reported to interact with ERp57 *in vitro*, suggesting that ERp27 binds ERp57 on the same binding site as the lectins. This data together has suggested a role for ERp27 in recruiting substrates to ERp57 (Alanen et al., 2006).

Moreover, ERp57 lacks a substrate binding site and binds its substrates through a CNX/CRT complex as they are able to recognise the suitable substrates and recruit them to ERp57 (Russell et al., 2004). Based on that model, ERp27 could potentially enable ERp57 to interact with a wide range of substrates that bind to ERp27 (Alanen et al., 2006). Hence, ERp27 might be working either in sequence or competing for the lectins that bind ERp57.

Under ER stress conditions, ERp27 was found to function as a chaperone by selectively binding to misfolded or unfolded proteins which suggest other molecular functions and physiological roles for this redox-inactive PDI member (Kober et al., 2013). It was also established that the expression of ERp27 increases greatly as part of the UPR under

cellular stress conditions. That is in line with an ERp57 independent function (from CNX/CRT) following infection with simian virus 40 (Schelhaas et al., 2007), suggesting that under regular cellular conditions CNX/CRT replaces the ERp27/ERp57 interaction (Kober et al., 2013).

Previous researches have consequently raised the following questions which we are aiming to answer;

1. Does the ERp27/ERp57 interaction compete with the CNX/CRT/ERp57 complex?
2. If so, then does ERp27 recruit non-glycosylated protein substrates to ERp57 to fold, just as CNX and CRT brings N-glycosylated proteins to ERp57 to fold?

So far none of the previous research has investigated whether the ERp27/ERp57 interaction compete with the complex of CNX/CRT/ERp57 or if these interactions occur sequentially and therefore the aims of this project are;

1. To investigate the interaction between ERp27 and ERp57 both *in vitro* and *in vivo*.
2. To compare the interaction of ERp57/ERp27 and CNX/CRT in order to define whether or not the ERp27 interaction could compete with ERp57/CNX/CRT complex.
3. To investigate the physiological role of ERp27.

To be able to achieve the aims and start *in vitro* assays we commenced a series of protein purifications which are explained in detail in the first results chapter. These include the purification of wild type (WT) ERp27 and two mutants: ERp27-I196W, which prevents ERp27 binding to client proteins and ERp27-E231K, which prevents ERp27 binding to ERp57.

Additionally, we have sub-cloned CRT into the RSFDuet-1 vector (3829 bp), which is engineered to co-express target proteins in *E. coli* and additionally to produce native unfused or fused protein to a His-tag and sequences for detection and purification of protein complexes. Consequently, CRT was expressed and purified with a good yield. Moreover, we mutated the Arginine (ARG, R 282) of ERp57 into Alanine (Ala, A) to study binding to CRT. The ERp57-R282A mutant will prevent ERp57 binding to CRT.

Isothermal titration calorimetry (ITC) experiments were carried out to investigate protein-protein interactions. Furthermore, a protein cross-linking assay was applied *in vitro* as

well as *in cellulo* which is explained in detail in the second results chapter. An antibody to ERp27-WT has also been raised and characterised using a variety of mammalian cell lines; PANC-1, INS-1, CHOS, and HEK. Further investigation of the ERp27 interaction with PDI proteins other than ERp57 or possibly other ER chaperones was also determined in results chapter three.

2 Materials and methods

2.1 List of chemicals

Chemicals	Supplier
Acetic Acid	Fisher (A/0400/PB17)
Acetone	BDH (1000346)
Ammonium bicarbonate	Sigma (A6141)
Ammonium Sulphate (NH ₄) ₂ SO ₄	ICN (808211)
Ampicillin	Sigma (A0166)
Bacto agar	Melford (M1002)
Bacto Tryptone	Melford (T1332)
Bacto Yeast Extract	Melford (Y1333)
BMH	Pierce (22330)
Brilliant Blue G250	Sigma (0770)
Bromophenol Blue	Aldrich (114391)
DMSO	Sigma
DSG	Pierce (20593)
DSP	Pierce (22585)
DTT	Fisher (D/D351/43)
EDTA	Fisher (D/0700/53)
Ethanol	Fisher (E/0650DF/17)
Formaldehyde	Fisher (F/1501/PB17)
G418	Sigma (A1720)
Glucose	Sigma (G8270)
Glycerol	Fisher
Glycine	Fisher (G/0800/60)
HEPES	Fisher (BP310-100)
Hydrochloric acid (HCL)	Fisher (H/1200/PB17)
Kanamycin	Roche (10106801001)
Lipofectamine 2000	Invitrogen (1168-019)
Lysozyme	Sigma (L6876)
MegaTran	Generon (TT200002)
Mercaptoethanol	Sigma M3148
Methanol	Fisher (M/4000/17)
N-Ethylmaleimide (NEM)	Sigma (E3876)
Phenol: chloroform: isoamyl alcohol	Sigma (77617)
Phosphoric Acid (H ₃ PO ₄)	Fisher (O/0500/PB08)
PMSF	Sigma (P7626)
Potassium Acetate	BDH (103504X)
Protease inhibitor cocktail tablets	Roche (04693159001)
Protein A Sepharose	Zymed (10-1042)
Silver nitrate (AgNO ₃)	Fisher (S/1286/46)
Sodium Carbonate (Na ₂ CO ₃)	BDH (10240)
Sodium Chloride (NaCl)	Fisher (S/3160/65)
Sodium Dodecyl sulphate (SDS)	Fisher (S/5200/53)
Sodium hydroxide (NaOH)	BDH (102524)
Sodium Phosphate (NaH ₂ PO ₄)	Fisher (BP329-1)
TBST	Sigma

TCEP	Thermo (20490)
TEMED	Sigma (T9281)
Tris	Fisher (BP152Y)
Triton X-100	Sigma (T8520)
Trypsin	DIFCO (215240)
Tween	Sigma (P1754)
Imidazole (C ₃ N ₂ H ₄)	Sigma (10125)

2.2 List of antibodies

Antibodies	Supplier
Anti-CRT rabbit	Stressgen (SPA-600)
Anti-CNX	Sigma
Anti-ERO1 monoclonal	Obtained from Roberto Sitia (Sitia <i>et al</i> , 2010)
Anti-ERp27 rabbit	Raised against ERp27 purified protein
Anti-ERp57 Rabbit	Sigma
Anti-His mouse	Proteintech (660055)
Anti-myc 9E10 mouse	Fisher
Anti-myc rabbit	Santacruz
Anti-myc conjugate (4A6) mouse	Millipore (16-212)
Anti-Myc-Trap agarose conjugate camel	Chromotek
Anti-V5 monoclonal	Generon
Anti-V5 agarose conjugate mouse	sigma
Licor secondary 800 mouse	Abcam
Licor secondary 680 mouse	Abcam
Licor secondary 800 rabbit	Abcam
Licor secondary 680 rabbit	Abcam

2.3 Protein expression and purification

Protein was purified using the general scheme outlined in figure 2.1 as previously described (Alanen et al., 2006). Cells were pelleted by centrifugation (10,000 rpm for 25 min), and the pellet re-suspended in 1/10th volume of buffer A (50 mM NaH₂PO₄ buffer pH 8.0, containing 300 mM NaCl, 5 mM imidazole). The cells were lysed using a French press three times, and the debris was removed by centrifugation (10,000 rpm for 25 min). The supernatant was filtered through a 0.45 μM filter before being applied to a nickel agarose affinity chromatography column, equilibrated in buffer A. After loading, the column was washed with buffer A, containing 5 mM imidazole, before the His-tagged proteins were eluted using a linear gradient of 5-500 mM imidazole in buffer A. Eluted fractions were checked for purity by SDS-PAGE, and fractions containing fewest contaminant proteins were further purified by gel filtration.

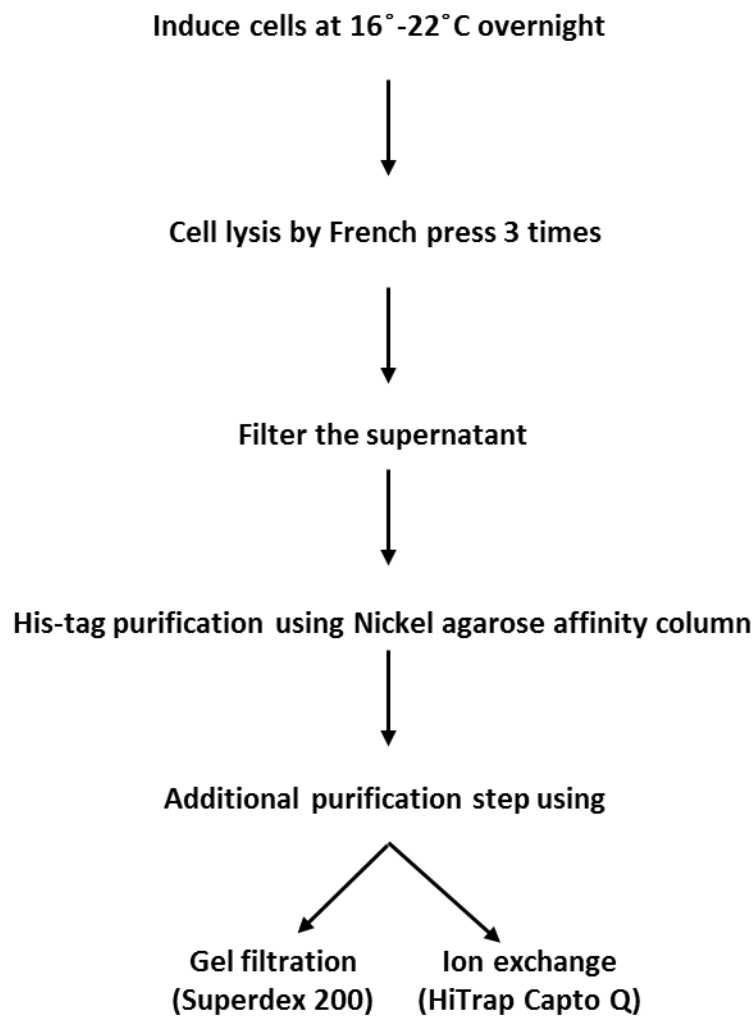


Figure 2.1, Protein purification steps.

A flow diagram shows the protein purification steps. Cells were pelleted (10,000 rpm for 25 min) then lysed by French press three times. The debris removed by centrifugation (10,000 rpm for 25 min). The supernatant was then filtered by 0.45 μ M filter and purified using a nickel agarose affinity chromatography column where the protein will be partially purified. Additional purification was by gel filtration chromatography (GFC Superdex 200) or ion-exchange (HiTrap Capto Q).

2.4 Colloidal Coomassie blue stain

After gel electrophoresis the proteins were visualized by Coomassie blue staining (10 % phosphoric acid (H_3PO_4), 10 % ammonium sulphate ($(\text{NH}_4)_2\text{SO}_4$, 0.12 % Coomassie G 250 (brilliant blue), 20 % Methanol) overnight. Gels were de-stained by dH_2O and scanned the next day.

2.5 Gel filtration (Superdex 200)

Fractions from the nickel agarose affinity chromatography column were combined and concentrated to 1 ml using a centrifugal concentrator (Satorius, Vivaspin 6, membrane 10,000 Mw). The membrane was washed with dH_2O prior to adding the sample (4 ml) to the concentrator. Subsequently, the sample was centrifuged at 3000 Xg for 25 min. The gel filtration column was equilibrated with 50 mM Tris buffer pH 7.5, containing 150 mM NaCl, prior to loading 1 ml sample. Fractions that contain the purified protein were combined, aliquoted and stored at -80°C to be used in other molecular assays.

2.6 Ion-exchange chromatography

Samples were concentrated as for gel filtration samples to a final volume (1 ml) using a centrifugal concentrator. The protein was then diluted using 5 ml of ion exchange buffer (50 mM Tris buffer pH 7.5, containing 10 mM NaCl), and centrifuged at 3000 xg for 20 min before loading onto a HiTrap Capto Q (anion exchange) 1 ml column (GE. Healthcare). Proteins were eluted with ion exchange buffer B (50 mM Tris buffer pH 7.5, containing 1 M NaCl). Eluted fractions were analysed by SDS-PAGE and protein visualised by silver staining.

2.7 Silver staining

Gels were fixed in [MeOH (50 %), acetic acid (12.2 %), formalin (0.05 %)] for 10 min, then washed with EtOH (35 %) for 5 min and sensitised by immersing in $\text{NO}_2\text{S}_2\text{O}_3$ (0.02 %) for 2 min. The gels were stained with silver nitrate solution [0.02 % AgNO_3 , 0.076 % formalin 35 % formaldehyde] for 20 min, and developed by incubating in [Na_2CO_3 (6 %), formalin (0.05 %), formaldehyde (35 %), $\text{Na}_2\text{S}_2\text{O}_3$ (0.0004 %)]. The staining was stopped by incubating the gel in [MeOH (50 %), acetic acid (12 %)].

2.8 Gel electrophoresis and western blot

Each sample was mixed with an equal volume of SDS sample buffer (240 mM Tris/HCl buffer pH 6.8, containing 40 % glycerol, 8 % SDS, 0.04 % bromophenol blue, 50 mM DTT), then heated to 105 °C for 5-10 min followed by centrifugation at 16,162 xg for 10 sec. The samples were electrophoresed (2 h, 20 mA) in 1X running buffer (0.25 M Tris, 1.52 M glycine, 0.02 M SDS). Samples were transferred to nitrocellulose membrane (LiCor) in transfer buffer containing (25 mM Tris/HCL, 20 % methanol, 0.1 % SDS, 192 mM glycine), for 1 h, 300 V. The membrane was blocked with 5 % blocking buffer (5 % non-fat milk in TBST 50 mM Tris/HCL buffer pH 7.5, containing 150 mM NaCl, 0.1 % Tween), for either 1 h at room temperature or overnight at 4 °C. Membranes were incubated overnight at 4 °C with ERp27 antibody which was raised to the purified protein. After 3 washes (5 min each) with TBST, the membrane was incubated with anti-rabbit 800 secondary antibody diluted 1/5000 or 1/10,000. then washed 3 times (5 min each) with dH_2O and scanned using the Odyssey Sa scanner. Anti-myc mouse antibody was used in some of the experiments along with the ERp27 antibody. In this case, the secondary antibody used was anti-mouse 680 diluted 1/5000 or 1/10,000.

2.9 Transformation

Plasmid DNA was mixed with 50 µl of competent cells [BL21 (DE3) or (XL1)] and incubated on ice for 30 min. The cells were heat shocked at 42 °C for 45 secs and immediately placed on ice for 2 min before adding 450 µl of LB broth. Cultures were shaken for 1 h at 37 ° C, prior to plating 200 µl of the culture was spread on antibiotic resistant plates (ampicillin 50 mg/ml or kanamycin 50 mg/ml) and incubated overnight at 37 ° C.

2.10 Mini prep purification of DNA by alkaline lysis

The culture (1.5 ml) was pelleted by centrifugation at 12,460 xg for 1 min. The supernatant was discarded, and centrifugation repeated. The pellet was re-suspended in 100 µl of GTE buffer (25 mM Tris-Cl buffer pH 8.0, containing 50 mM glucose, 10 mM EDTA). Freshly made NaOH/SDS solution (200 µl) was added and samples incubated on ice for 5 min. Then 150 µl of 5 M potassium acetate solution pH 4.8 was added, mixed and centrifuged at 16,162 xg for 5 min to pellet all debris and chromosomal DNA. The supernatant was transferred to a new tube with an equal volume of phenol: chloroform: isoamyl alcohol (25:14:1) and centrifuged at 16,162 xg for 2 min. The upper phase was removed to another tube with an equal volume of phenol: chloroform: isoamyl alcohol and centrifuged at 16,162 xg for 2 min. The upper phase was removed to another tube with 800 µl 95 % ethanol and centrifuged at 16,162 xg for 5 min. The supernatant was discarded, and 1 ml of 70 % ethanol was added to the pellet and centrifuged at 16,162 xg for 5 min. After air-drying the pellet, 30 µl water was added. Samples of each DNA mini-preparation were then sequenced (GATC).

2.11 Sub cloning of DNA fragments into vectors by PCR or restriction digestion

DNA fragments for cloning were prepared by means of PCR (94 ° C for 5 min, then 25 cycles of 94 ° C for 30 secs, 62 ° C for 1 min, 72 ° C for 1.5 min, and 72 ° C for 7 min). The vector was linearised and PCR products cleaved by incubation with two different enzymes; Eco RI and Hind III. All of the digestion products were separated on 1 % agarose gel and correct sized bands were excised from the gel. The DNA was purified using Qiagen Qiaquick Gel Extraction Kit. Subsequently, the DNA fragment was ligated into the vector using T4 DNA ligase. Ligation reactions were transformed and plated onto antibiotic resistant plates and, finally, checked by sequencing.

2.12 Site Directed Mutagenesis

The sample was prepared as follows; 1:10 dilution of 50 ng parental DNA, 10X Accuzyme buffer, MgCl₂, 10 µM forward primer (CAACTACTGGAGAAACGCGGTAATGATGGTGGCA), 10 µM reverse primer (TGCCACCATCATTACCGCCTTTCTCCAGTAGTTG), 10 µM mixed dNTP, DMSO, dH₂O to a final volume of 50 µl, and finally Accuzyme enzyme. Samples then underwent heating cycles; 95 ° C (30 secs), 60 ° C (1 min), 72 ° C (8 min), 72 ° C (10 min), for 25 cycles. Dpn I restriction enzyme was added to digest the parental DNA. Finally, the DNA was used to transform XL1 blue E. coli competent cells and colonies were picked. Mini preps were carried out and checked by sequencing (GATC).

2.13 *In vitro* protein cross-linking

Proteins were mixed to prepare a 9 µl volume cross-linking reaction in 0.2 mM Sodium phosphate buffer (NaH₂PO₄) pH 7.4 incubated on ice for 10 min. Disuccinimidyl glutamate (DSG) (1 mM), which is amino group specific and non-cleavable, was added and incubated for 30 min at room temperature. Each sample was mixed with an equal volume of SDS sample buffer (240 mM Tris/HCl buffer pH 6.8, containing 40 % glycerol, 8 % SDS, 0.04 % bromophenol blue, 50 mM DTT), then heated to 105 ° C for 5-10 min followed by centrifugation at 16,162 xg for 10 secs.

The samples were electrophoresed (2 h, 20 mA) in running buffer (25 mM Tris, 1.92 mM Glycine, 0.01 % SDS). Samples were transferred to nitrocellulose membrane (LiCor) in transfer buffer for 1 h, 300 V. The membrane was blocked with 5 % blocking buffer for either 1h at room temperature or overnight at 4 °C. Following that, the membrane was incubated overnight at 4 °C with rabbit anti-ERp27, which was raised against the purified protein, rabbit anti-ERp57, mouse anti-His 1/5000 (Proteintech 66005), or rabbit anti-CRT 1/1000 (Stressgen SPA-600) antibodies. After 3 washes (5 min each) with TBST, the membrane was then incubated with either rabbit 800 or mouse 800 secondary antibodies diluted 1/5000 or 1/10,000. After 3 washes (5min each) with dH₂O the membrane was scanned using an Odyssey Sa scanner.

2.14 Immunoprecipitation technique

Cell lysate was prepared by lysing the cells in 200 µl of lysis buffer containing (1 % Triton X100, 50 mM Tris buffer pH 8, 150 mM NaCl, 5 mM EDTA, protease inhibitor cocktail). After 5 min incubation on ice, nuclei and large debris were removed by centrifugation. Immunoprecipitations were carried out using cell lysis buffer and specific antibody. Cell lysates were precleared by incubating with Protein A Sepharose. Aliquots of the precleared lysate were incubated with a specific antibody either monoclonal V5 1/1000 (Invitrogen) or V5 agarose beads (Sigma) overnight at 4 °C. Immunoisolates were washed 3 times with immunoprecipitation buffer (50 mM Tris-HCl pH 7.5, 1 % Triton X-100, 150 mM NaCl, 2 mM EDTA, 0.5 mM PMSF, 0.02 % Na-azide). Immunoisolates were then boiled with electrophoresis sample buffer containing 2 % SDS.

2.15 Transient and stable transfections

Mammalian cells were transfected using transfection reagents; PEI, MegaTran (TT200002 MegaTran 1.0 (0.5 ml) Generon), or Lipofectamine 2000 for 24 h.

2.16 *In cellulo* protein cross-linking

HT1080 cells in adherent culture were treated with 0.5 mM BMH (Pierce) at 37 °C. After that, the cross-linker was quenched with 10 mM DTT. Subsequently, the cells were lysed and V5 tagged ERp57 was immunisolated prior SDS-PAGE and immunoblotted.

In other experiments, we used ERp57-WT cells in adherent culture which were treated with either 0.5 mM BMH (Pierce) or 1 mM DSP (Pierce) at room temperature. The reaction was quenched with 10 mM DTT or 10 mM Tris/HCL buffer pH 7.5. Following that, cells were lysed and V5-tagged ERp57 as well as myc-tagged ERp27 were detected by immunoblotting.

2.17 Mass spectrometry following DTT elution of substrate-trapped mixed disulphide

Eight 15 cm dishes of HT1080 cells or HT1080 cells expressing V5-tagged ERp57 were grown to confluence. Freshly made DSP (Pierce) cross-linking reagent was added to four of the dishes for 30 min at room temperature. The cross-linker was quenched with 10 mM Tris/HCL buffer before washing the cells for 5 min with ice-cold phosphate-buffered saline (PBS) containing 20 mM NEM. After that, any excess of PBS/25 mM NEM was removed and 1 ml of ice-cold lysis buffer [50 mM Tris pH 8.0, 1 % Triton X-100, 150 mM NaCl, 2 mM EDTA, 0.5 mM PMSF, 20 mM NEM and EDTA-free protease inhibitor cocktail (Roche)] was added to each dish for 5 min. Subsequently, the cells were scraped off the dishes (with or without treatment with cross-linker) and transferred to 15 ml falcon tubes. The cell lysates were incubated on ice for 20 min before being centrifuged for 20 min at top speed at 4 °C. The supernatant was transferred to a fresh tube (4 ml each in total). The supernatant was precleared using 10 % PAS (100 µl), 30 min at 4 °C. The samples were centrifuged at 3000 xg for 3 min and the supernatant transferred to a fresh 15 ml tube. Anti-V5 agarose beads (75 µl) (Sigma) were added to the supernatant and samples were incubated overnight at 4 °C on a rocker. The samples were centrifuged at 3000 xg for 3 min, the supernatant was removed, and the beads transferred to a 1.5 ml microfuge tube. The beads were washed 3 times with 500 µl washing buffer (50 mM Tris/HCL pH 8.0, 1 % Triton X-100, 150 mM NaCl, 2 mM EDTA, 0.5 mM PMSF, 0.02 %

sodium azide). The beads were incubated with freshly made 10 mM DTT (200 μ l) for 10 min at room temperature to elute the cross-linked proteins. Ice-cold 12 % TCA (800 μ l) was added to the DTT-elute and kept on ice for 10 min. The sample was centrifuged at 15,000 xg for 20 min then the supernatant was removed, leaving a small pellet visible at the bottom of the tube. Ice-cold acetone (500 μ l) was added and then the tube was centrifuged at 15,000 xg for 10 min. This wash step was repeated 3 times. Subsequently the acetone was completely removed, and the pellet allowed to air-dry for 10 min before adding 50 μ l of 25 μ M ammonium bicarbonate. Finally, the samples were dispatched for LC/MSMS analysis at the University of St. Andrews or the University of Glasgow Polyomics facility.

3 Protein expression and purification, *In vitro* protein interaction by isothermal titration calorimetry (ITC)

3.1 Introduction

ERp27 is a non-catalytic human PDI family member that was identified and characterised by the Ruddock group (Frickel et al., 2002). It is a 27.7 kDa endoplasmic reticulum (ER) protein. ERp27 gene expression was analysed and it was found to be expressed in various human tissues such as; kidney, lungs, spleen, thymus, bone marrow and highly expressed in the pancreas (Alanen et al., 2006, Kober et al., 2013, Lash et al., 2000).

Human ERp27 homology with the b' domains homologous to the PDI protein has been highlighted (Alanen et al., 2006, Amin et al., 2013) as well as other PDI family members. ERp27 and PDI have the highest homology (33.5 %) (Alanen et al., 2006, Okumura et al., 2015) in contrast to other family members such as; ERp57 (16.5 %), PDIp (28.1 %). ERp29 is another non-catalytic member of the PDI family did not show any significant homology with ERp27 (Alanen et al., 2006).

Biophysical analysis of mature ERp27 was carried out to characterise protein function. ERp27 (Glu²⁶-Leu²⁷³) as well as the isolated domain 1 of ERp27 (Glu²⁶-Leu¹⁴¹) both with N-terminal his tags, were expressed in *E. coli* then proteins were purified by a combination of both metal affinity and ion-exchange chromatography. Analysis of the mass of the purified protein by matrix-assisted laser desorption/ionization MALDI-MS, an ionisation technique that uses laser energy to absorbing matrix to create ions from large molecules to tiny fragments, gave a mass of 28,838.9 Da for His-tagged ERp27 and for the His-tagged domain 1 construct the mass was 13,795.9 Da. Purified ERp27 then was evaluated by various approaches such as far-UV CD (Alanen et al., 2006).

An investigation of ERp27 peptide binding capability was carried out. Since there is a considerable degree of homology between the b' domain of ERp27 and the PDI b' domain they were both tested for binding a 14-residue peptide, Δ -somatostatin, by applying a cross-linking assay. The b' domains of ERp27 and PDI were shown to bind the peptide and the interaction was hydrophobic (Alanen et al., 2006, Amin et al., 2013).

ERp27 has been reported to interact *in vitro* with the oxidoreductase ERp57, which is a well-known member of the PDI family. The interaction was investigated by applying a cross-linking approach which revealed that ERp57 has the ability to bind either ERp27 or

the lectin calreticulin-P domain at the same binding site (Alanen et al., 2006, Frickel et al., 2002, Wijeyesakere et al., 2011). However, an interaction between ERp27 and the CRT-P domain was not observed nor was an interaction between ERp27 and PDI (Alanen et al., 2006).

The peptide-binding site of the b' domain of human PDI was shown to be within a hydrophobic pocket mainly containing the side chains of Leu²⁵⁹, Leu²⁶¹, Phe²⁷⁵, and Ile²⁸⁹. To identify the calreticulin interaction site within ERp57 an alignment of the b' domains of human PDI and ERp57 was carried out. The corresponding residues in ERp27 (Leu¹⁶⁶, Met¹⁶⁸, Tyr¹⁸², and Ile¹⁹⁶) were indicated to be semi-conserved suggesting that the peptide binding site location might be the same in both proteins.

To test this hypothesis, mutants were made in the ERp27 residues, the proteins expressed and tested for binding the 14 residue Δ -somatostatin peptide. Results indicated that mutations in both Met¹⁶⁸(M168W) and Ile¹⁹⁶(I196A, I196L, and I196W) decreased the peptide-binding site significantly. A small decrease in the binding was noticed with Y182W and no change was shown with L166W mutant compared to the wild type protein. The Ile-196 mutation has shown the greatest effect on peptide binding. The site was found to be consistent between PDI and ERp57, which revealed that a greatest effect on the peptide binding site with the homologous residues in PDI (Ile²⁸⁹, and Phe²⁹⁹). However, no discernible effects of these mutations was observed on the protein structure (Alanen et al., 2006).

An ERp27 mutant, which prevents peptide binding as well as mutants of the ERp27 b' domain, within the region homologous to the CRT/ERp57 binding site (DEWD), were used to study the interaction between ERp27 and ERp57. Results revealed that the ERp27 peptide-binding site mutants can still form cross-links with ERp57 suggesting that this site is not involved in their binding. However, ERp27 cross-links with ERp27 containing mutations within the DEWD site were very much reduced. Consequently, this implies that ERp57 binds both ERp27 and CRT-P domain at the same site (Alanen et al., 2006) and that the ERp27 peptide binding site is not required for its interaction with ERp57. ERp29 was found to form a complex with the lectin CRT with a similar affinity to CRT interaction with ERp57 suggesting a competition with CRT for binding ERp57 (Sakono et al., 2014).

Since the cross-linking results demonstrating an interaction between ERp27 and ERp57 were relatively poor it was further investigated by Nuclear Magnetic Resonance Spectroscopy (2D NMR). The NMR approach was applied to study the interaction and to find out if it is mediated by the b'-like domain. ^1H and ^{15}N heteronuclear single-quantum coherence (HSQC) spectra were collected for both domain 1 and the full length ERp27 labelled with ^{15}N . Unlabelled ERp57 addition to domain 1 of ERp27 did not affect the interaction. Consequently, no peak shift was recognised. However, addition of unlabelled ERp57 to the full length ERp27 resulted in significant changes in the ERp27 spectrum. That suggested a tight binding of ERp57 to ERp27 via the b'-like domain (Alanen et al., 2006).

These findings have raised the following questions;

- 1- Does ERp27 compete with CRT P-domain for binding ERp57?
- 2- If so, does ERp27 bring non-glycosylated protein to ERp57 to fold just as CNX/CRT brings glycoproteins to ERp57 to fold?

Accordingly, the aims of this part of the project are;

- 1- To study the interaction between ERp27 and ERp57 both *in vitro* and *in cellulo* (mammalian cells).
- 2- To compare the interaction between ERp57 and ERp27 or CRT to determine if there is a competition between ERp27 and CRT-P domain for binding ERp57.

To be able to achieve the aims and discuss the interplay between the three proteins, (ERp27, ERp57, and the soluble lectin CRT) protein expression and purification plus protein-protein interaction *in vitro* assays were carried out. The following proteins were expressed for further study: ERp27 WT, ERp27-I196W mutant, (which blocks the client protein binding site), ERp27-E231K mutant, (which had been previously shown to prevent binding to ERp57). ERp57 WT was also expressed and purified. Mutagenesis of ERp57 was carried out to mutate Arginine (Arg, R 282) into Alanine (Ala, A), which blocks the CRT binding site. The protein was then expressed and purified for further work.

Calreticulin was sub-cloned into the RSFDuet-1 vector (3829 bp) which is designed to co-express target proteins in *E. coli* and to produce native unfused or fused protein to His tag and sequences for detection and purification of protein complexes. After successfully sub

cloning, CRT was expressed on its own and purified for protein binding studies. Once we obtained sufficient amounts of all purified proteins other experiments were carried out to probe the interaction between ERp27 and ERp57. Additionally, an antibody to the purified ERp27 was raised and characterised against ERp27 expressed in different mammalian cell lines.

3.2 Results

3.3 Protein expression and purification

The following results were obtained from a series of experiments to express and purify ERp27-WT and two mutants; ERp27-I196W and ERp27-E231K. ERp57 WT was also expressed and purified as well as the mutant ERp57-R282A to enable its interaction with ERp27-WT to be studied. Calreticulin-WT was also expressed and purified to examine the interaction with ERp57-WT and furthermore to compare between the interaction of ERp57-WT with ERp27 or calreticulin by carrying out *in vitro* protein-protein interaction assays. In addition, an antibody to purified recombinant ERp27-WT was successfully raised to allow characterisation of its expression in a variety of different mammalian cell-lines.

3.3.1 ERp27-WT expression and purification

This experiment was carried out to produce purified protein for binding studies. Initially, the plasmid was transformed in the presence of the antibiotic required for expression using BL21 (DE3) *E. coli* bacterial strain competent cells that are compatible with Isopropyl-1-thio- β -D-galactopyranoside IPTG induction for high-level expression. A single colony was picked for making 1 l bacterial culture using lysogeny broth (LB), which was incubated for 2-3 h at 37 °C in a shaking incubator. An aliquot (1 ml) of the culture was taken out before induction (non-induced fraction) and kept at room-temperature. The remaining culture was induced with 1 mM IPTG then transferred to another shaking incubator at 16-22 °C overnight. An aliquot (1 ml) of the induced culture was taken and both non-induced and induced samples were then prepared to be loaded on a SDS-PAGE. SDS sample buffer was added to both samples, heated up to 105 °C for 5 min before being separated by SDS-PAGE and stained with Coomassie blue. It was noticed that ERp27-WT expression was leaky. Consequently, BL21 (DE3) PLYS strain competent cells were used which are known for ability to prevent leaky expression. However, there was no expression in this case. LB broth did not show any difference before and after induction. Subsequently, terrific broth (TB) and auto induction media (AI) were used to assess protein expression. It was noticed that expression did improve using AI. Finally,

protein was expressed in TB broth, however, it was difficult to conclude whether expression has taken place as the signal was quite diffuse as shown in (Fig 3.1A). To verify that the protein was expressed a western blot was carried out using anti-His antibody which confirmed ERp27 expression (Fig 3.1B) where a single protein band at the correct size (27 kDa) was observed (indicated with an arrow). At this stage, it can be concluded that ERp27 has successfully expressed.

Following expression, cells were pelleted at 10,000 rpm for 25 min at 4 °C. Pellets were re-suspended in 1/10th volume of buffer (50 mM NaH₂PO₄ buffer, pH 8.0 containing 300 mM NaCl, 5 mM imidazole). After that, cells were lysed for protein purification using a French pressure cell press. Cells were added into the cylinder where they undergo high pressure and are squeezed through a valve. During passage, cells experience decompression and shear stress resulting in cellular disruption. Once the lysate was obtained it was filtered through a 0.45 µM filter and the protein was purified using a nickel agarose affinity chromatography column which was equilibrated beforehand with His Buffer A, pH 8.0, and has the ability to bind His-tagged protein. The protein was washed with His Buffer A, (containing 5 mM imidazole, 300 mM NaCl) before the His-tagged protein was eluted using a linear gradient of 5-500 mM imidazole (Fig 3.1C, fractions 7, 8, 9).

At this point, the protein was partially purified containing several contaminants. The fractions containing ERp27 were combined and concentrated to 1 ml then purified further using gel filtration chromatography column Superdex 200 as an addition purification step to remove contaminated protein. The gel filtration column was equilibrated with 50 mM Tris buffer pH 7.5, containing 150 mM NaCl prior loading 1 ml protein sample. A typical elution profile is presented in Fig 3.1D. Although most contaminants were removed, the presence of high molecular weight proteins was noticed, which suggested that ERp27 might have the ability to form aggregates at higher concentration. Western blotting was carried out using anti-His antibody confirming that these higher molecular bands were ERp27 (Fig 3.1E). Subsequently, as an attempt to remove those aggregates, we carried out ultra-centrifugation. Two protein samples were prepared in which one was centrifuged at 100K rpm for 30 min and the other one was not. Both fractions were checked by SDS-PAGE then stained by Coomassie blue (Fig. 3.1F). The centrifuged fraction 3 showed little difference compared to fraction 2. Hence, the protein was successfully, purified with a

high yield (2 mg/l) but contained some aggregates as a minor contaminant. Some of the purified protein was then used as an antigen to raise a polyclonal antibody to ERp27-WT in rabbits. Initially, the protein was freeze-dried where the solvent sublimates from solid phase to gas phase directly. This procedure has four main steps. First, pre-treatment which can vary depends on its requirements for freeze-dry. In this case, the protein was concentrated prior to freeze-drying. Secondly, freezing-phase, the most critical stage of the entire process where the protein was placed in a flask inside a shell-freezer where the process took place. Thirdly, primary drying phase, the sample experienced low pressure and elevated temperature for sublimation. Almost 95 % of the water in the sample is sublimated. Finally, secondary drying phase where the temperature is raised higher than the previous stage almost above 0 °C aiming to remove any unfrozen water left after the primary drying. Once this operation was complete the freeze-dried protein was sent out to a special lab for antibody production. The rest of the protein was combined, aliquoted then snap frozen in liquid nitrogen and stored in – 80 °C to be used in future assays.

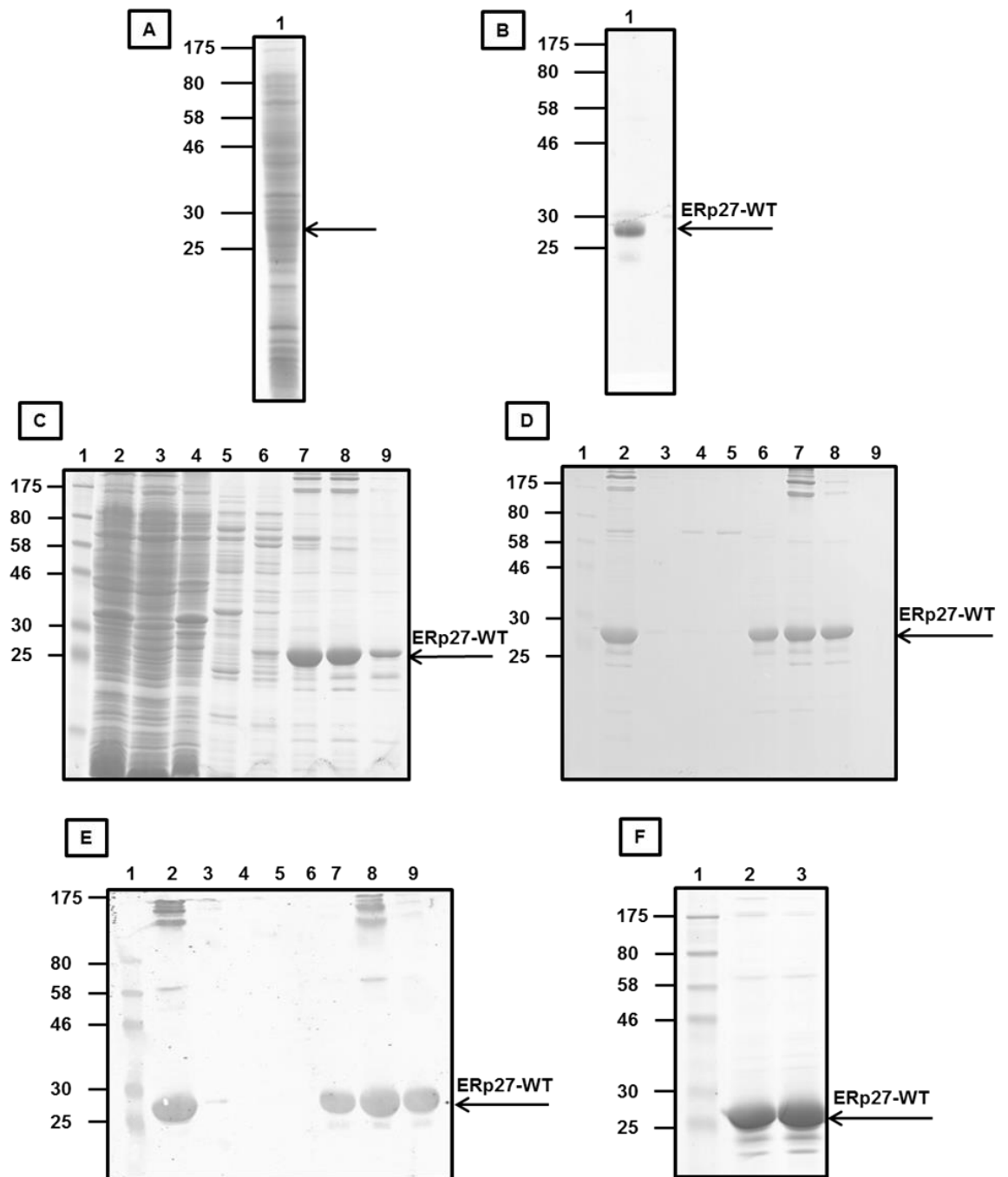


Figure 3.1, ERp27-WT expression and purification.

A, Coomassie-stained gel of *E. coli* BL21 (DE3) cell lysate from the ERp27-WT transfectants. **B**, western blot using anti-His antibody of *E. coli* lysate separated as in A. **C**, Coomassie-stained gel of fractions eluting from a nickel agarose affinity chromatography column. Arrow indicates a major band at 27 kDa most likely ERp27. **D**, Coomassie-stained gel of fractions eluting from a gel filtration column. Lanes 6, 7, 8 are the purified ERp27-WT. **E**, western blot using anti-His antibody. Lanes 7, 8, 9 are the purified ERp27-WT. **F**, Coomassie-stained gel of ERp27-WT ultra-centrifugation at 100K rpm for 30 min. Lane 2 is non-centrifuged fraction and lane 3 is centrifuged fraction.

3.3.2 ERp27-I196W expression and purification

Similar to the WT protein this experiment was carried out to produce purified protein for binding studies. The expression was examined under different conditions where two fractions of *E. coli* proteins were separated by SDS-PAGE and stained with Coomassie blue. The total cellular proteins were analysed either before or after induction with 1 mM IPTG (Fig. 3.2A, compare fractions 1 and 2). Both fractions contained a protein at 27 kDa; however, the induced fraction showed a stronger protein band at 27 kDa compared to the non-induced sample. A nickel agarose affinity column was used for the same purification method as the wild type protein. His tagged protein was bound to the column and eluted with imidazole (Fig. 3.2B, fractions 6, 7, 8, 9). However, contaminants were co purified with ERp27. To achieve a better separation of ERp27 from the contaminants a fresh purification was carried out with a gradient elution from the nickel agarose chromatography column with (5-500 mM) imidazole. Subsequently, ERp27 was separated from the contaminants more efficiently (Fig. 3.2C). The purification then was repeated demonstrating reproducibility of the protocol (Fig. 3.2D, fractions, 2, 3, 4, 5, 6). Although the purification of the eluted fractions was partially successful, the output still contained some additional proteins, so another polishing step was carried out using a gel filtration column. This column successfully purified ERp27 (Fig. 3.2E) with high yield (3.5 mg/l) and the purified fractions were then combined, aliquoted and stored at – 80 °C for future work.

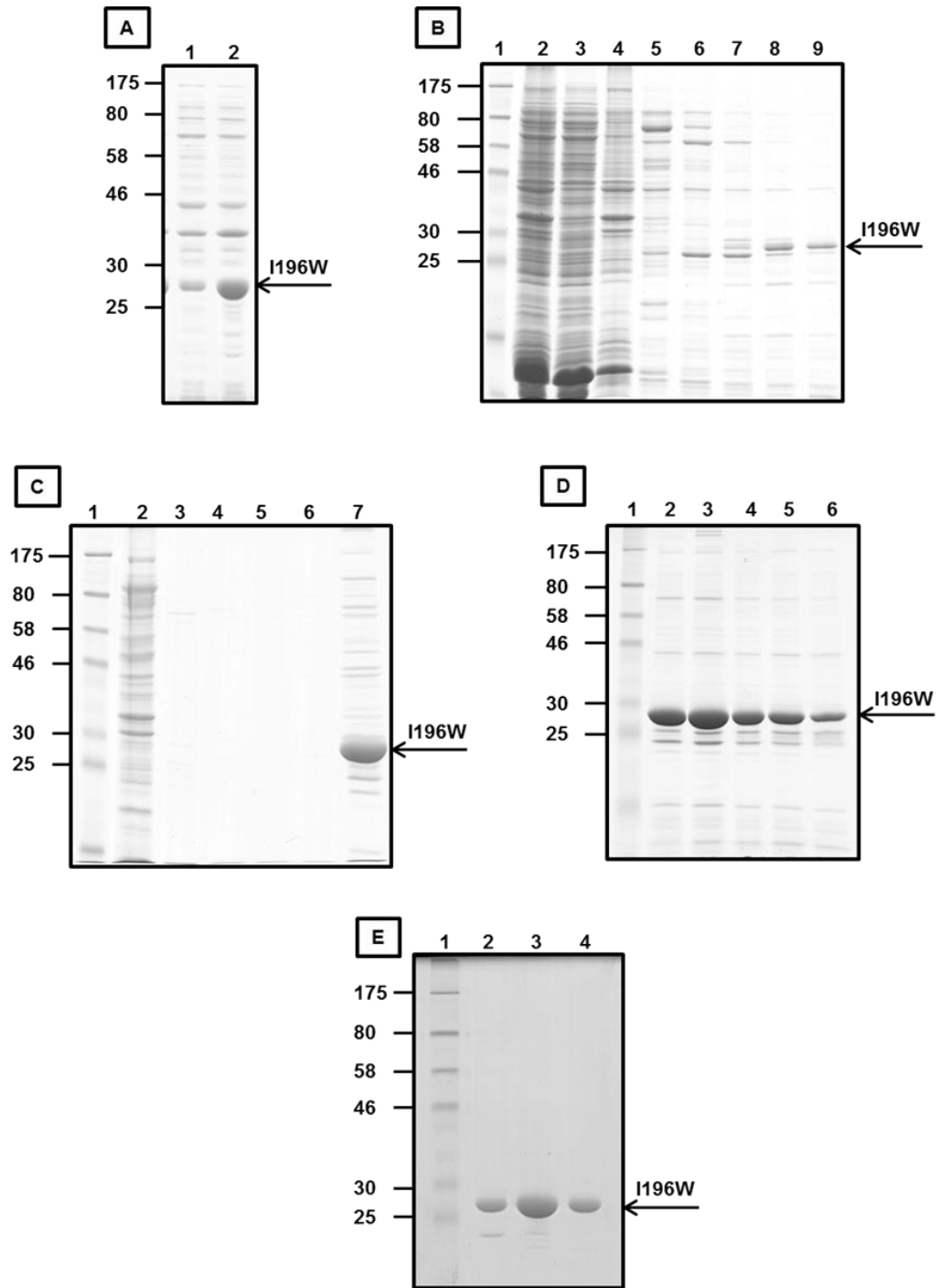


Figure 3.2, ERp27-I196W expression and purification.

A, Coomassie-stained gel of an *E. coli* BL21 (DE3) cell lysate from ERp27-I196W transfectants. Lane 1, non-induced, Lane 2, induced with 1 mM IPTG. **B**, Coomassie-stained gel of fractions eluted from a nickel agarose affinity chromatography column. Lanes 1, 2, 3, 4, 5, contain flow-through, Lanes 6, 7, 8, 9, contain ERp27-I196W. **C**, Coomassie-stained gel of fraction eluted from a nickel agarose affinity chromatography column. The purification was carried out with a linear gradient 5-500 mM imidazole. Lane 1, contains flow-through, Lanes 2, 3, 4, 5, 6, contain flow-through, Lane 7, contains ERp27-I196W. **D**, Coomassie-stained gel of fractions eluted from a nickel agarose affinity chromatography column. Lanes 1, 2, 3, 4, 5, 6, contain ERp27-I196W. **E**, Coomassie-stained gel of fractions eluted from a gel filtration column. Lanes 1, 2, 3, 4, are the purified ERp27-I196W.

3.3.3 ERp27-E231K expression and purification

Similar to the previous approach, two cultures of *E. coli* transformed with ERp27-E231K were tested under different conditions in which the first was non-induced whereas the second was induced with 1 mM IPTG to assess protein expression. *E. coli* proteins were separated by SDS-PAGE and visualised using Coomassie blue staining (Fig. 3.3A). It was noticed that the induced fraction provided higher expression compared to the non-induced fraction and the protein bands appeared at about 27 kDa. Following the expression test, protein purification was carried out by a nickel agarose affinity column. The protein was eluted with an imidazole gradient (5-500 mM) with ERp27 as indicated in fractions 4, 5, 6, 7 (Fig. 3.3B). Unfortunately, the purification gave a different outcome compared to the previous protein purifications as the protein peaks did not separate and the purity was low. However, the purification was taken further by ion-exchange chromatography to remove the contaminants. Samples were concentrated as for gel filtration to a final volume of 1 ml using centrifugal concentrators. The protein was then diluted by 5 ml of ion exchange buffer A (50 mM Tris buffer, pH 7.5 containing 10 mM NaCl), and centrifuged at 3000 xg for 20 min before loading it onto HiTrap Capto Q (anion exchange) 1 ml column (GE Healthcare). The protein was eluted with ion exchange buffer B (50 mM Tris buffer pH 7.5, containing 1 M NaCl). Eluted fractions were separated by SDS-PAGE and protein was visualised using silver staining. As shown in Fig. 3.3C the protein was effectively purified. After that, a fresh purification was carried out. As indicated in Fig. 3.3D the protein bound to the column and was eluted in fractions 5, 6, 7, 8, 9. At this stage the protein was still contaminated, and the purification needed to be taken further but this time through gel filtration instead of ion-exchange (Fig. 3.3E). The protein was purified but similar to the wild type, higher molecular bands appeared which suggested this protein has the tendency to form aggregates at high concentration. To remove these aggregates, ultra-centrifugation took place. As suggested in Fig. 3.3F, by comparing non-centrifuged with centrifuged fractions, it appears that there was no significant change. At this point of the purification the protein was partially purified with a high yield (3.5 mg/l) with some minor aggregation. Fractions were combined, aliquoted, snap-frozen and stored at -80°C for future assays.

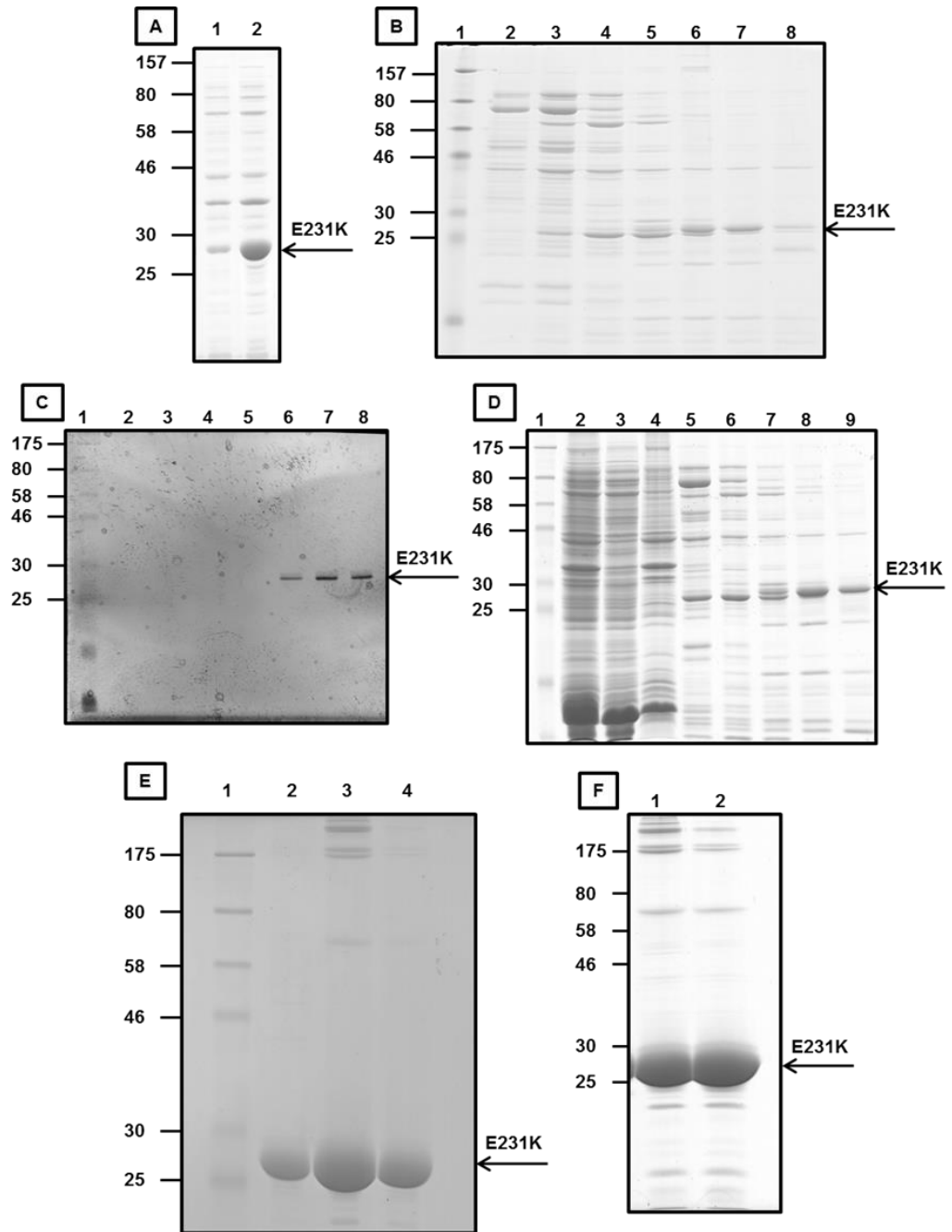


Figure 3.3, ERp27-E231K expression and purification.

A, Coomassie-stained gel of *E. coli* BL21 (DE3) cell lysate from the ERp27-E231K transfectants. Lane 1 is non-induced, and Lane 2 is induced with 1 mM IPTG. **B**, Coomassie-stained gel of fractions eluting from a nickel agarose affinity chromatography column, protein was eluted with linear gradient 5-500 mM imidazole. Lanes, 4, 5, 6, 7, contain ERp27-E231K. **C**, silver stained gel of fractions eluting from an ion-exchange column. Lanes, 6, 7, 8, are the purified protein. **D**, Coomassie-stained gel of fractions eluting from a nickel agarose affinity chromatography column, protein was eluted with a linear gradient 5-500 mM imidazole. Lanes, 5, 6, 7, 8, 9, are ERp27-E231K. **E**, Coomassie-stained gel of fractions eluting from a gel filtration column. Lanes, 2, 3, 4, are the purified ERp27-E231K. **F**, Coomassie-stained gel of ERp27-E231K ultra-centrifugation at 100K rpm for 30 min. Lane 1 is non-centrifuged fraction and lane 2 is the centrifuged fraction.

3.3.4 ERp57-WT expression and purification

This protein purification was carried out to produce enough protein for biochemical assays. Protein expression was tested following cell lysis and separation of ERp57 protein by SDS-PAGE. As shown in (Fig 3.4A) fraction 2 is non-induced while fraction 3 is induced by 1 mM IPTG. Coomassie blue staining confirmed protein expression with a clear band at 57 kDa representing ERp57. A western blot was carried out using an anti His antibody which confirmed protein expression after IPTG induction (Fig 3.4B). ERp57 was then purified using nickel agarose affinity chromatography. The protein was bound by the column and eluted with an imidazole gradient (5-500 mM) in fractions 7, 8, 9, 10 (Fig 3.4C). At this point, contaminants were still present so a further separation of the proteins by gel filtration chromatography was carried out. The protein was eluted in fractions 5, 6, 7, 8 (Fig 3.4D). Purification was successful, and the protein yield obtained was 4 mg/l. The purified fractions were combined, aliquoted, snap-frozen in liquid nitrogen and stored at – 80 °C for future work.

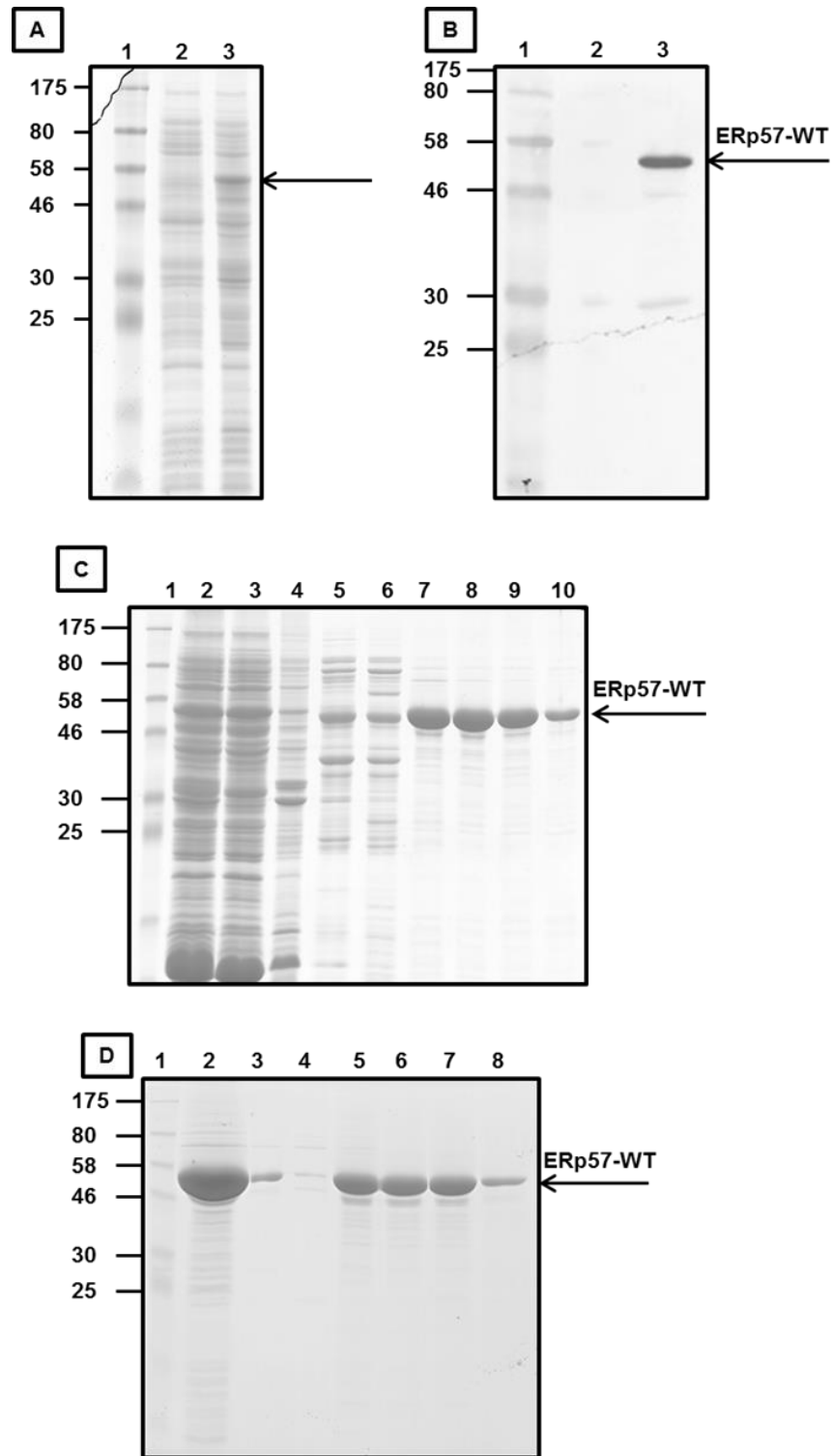


Figure 3.4, ERp57-WT expression and purification.

A, Coomassie-stained gel of an *E. coli* BL21 (DE3) cell lysate from ERp57-WT transfectants. Lane 2, is non-induced ERp57-WT, lane 3, is induced. **B**, western blot using anti-His antibody of *E. coli* lysate separated as in A, lane 3, ERp57-WT. **C**, Coomassie-stained gel of fractions eluting from a nickel agarose affinity chromatography column. Lanes 7, 8, 9, 10 contain ERp57-WT. **D**, Coomassie-stained gel of fractions eluting from a gel filtration column. Lanes, 5, 6, 7, 8, are the purified ERp57-WT.

3.3.5 ERp27-antibody testing

As ERp27-WT was successfully purified, it was then freeze-dried and sent out for antibody production as mentioned earlier. Two rabbits were injected to produce antibodies. Upon receiving the first bleeds of the antibody it was tested on several cell lines for its ability to recognise ERp27 in mammalian cells. A series of western blots were carried out on a variety of cell lines including; HT1080, HEK 293, CHOS and Panc1 as well as HT1080 cells expressing exogenous ERp27-WT or ERp27-E231K. First bleeds were tested on all cell lines except Panc1. The majority produced negative outcomes however; ERp27-WT and ERp27-E231K cell lines provided positive results. The ERp27-E231K data is presented here as it represents the clearest results (Fig. 3.5). Lane 1 (Fig. 3.5A) represents 1X dilution and lane 2 is 10X dilution of ERp27-E231K cell line lysate. Both were tested by immunoblotting using the ERp27 antibody and as indicated in lane 1 there was a strong signal around 30 kDa as well as some non-specific bands at higher molecular weight. Accordingly, we stripped and re-probed the same blot with anti-myc antibody (mouse monoclonal) as a positive control as the exogenously expressed protein contains a myc-tag (Fig. 3.5B). The anti-myc antibody confirmed that the raised polyclonal ERp27 antibody recognised ERp27 which is abundant in lane 1 compared to lane 2. By overlaying (Fig. 3.5A) and (Fig. 3.5B), we could see that the signal from ERp27 antibody overlaid with the signal from the anti-myc antibody as indicated by yellow bands at the same size (Fig. 3.5C). Furthermore, additional experiments were carried out upon receiving the final bleed on ERp27-WT and the Panc1 cell lines. Positive outcomes were obtained from ERp27-WT cell line however; the Panc1 cell line was negative. The conclusion that was drawn at this point is, first bleeds were shown to function positively by recognising ERp27 although it gave negative results with the majority of the tested cell lines suggesting a limited amount of ERp27 in these cell-lines.

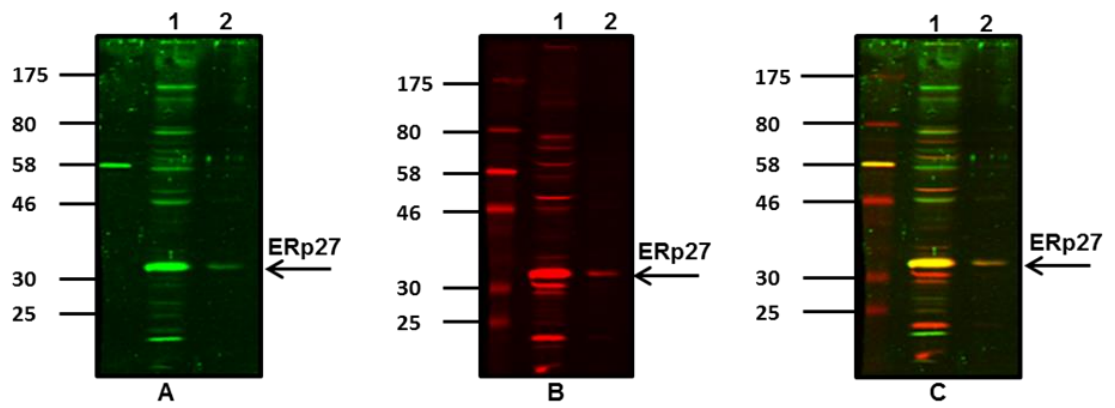


Figure 3.5, ERp27 anti body testing on ERp27-E231K cell line.

A, western blot using anti-ERp27 antibody. Lanes 1, 1X dilution and 2, 10X dilution of ERp27 lysate. **B**, western blot using anti-myc antibody. Lanes 1, 1X dilution and 2, 10X dilution of ERp27 lysate. **C**, overlaying gel of A and B showing signals from both ERp27 antibody and anti-myc antibody as yellow bands.

3.3.6 Calreticulin WT expression and purification

This purification was carried out to produce adequate CRT for binding studies. Two fractions of *E. coli* lysates were separated by SDS-PAGE and visualised by Coomassie blue stain (Fig 3.6A) where lane 1 is non-induced and lane 2 is induced. It was noticed that the protein was abundant within the induced sample and major induced protein migrated at 57 kDa. The lysate was loaded onto a nickel agarose affinity column. Bound protein was eluted, separated by SDS-PAGE and visualised by Coomassie blue stain (Fig 3.6B).

Fractions 2, 3, 4, and 5 contain CRT. As the protein still contains some contaminants it was purified further by gel filtration chromatography (Fig 3.6C). Fractions 1, 2, 3, 4, 5, and 6 contain CRT-WT. The protein at this stage was relatively pure with a good yield (5 mg/l). Fractions containing the purified protein were then combined, aliquoted, snap-frozen by liquid nitrogen and stored for future assays.

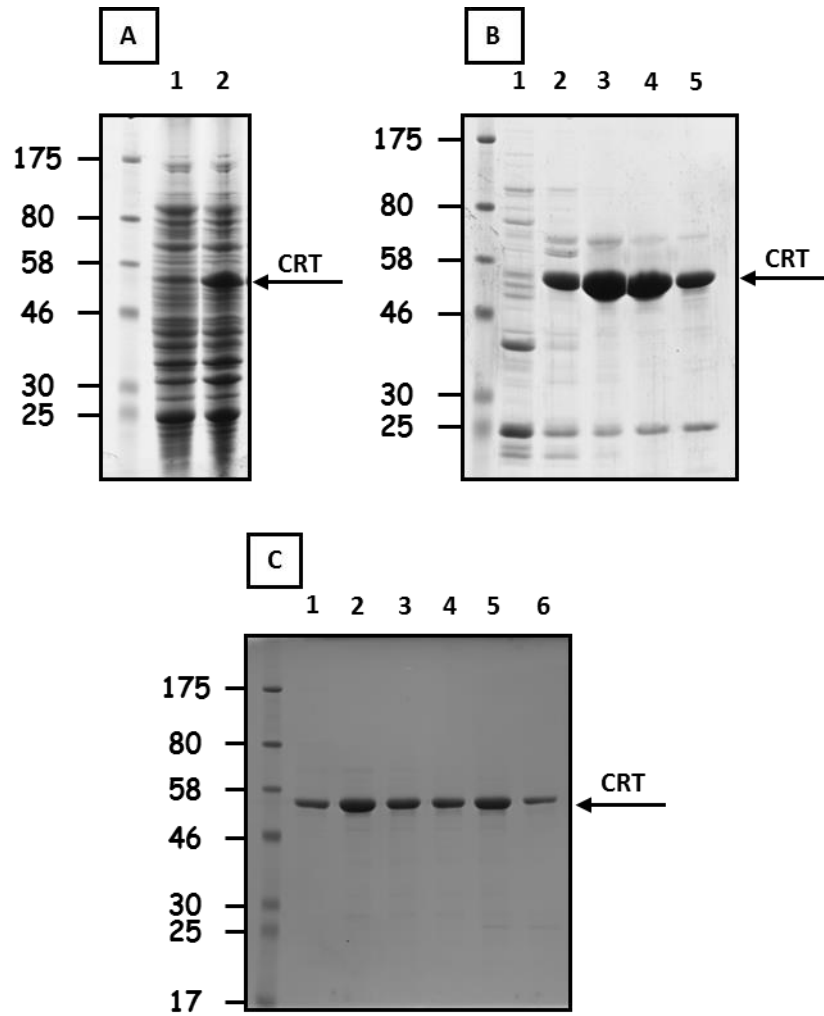


Figure 3.6, Calreticulin-WT (CRT) expression and purification.

A, Coomassie-stained gel of fractions eluting from a nickel agarose chromatography column. Lanes 2, 3, 4, 5 are purified CRT. **B**, Coomassie-stained gel of fractions eluting from a gel filtration column. Lanes, 1, 2, 3, 4, 5, and 6 are the purified CRT.

3.3.7 ERp57-R282A expression and purification

This experiment was designed as previous experiments to express and purify the protein for binding studies. *E. coli* proteins were checked by SDS-PAGE then analysed and visualised by Coomassie blue stain. The first purification step was by Nickel agarose affinity chromatography. The protein bound to the column was eluted with imidazole gradient (5-500 mM). Fractions 2, 3, 4, 5, and 6 (Fig. 3.7A) containing ERp57-R282A were combined and concentrated as explained earlier for further purification. Gel filtration chromatography was carried out as a further purification step as shown in (Fig. 3.7B) where fractions 7, 8, 9, 10, 11, and 12 contain the purified ERp57-R282A with a yield of (6 mg/l). The protein was combined, aliquoted, and snaps frozen and stored at -80°C .

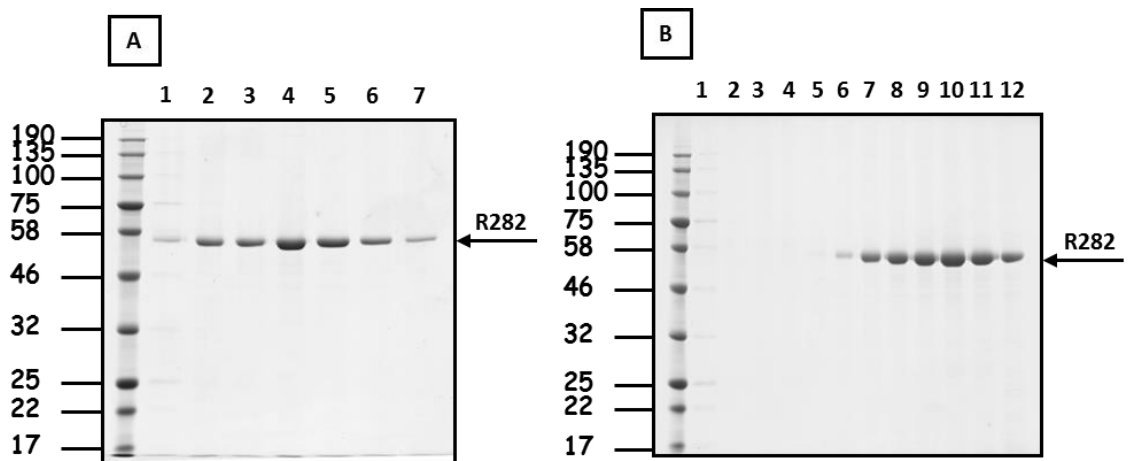


Figure 3.7, ERp57-R282A expression and purification.

A, Coomassie-stained gel of an *E. coli* cells BL21 (DE3) lysate from ERp57-R282A transfectants. Lane 1, none induced ERp57-R282A, lane 2, induced. **B**, Coomassie-stained gel of fractions eluting from a nickel agarose chromatography column. Lanes 1, 2, 3, 4, 5, 6, and 7 contain contaminant ERp57-R282A. **C**, Coomassie-stained gel of fractions eluting from a gel filtration column. Lanes, 6, 7, 8, 9, 10, 11, and 12 are the purified ERp57-R282A.

3.4 Isothermal titration calorimetry ITC

After obtaining a good yield of all the wild type proteins and their mutants some *in vitro* assays were carried out to assess protein-protein interaction. Isothermal titration calorimetry (ITC) a physical technique which determines a direct measurement of the thermodynamic parameters of interactions in solution. It is usually used to investigate interactions between small molecules like medicinal compounds and larger molecules such as proteins. The device consists of a sample cell that contains the macromolecule, the reference cell which contain water or buffer as a direct comparison to the sample cell as well as a syringe that holds the ligand particles that is titrated into the sample cell. As the first injection is made, the macromolecules will bind to the ligand generating heat that appears as a spike signal. The spike will return to the baseline before the next injection. The more injections the more binding occurs between macromolecules and ligands. Consequently, more heat is generated, and signals appear. Once they reach saturation no more interaction takes place and accordingly no heat change occurs. By applying this technique, it is intended to investigate the binding affinity between ERp27-WT and ERp57-WT then compare it to ERp57-WT and CRT binding affinity that has been determined previously by (Frickel et al., 2002) where protein samples of ERp57 and CRT (189-288) were prepared, purified and filtered into a buffer containing 25 mM Tris HCl, pH 7.0 and 10 mM β -mercaptoethanol. Protein concentration were measured after gel filtration. ERp57 (0.2 mM) was loaded into the cell. The protocol comprises 24 12 μ l injections of 0.2 mM CRT (189-288) where the duration was 10 secs allowing 5 min between injections for equilibration. The stirring rate was 200 rpm. At the end of the experiment data were analysed based on 1:1 binding model.

Our samples were prepared for ITC as follows. In the first attempt, proteins were purified and polished by gel filtration chromatography in 50 mM HEPES pH 7.5 containing 150 mM NaCl and 1 mM TCEP. The concentration obtained following gel filtration were; 13.43 μ M ERp57, 43.67 μ M ERp27, and 55.21 μ M CRT. Prior ITC samples were concentrated using (Satorius, Vivaspin 6, membrane 10,000 Mw) and centrifuged at 3000 xg for 30 min at 4 °C as an attempt to achieve a concentration compatible for the ITC device (300 μ l of 10-20 μ M for the cell and 100 μ l of 200 μ M for the syringe).

Following that, samples were dialysed using dialysis buffer (50 mM HEPES pH 7.5 containing 150 mM NaCl and 1 mM TCEP) as the protein and the ligand must be in identical buffers to avoid false heat masking the heat of interaction. Proteins were spun down for 5 min to remove precipitates before injection of their estimated concentrations after this centrifugation were; 7.44 μ M ERp57 and 29.27 μ M ERp27. ERp27 was then titrated into ERp57. Following subtraction of the appropriate heats of dilution control experiments gave no evidence of interaction (Fig 3.8A). Thereafter, ERp57 was injected into CRT. The first few injections showed evidence of heat of interaction (Fig, 3.8B). The K_D between CRT and ERp57 was calculated to be 0.26 μ M +/- 0.8 μ M.

As ERp27/ERp57 interaction did not show any heat generation more attempts were carried out by purifying both proteins and concentrating them close enough to the required concentration for binding, however, the desired concentration was never obtained. In addition, the experiment was repeated using the same buffer used previously (Frickel et al., 2002). Samples were dialysed for 2 days at 4 °C before injection. Unfortunately, the ERp27 concentration was not suitable for ITC and the experiment could not be repeated. The ERp57 and CRT binding experiment was repeated regardless of the ERp57 low concentration of 7.44 μ M. CRT was diluted to 100 μ l for this repeat experiment. The heats were extremely small due to the very low concentration of ERp57 (Fig, 3.8C). The stoichiometry of binding was also less than one which may reflect changes of concentrations. The negative values of enthalpy and entropy suggested that CRT/ERp57 binding is favourable and might be driven by hydrogen and hydrophobic interactions. The K_D of this interaction is 0.429 μ M +/- 1.8 μ M.

This set of experiments were carried out in a chemistry lab where the instrument gives an association constant value K_A which is the favoured parameter for chemists. However, as biochemists we prefer to report in terms of dissociation constant K_D which was calculated according to this equation: $K_D = [P]_{free} [L]_{free} / [PL] = 1 / K_A$. This explains the difference between the K values on the graph and in the text and figure legend.

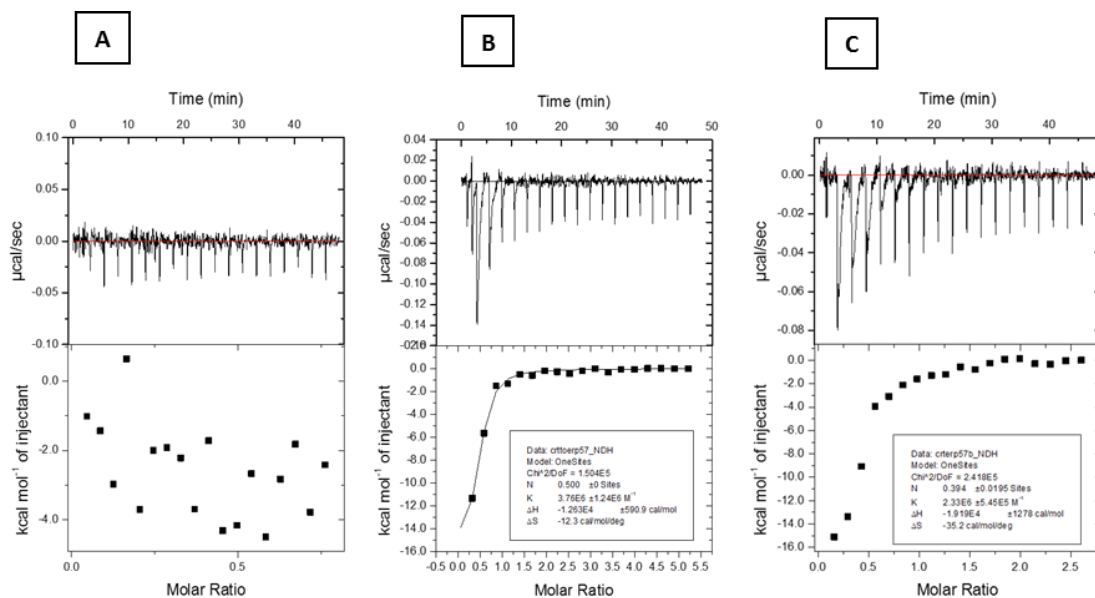


Figure 3.8, Isothermal titration calorimetry (ITC).

Binding isotherm describing the formation of, **A**, The interaction between ERp27 (29.27 μM) and ERp57 (7.44 μM). The signal is scattered, and no interaction observed due to the low concentration of both proteins. **B**, The formation of CRT (>200 μM) and ERp57 (7.44 μM) complex. The signal of the heat change and the sigmoidal curve have indicated the tight binding between the two proteins, The K_D obtained is (0.26 μM). **C**, A repeat of the interaction between CRT and ERp57. The K_D obtained is (0.429 μM).

3.5 Discussion

This first chapter aimed to produce sufficient recombinant protein for ERp27, ERp57, CRT and mutants thereof for further interaction studies. The purifications were successful providing protein at sufficient yield for future work. A leaky expression was experienced when expressing ERp27-WT. As an attempt to overcome that issue PLYS cells were used instead of BL21 (DE3) cells which are a bacterial strain that limits leaky protein expression. Unfortunately, expression was not successful. The following option was to assess other types of media for protein expression; terrific broth (TB) and auto induction (AI) were used. TB broth showed the best expression with BL21 (DE3) competent cells when induced with 1 mM IPTG at 16-22 °C overnight compared to both AI culture and LB broth which were used initially. As soon as that matter was solved it was applied to the rest of the proteins. ERp27-WT and ERp27-E231K both have the tendency to form aggregates at high concentration. These accumulations appeared as bands at higher molecular weight after proteins were polished by gel filtration column. It is thought that aggregation occurs because of the high concentration of the protein obtained after purification and by diluting the protein those higher bands might be removed. As an attempt to remove those aggregates, an ultra-centrifugation was carried out at 100K rpm for 30 min however no significant change was noticed post centrifugation. It was suggested to take the purification further by running another gel filtration column which might remove these higher bands. Yet, proteins were sufficiently purified at this point for use in other molecular assays.

Our ITC results between CRT and ERp57 has confirmed their interaction and the K_D is 0.26 μM +/- 0.8 μM . However, given that the concentration of CRT was found to be 3.6-fold higher than expected (i.e. 200 μM) it was advisable to repeat this experiment using a CRT concentration between 75-100 μM so that the reaction is not saturated within the first 2-3 injections in addition to increasing ERp57 concentration in the cell. Consequently, another attempt was carried out however the heat change were extremely small due to the very low concentration of ERp57. The stoichiometry of binding was also less than one which may reflect changes of concentrations. The negative values of enthalpy and entropy suggested that CRT/ERp57 binding is favourable and might be driven by hydrogen and hydrophobic interactions. The K_D of the second run is 0.429 μM +/- 1.8 μM . Ideally;

we should aim to increase the ERp57 concentration in the cell to improve the accuracy of heat detection. As a comparison, the Ellgaard group have studied CRT (189-288)/ERp57 interaction. The NMR results proved the binding between those proteins and characterised CRT P-domain as the binding site for ERp57. Further investigation determined the thermodynamic stability of the interaction. The K_D values obtained by ITC and TROSY-NMR are; $9.1 \pm 3.0 \mu\text{M}$ at 8°C and $18 \pm 5 \mu\text{M}$ at 20°C , respectively (Frickel et al., 2002).

Moreover, the ITC results of ERp27/ERp57 interaction did not show any heat generation due to the low concentration for both proteins. More purification and concentration attempts were carried out for both proteins, however during sample preparation, obtaining more concentrated proteins using centrifugal concentrator was difficult. It was noticed that after exceeding certain concentration ERp27 and ERp57 started to aggregate, probably due to the intrinsic insolubility of both proteins. It was suggested that an exact buffer match followed by an extensive dialysis should preclude heats of ionisation. Consequently, the experiment was repeated with the same buffer from published work (Frickel et al., 2002). Samples were dialysed for 2 days at 4°C before injection. Unfortunately, the ERp27 concentration was still lower than the ITC requirements and accordingly could not be repeated. However, that does not mean there is no interaction taking place between ERp27 and ERp57, but it could not be detected.

The Ruddock group have looked at ERp27/ERp57 binding by applying various techniques including 2D NMR and cross-linking assays. The 2D NMR results show a very tight binding between ERp27 and ERp57 after comparing $^1\text{H}/^{15}\text{N}$ HSQC spectra for domain 1 and the full length ^{15}N labelled ERp27. In the presence of a small excess of unlabelled ERp57 no peak shifts were observed with domain 1 but significant peak shifts were determined with the full length ERp27 which confirmed the tight binding between ERp27 and ERp57 (Alanen et al., 2006). Additionally, the ERp27 b' domain was found to be conserved with the PDI b' domain and similarly bound the 14 peptide, Δ -somatostatin. This fact suggested a possible interaction between ERp27 and a wide range of unfolded or partially folded polypeptides. It was also found that the loop between β_4 and β_5 in ERp27, which has the sequence of Asp-Glu-Trp-Asp. Similar motif was also found within the CRT P-domain which has the ability to bind ERp57. It was speculated that ERp57 can also bind ERp27 via this loop. Furthermore, cross-linking results have revealed that ERp57 can form cross-

links with either the ERp27 or CRT P-domain under certain conditions. As ERp57 binds to both motifs on the CRT P-domain and ERp27 using the same binding site on its b' domain it is not possible to bind them simultaneously. Moreover, since ERp57 is involved with the (ER) resident lectins CNX and CRT for glycoprotein folding and in quality control, ERp27 overexpression might influence that binding or function or it may operate to bring non-glycosylated proteins to ERp57 to fold, just as N-glycosylated substrates are brought to ERp57 by CNX and CRT to fold. Nevertheless, it is still unknown under what conditions or physiological circumstances the ERp57/ERp27 interaction happens. Interaction was not observed between ERp27 and PDI or between ERp27 and CRT P-domain (Alanen et al., 2006). In those experiments, the ERp27/ERp57 interaction was investigated using cross-linking assays and will be discussed in the next results chapter.

With regard to the raised polyclonal anti body to the purified ERp27-WT, first bleeds from both rabbits have been shown to successfully recognise ERp27 in some transfected cell lines, specifically ERp27-WT and ERp27-E231K cell lines. However, they produced negative results with the cell lines HEK 293, and CHOS suggesting these cell lines have limited amounts of ERp27. Final bleeds were tested only on ERp27-WT and the Panc1 (pancreas/duct) cell line which was provided by Dr. Karen Cosgrove, University of Manchester. It has been reported previously that the pancreas has the highest levels of ERp27 (Kober et al., 2013, Lash et al., 2000). Yet ERp27 might not be expressed in this particular cell line so other pancreas cell lines were investigated. The MIN6 Cell line (which was supplied by Dr. Kevin Docherty) University of Aberdeen, was tested. Initially this cell line needed special media to grow and while growing it was recognised that cells are growing in clusters and possibly vertically rather than horizontally. A cell lysate was made and tested with ERp27 antibody. Unfortunately, ERp27 was not recognised within this cell line either.

4 *In vitro* and *in cellulo* protein-protein interaction by cross-linking assay

4.1 Introduction

The oxidoreductase ERp57 is a PDI enzyme that is known for its significant role in catalysing isomerisation of non-native disulphide bonds in glycoproteins (Frasconi et al., 2012). It operates as a chaperone, disulphide isomerase, and oxidoreductase together with calnexin and calreticulin. It is also considered an effective factor in the CNX and CRT cycle (Williams, 2006). ERp57 has generally been known and referred to as a glycoprotein-specific oxidoreductase for its significant role in nascent glycoprotein folding when associated with CNX and CRT (Ellgaard and Frickel, 2003).

This interaction between ERp57 and the two endoplasmic reticulum resident lectins, CNX and CRT was previously investigated by a cross-linking assay in mammalian cells (Jessop et al., 2009a). ERp57 has also shown the ability of binding the non-glycosylated substrates such as viruses (Schelhaas et al., 2007) which suggests that ERp57 can function independently from the CNX and CRT cycle.

To determine the reasons why polyoma virus, simian virus 40 (SV40) uses an elaborate entry pathway and to define the possible roles of the ER in this process, the uncoating and the penetration of the SV40 virus were analysed. It was found that the ER route of entry allows SV40 to take advantage of the protein folding and quality control machinery in the ER before exploiting components of the ER-associated degradation (ERAD) to exit the ER lumen to the cytosol (Schelhaas et al., 2007).

The isomerisation of disulphide bonds within the interpentamer in the virus plays a significant role in the entry process. During ERp57 catalysed disulphide isomerisation reactions in the lumen of the ER, pentamers are disconnected from a large network of disulphide crosslinked virus protein 1 (VP1) molecules in the capsid, the initial step for uncoating SV40. It was indicated that the modified virus exploits the ERAD pathway as a way to cross to the cytosol by depending on PDI, Derlin-1, and Sel1L. The SV40 overall strategy was found to be similar to that of cholera toxin, however, more elaborate due to the particles structural complexity (Schelhaas et al., 2007, Tsai et al., 2001).

To establish whether ERp57 can form mixed disulphides when not associated with CNX and CRT, the interaction between ERp57/CNX/CRT was abolished using various mutations

of ERp57. Mixed disulphides between the enzyme and substrates can be trapped when the second cysteine of the CXXC active site on ERp57 is mutated into alanine. Subsequently, Arginine 282 within the b' domain of ERp57 was mutated into Alanine that abrogates the CRT binding site. Moreover, various stable cell lines were made which include; wild type ERp57, a single point mutant R282A, a double mutant Cys2,7 in which cysteines on both CXXC active sites are mutated into alanine CXXA as well as a triple mutant cys 2,7 R282A (Jessop et al., 2009a).

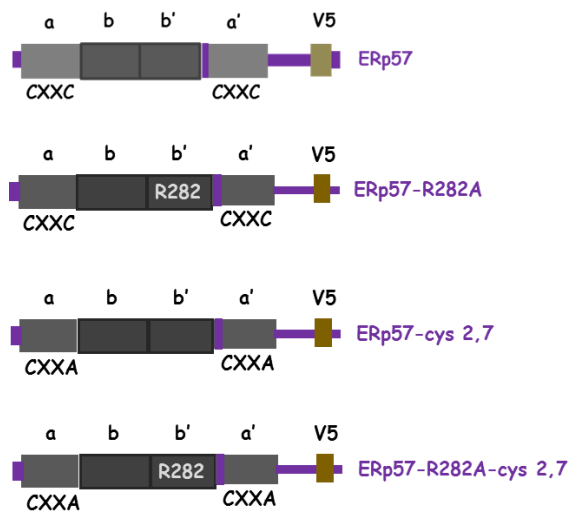


Figure 4.1, schematic diagram showing the domain structure of V5-tagged ERp57, single point mutant ERp57-R282, double mutant ERp57-cys 2,7, and triple mutant ERp57-cys 2,7-R282.

The diagram depicts the domain organisation of ERp57. The domains; a, b, b', and a' are indicated for ERp57 and all mutants.

A cross-linking agent was added to the transfected cells to verify that the R282A mutation stops complex formation between ERp57 and CNX/CRT. Cells were lysed and immunoprecipitated using the V5 antibody and then the immunoisolated material was separated by SDS-PAGE and visualised using either CNX or CRT antibodies by western blotting. Results revealed that cross-links were formed with both CNX and CRT within the wild type and cys 2,7 cells and it was noticed those complexes form to a lesser extent in the case of CNX.

Both lectins are absent in the un-transfected cells which confirmed ERp57 interaction specificity. Furthermore, no sign of interaction was detected with R282A or cys 2,7 R282A cells which means successful creation of stable cell lines of ERp57 that are not associated with either CNX or CRT but can form a mixed disulphide with substrate proteins (Jessop et al., 2009a).

ERp57 has also been shown to form complexes with the non-catalytic member of the PDI family ERp27. The b' domain of ERp27 contains a sequence of Asp-Glu-Trp-Asp similar to that on the P-domain of CRT which suggests that both ERp27 and CRT interact with ERp57 on the same binding site. This interaction of ERp57 with ERp27 was investigated by *in vitro* cross-linking.

Previous work has demonstrated that cross-links can be formed between the two wild type proteins. Complexes also formed between the client protein mutant of ERp27 and ERp57; however, the interaction between ERp27 and the CRT binding mutant of ERp57 was very much reduced. This suggests that ERp57 binds ERp27 using the same binding site for CRT. That was accordingly confirmed by the E231K mutant of ERp27 which dramatically reduced the interaction with ERp57 (Alanen et al., 2006).

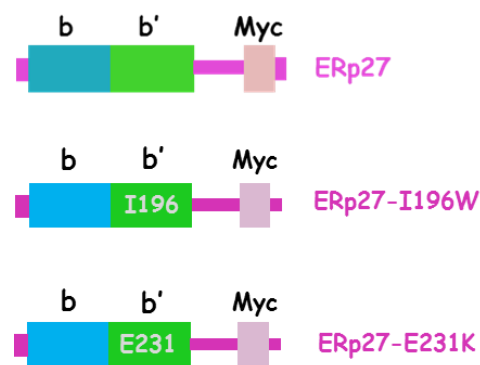


Figure 4.2, Schematic diagram showing the domain structure of Myc-tagged ERp27, ERp27-I196W, and ERp27-E231K.

The diagram depicts the domain organisation of ERp27 and both mutants. The domains; b, and b', are indicated for ERp27 as well as the mutants.

Our investigation of the interaction of ERp27 with ERp57 by isothermal titration calorimetry (ITC) was unsuccessful due to low protein concentrations. To study the interaction of ERp27 and ERp57 both *in vitro* and *in cellulo*, a biochemical assay, cross-linking, was used to establish if any interaction can be detected either in solution or within living cells and to compare ERp57 and ERp27 interaction to the ERp57 and CRT interaction. Purified proteins were used for the *in vitro* investigation while mammalian cells were used for the *in-cellulo* study.

4.2 Results

4.2.1 *In vitro* cross-linking

To investigate the formation of cross-links between purified proteins in solution, His-tagged recombinant proteins were expressed and purified and include; ERp27-WT, I196W and E231K mutants, ERp57-WT and R282A mutant, as well as calreticulin-WT (CRT) (Figures 4.4, 4.5 and 4.6). To determine the optimum concentration of the cross-linking agent to use, various concentrations of disuccinimidyl glutarate (DSG) were tested (0.02 mM, 0.01 mM, 0.2 mM, 0.1 mM, 1 mM, 2 mM, and 5mM). A 1 mM concentration of DSG was found to be the best. A 10 μ l cross-linking reaction was made as following; 3 μ g of each protein (worked out depending on protein concentration obtained after purification), 2 μ l of phosphate buffer pH 7.2, and dH₂O up to 10 μ l placed on ice for 10 min prior addition of 1 μ l of DSG. After addition of DSG, the reactions were placed at room temperature for 30 min. The reactions were stopped by adding SDS sample buffer, boiled at 105 °C for 5-10 min and then separated by SDS-PAGE under reducing conditions. Subsequently, a western blot was carried out to assess the presence of proteins and their complexes using different antibodies.

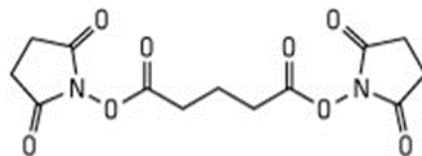


Figure 4.3, The chemical structure of the disuccinimidyl glutarate (DSG) cross-linking agent.

An anti-His western blot confirmed the presence of all proteins with and without DSG (Fig 4.4A). ERp27 protein bands appeared at 27 kDa (lanes 1, 4, 7-9 and 11), while ERp57-WT was observed at 57 kDa (lanes, 2, 5, and 7- 11). CRT bands migrated at about the same size as ERp57 at 57 kDa (lanes, 3, 6, 10, and 11). CRT bands were less evident compared to ERp27 and ERp57. However, it was apparent on later gels that CRT is abundant when probed with the CRT-antibody. That suggests that His-antibody is not able to recognise the His-tag on this particular protein. Cross-links formed between ERp27 and ERp57 at 84 kDa (Fig 4.4A, lane 7). The ERp27 mutants also engaged in complexes around 84 kDa. The I196W mutant confirmed that ERp27 does not require the peptide-binding site to interact with ERp57 (Fig 4.4A, lane 8). In addition, there was no effect of the E231K mutant on the

cross-links formed with ERp57 (Fig 4.4A, lane 9). This is different to what was found previously (Alanen et al., 2006) and suggests that the E231K does not prevent the interaction with ERp57 *in vitro*. High molecular bands were also observed between ERp27 wild type and both mutants with ERp57 (Fig 4.4A lanes 7-9)

The interaction between ERp57 and CRT was confirmed by a cross-linking product that appeared at about 100 kDa (Fig 4.4A, lane 10). Additionally, a competition experiment was carried out where ERp27, ERp57, and CRT were mixed together to establish if ERp27 would inhibit the interaction between ERp57 and CRT. A cross-linking product was observed between ERp57 and CRT around 100 kDa (Fig 4.4A lane, 11) which correspond to the cross-link in the absence of ERp27 (Fig 4.4A lane 10). In addition, no cross-links were observed between ERp27 and ERp57 within the same protein mixture using His antibody compared to the ERp27 and ERp57 western blots which suggest that His antibody cannot detect that specific signal due to its immunodetection and sensitivity.

An ERp27 western blot confirmed the cross-links between ERp27 and ERp57 around 84 kDa as well as the aggregates at higher molecular weight (Fig 4.4B, lanes 7- 9) which correspond to those cross-links seen with the anti His antibody (Fig 4.4A, lanes 7- 9). Additionally, a cross-link appeared at 84 kDa within the protein mixture (Fig 4.4B, lane 11) corresponding to those cross-links between ERp27 and ERp57 (Fig 4.4A, lanes 7- 9) suggesting that ERp27 has the potential to influence the ERp57 and CRT interaction. A western blot using an ERp57 antibody also verified cross-linking products of ERp57 with ERp27 around 84 kDa as well as the higher molecular weight bands (Fig 4.4C, lanes 7- 9) in addition to the complex at 100 kDa between ERp57 and CRT (Fig 4.4C, lanes 10 and 11). Similar to the ERp27 western blot, a cross-linking product appeared between ERp27 and ERp57 at 84 kDa (Fig 4.4C, lane 11) which corresponds to the cross-links of ERp27 and ERp57 (Fig 4.4B, lane 11). So, ERp57 interacts with ERp27 and CRT. The E231K mutant of ERp27 did not prevent the interaction with ERp57 in contrary to what was expected. Additionally, the peptide binding mutant of ERp27 is not required for the interaction with ERp57. Furthermore, ERp27 formed cross-links with ERp57 when mixed with CRT. That cross-link seemed stronger compared to the complex formed between ERp57 and CRT suggesting that ERp27 may be competing CRT for binding ERp57.

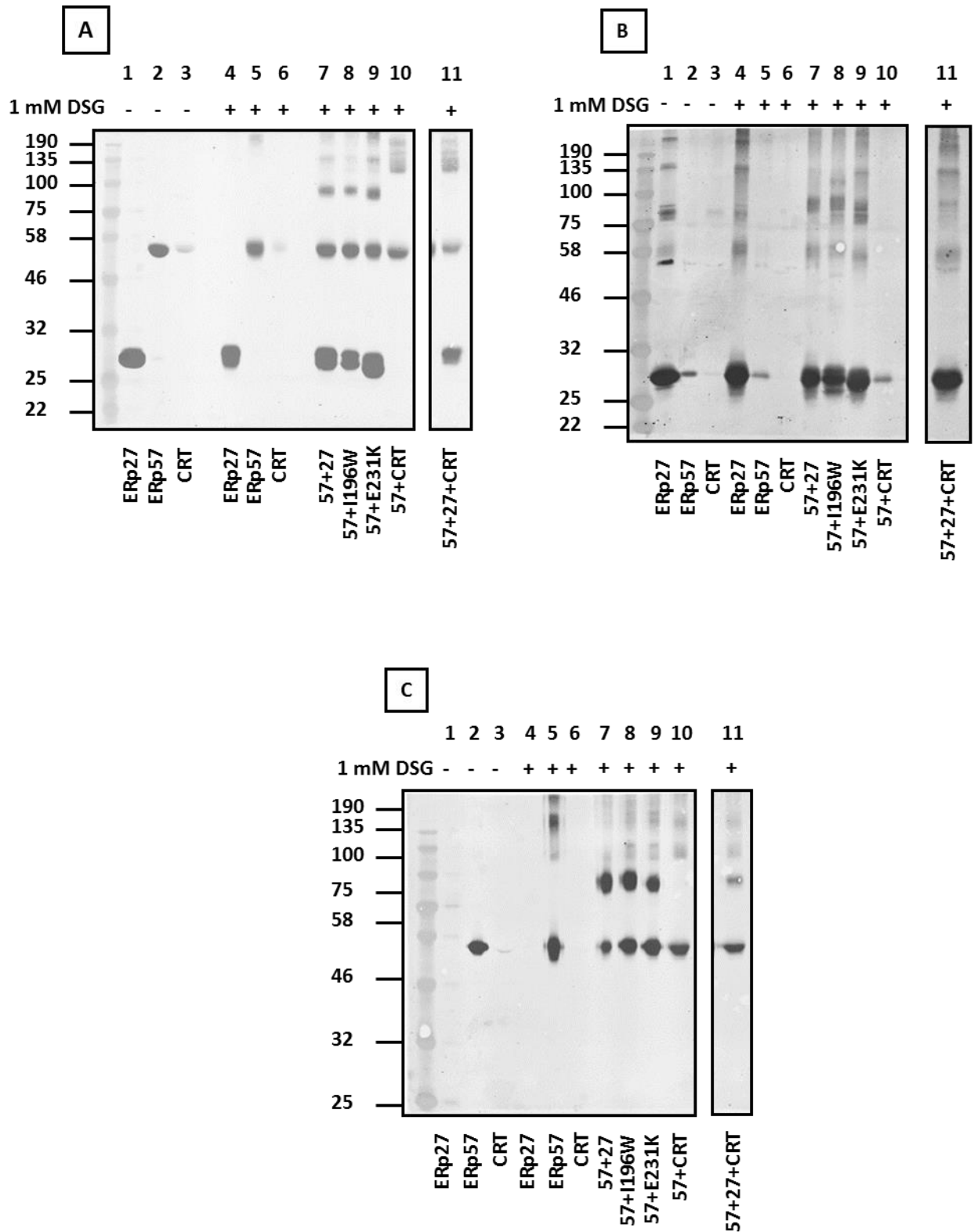


Figure 4.4, The interactions between ERp57 and ERp27 or ERp57 and CRT assessed by *in vitro* cross linking.

A representative western blot of *in vitro* cross-linking between purified protein components (all 3 μ g, ERp57-WT, ERp27-WT, ERp27-I196W, ERp27-E231K, and CRT) in 10 μ l of 0.2 M phosphate buffer, pH 7.2; 1 mM DSG, 30 min at room temperature. **A**, anti-His. **B**, anti-ERp27. **C**, anti-ERp57. Non-relevant lanes were cropped off the gels. (n = 8).

As the CRT concentration used in these experiments might be insufficient (Fig 4.4) its interaction with ERp57 was repeated as shown in (Fig 4.5). A western blot using a His-antibody showed ERp57-WT, and CRT at about 57 kDa (Fig 4.5A, lanes 2, 3, and 5- 11) though the intensities of protein bands vary between different lanes. Additionally, by comparing the anti-His to the anti-CRT western blots CRT seem to be abundant when probed with the CRT specific-antibody suggesting that His-tagged CRT is not detected by the His-antibody for some reason. The cross-linking products between ERp57-WT and CRT were observed around 100 kDa in the presence of DSG (Fig 4.5A, lane 10). CRT and ERp57 cross-links were also detected within the mixture of ERp57, ERp27, and CRT, which was made to investigate the effect of ERp27 on the ERp57/CRT complex (Fig 4.5A lane, 11). The cross-linking product formed between ERp57/CRT in Fig 4.5A lane 11 correspond to the cross-linking complex in Fig. 4.5A, lane 10. However, no cross-linking band for the ERp57 and ERp27 interaction was observed using the DSG cross-linker.

The same experiment was carried out using a CRT antibody and CRT was seen at 57 kDa (Fig 4.5B lanes, 3, 6, 10, and 11). A cross-linking product formed between ERp57 and CRT at 100 kDa (Fig 4.5B lanes, 10, and 11) which correspond to those cross-links formed in (Fig 4.5A lanes, 10 and 11). This confirms the interaction between ERp57 and CRT.

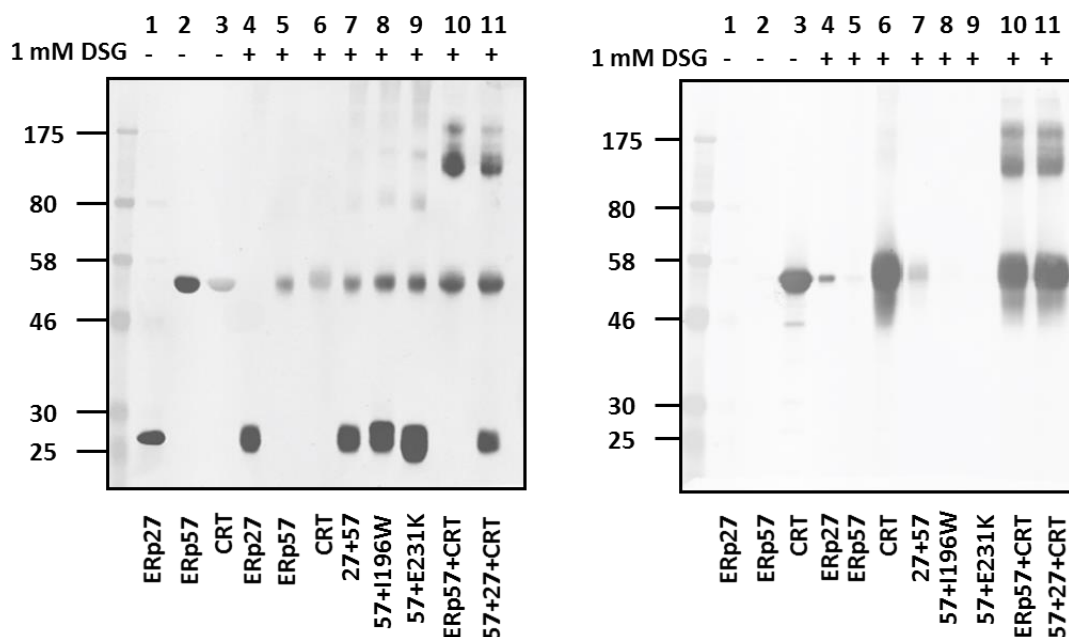


Figure 4.5, The interaction between ERp57 and CRT by *in vitro* cross linking.

A representative western blot of *in vitro* cross-linking between purified protein components (all 3 μ g, ERp57-WT, ERp27-WT, ERp27-I196W, ERp27-E231K, and CRT) in 10 μ l of 0.2 M phosphate buffer, pH 7.2; 1 mM DSG, 30 min at room temperature **A**, anti-His. **B**, anti-CRT. (n = 8).

A western blot using a His-antibody was carried out to determine the ability of the ERp57-R282A mutant to prevent binding to CRT (Fig 4.6A lanes, 5, 6, and 8). However, expression of the R282A protein was very low compared to ERp57-WT and CRT which migrate at 57 kDa (Fig 4.6A lanes, 1-4, and 7, 8). As seen before, the His-antibody did not recognise CRT and that may be because it cannot recognise the His-tag on this protein (Fig 4.6A).

However, when probed with the CRT-antibody it is obvious that the protein is abundant (Fig 4.6C). A cross-link was observed between ERp57 and CRT at 100 kDa (Fig 4.6A lane 7). ERp57-WT as well as ERp57-R282A were detected at 57 kDa when probed with an ERp57 antibody (Fig 4.6B lanes 1, 2, and 5-8) though ERp57-R282A expression was very low. A cross-link between ERp57 and CRT was seen at 100 kDa (Fig 4.6B lane 7) which corresponds to the cross-link in (Fig 4.6A lane 7); however, no cross-links were identified between ERp57-R282A and CRT (Fig 4.6B lane 8). An anti-CRT western blot has shown CRT bands at 57 kDa (Fig 4.6C lanes 3, 4, 7, and 8) in addition to cross-links with ERp57 at 100 kDa (Fig 4.6C lane 7). This has confirmed the interaction between ERp57 and CRT.

Unfortunately, due to the low levels of expression we could not determine using this approach whether the R282A mutation prevented ERp57 binding to calreticulin.

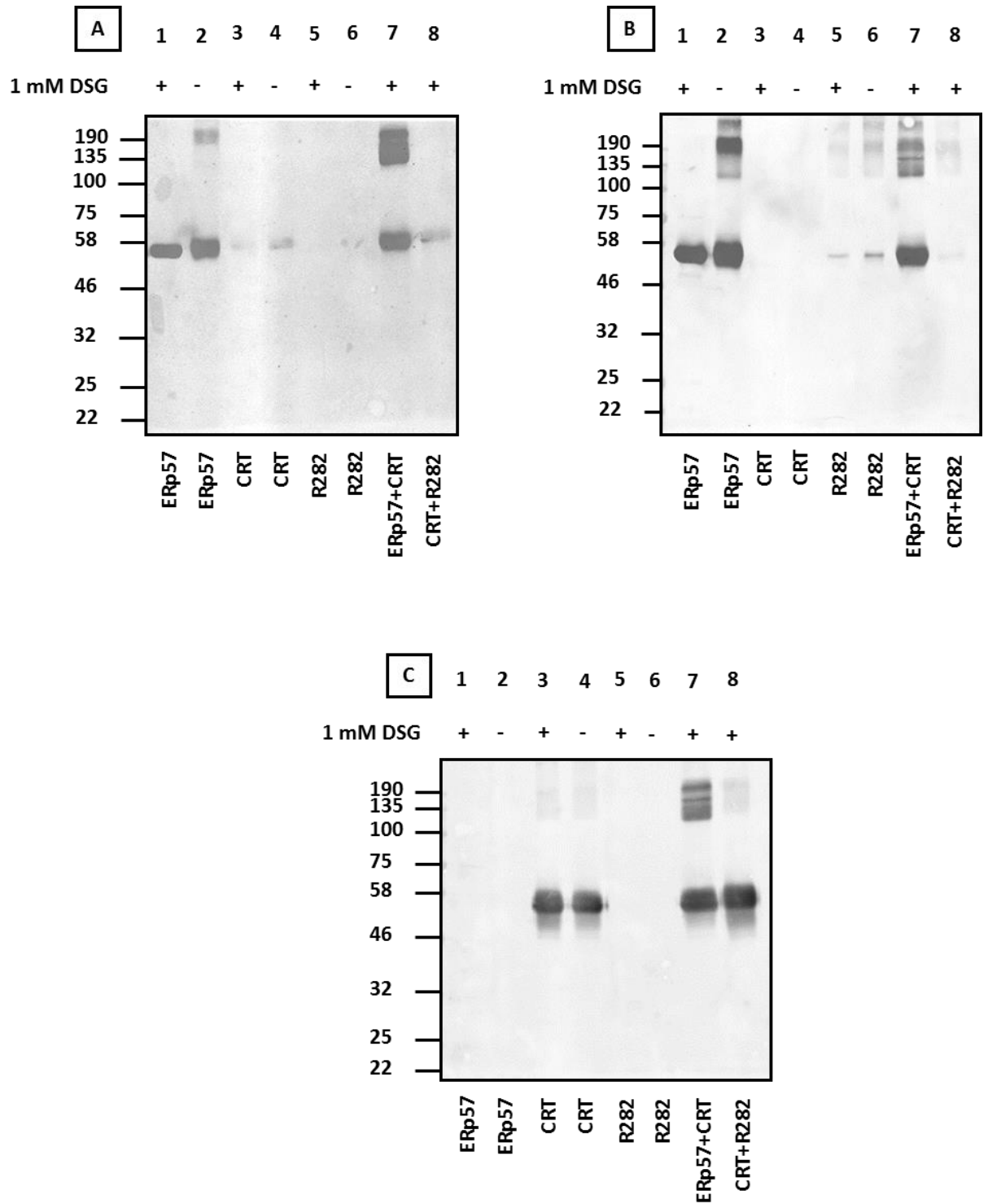


Figure 4.6, The interactions between ERp57 and CRT by *in vitro* cross linking.

A representative western blot of *in vitro* cross-linking between purified protein components (all 3 μ g, ERp57-WT, ERp57-R282A, and CRT) in 10 μ l of 0.2 M phosphate buffer, pH 7.2; 1 mM DSG, 30 min at room temperature. **A**, anti-His. **B**, anti-ERp57. **C**, anti-CRT. (n = 3).

4.2.2 *In cellular cross-linking*

The interaction between ERp57 and CRT was investigated in mammalian cells as done previously (Jessop et al., 2009a) to determine if it is occurring *in cellulo* as it is *in vitro*. V5-tagged wild type ERp57 as well as the R282A mutant were transfected into HT1080 cells. Myc-tagged ERp27 was co-transfected with ERp57-WT to determine if it will have any effect on the ERp57/CRT interaction. The cells were cross-linked with the non-cleavable sulfhydryl group specific cross-linking agent Bismaleimido-hexane (BMH) which was added to stabilise protein complexes.

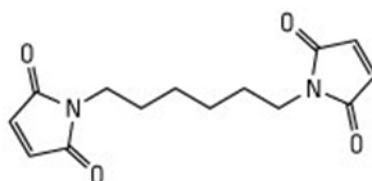


Figure 4.7, The chemical structure of the Bismaleimido-hexane (BMH) cross-linking agent.

The expressed V5-tagged ERp57 was immunoprecipitated and the immunisolated material was separated on reduced SDS-PAGE followed by a CRT western blot (Fig 4.8A). CRT was pulled down with ERp57 in the presence of BMH (Fig 4.8A lanes 2 and 4) and cross-links were also observed between CRT and ERp57 (lanes 2 and 4). ERp27 seems to enhance the immunisolation as stronger CRT and cross-links were observed in lane 4 compared to lane 2. Unlike ERp57-WT, CRT was not pulled down within the ERp57-R282A sample in the presence of BMH (Fig 4.8A lane 6) and consequently no cross-links formed. That has confirmed that the ERp57-R282A mutation prevents the interaction between ERp57 and CRT. This experiment was repeated and showed consistency (Fig 4.8B). However, a triplicate showed slightly different results (Fig 4.8C). The results taken together demonstrated that we could detect an interaction between exogenously expressed ERp57 and endogenous calreticulin using this cross-linking approach.

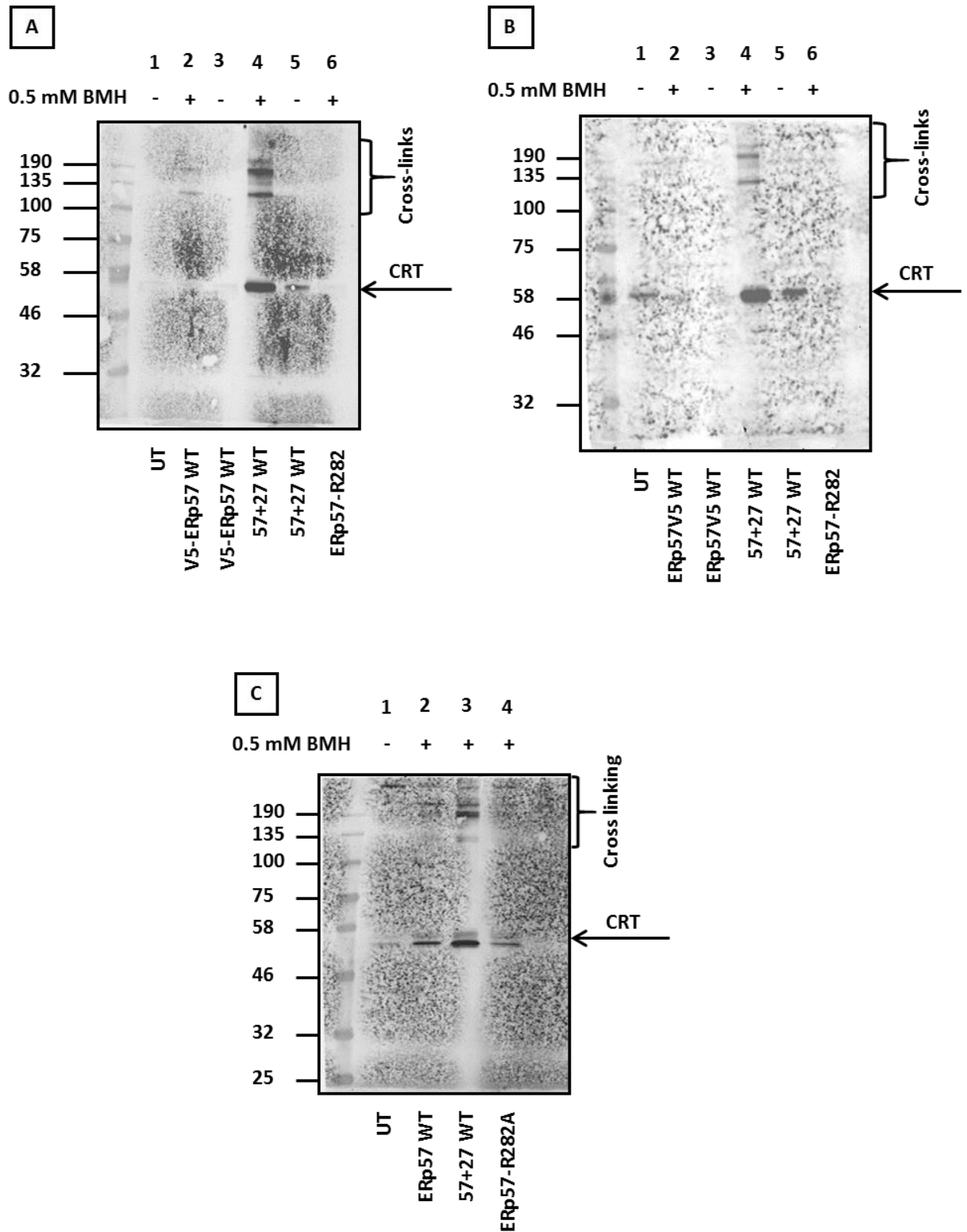


Figure 4.8, The interaction between ERp57 and CRT by *in-cellular* cross-linking and the R282A mutation in ERp57 abolishes the interaction with CRT.

A, HT1080 cells transfected with V5-tagged ERp57 (lanes 2- 6) as well as Myc-tagged ERp27 (lanes 4, and 5) or un-transfected (UT) cells (lane 1) were cross-linked with BMH and lysed, and the expressed V5-tagged ERp57 was immunisolated with V5-specific antibody. The immunisolated material was separated on a reducing SDS-PAGE gel, and CRT was identified following western blotting. **B and C**, are repeats. (n = 3).

To investigate the interaction between ERp57 and ERp27, V5-tagged ERp57 and Myc-tagged ERp27 constructs were co-transfected into HT1080 cells. Cells were co-transfected with ERp27 as the level of endogenous ERp27 was quite low in HT1080 cells (see chapter 3). Cells were cross-linked and lysed then lysates were analysed by reducing SDS-PAGE. The exogenously expressed proteins were detected by western blot using V5 and Myc antibodies (Fig 4.9). Proteins were expressed at 57 and 27 kDa, however, no cross-links were observed between ERp57 and ERp27. Interestingly, cross-links appeared within the ERp57 only fraction (Fig 4.9A lane 6). A Myc western blot showed a non-specific band around 100 kDa (Fig 4.9B) but cross-links were not observed.

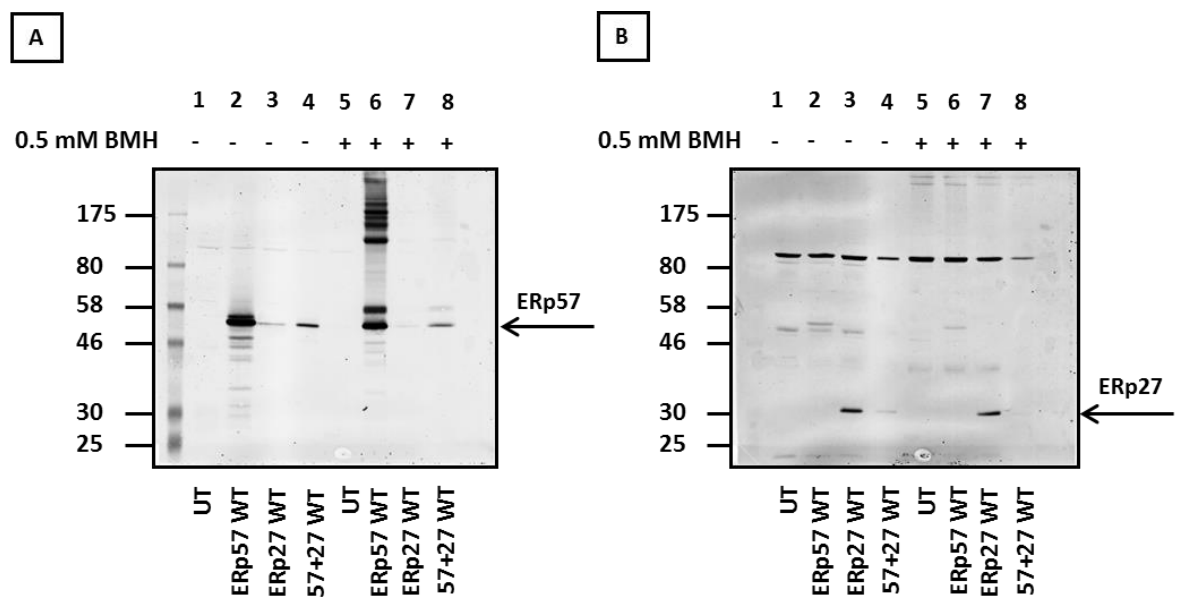


Figure 4.9, The interaction between ERp57 and ERp27 by *in-cellular* cross-linking.

HT1080 cells transfected with V5-tagged ERp57 (lanes 2, 4, 6, and 8) as well as Myc-tagged ERp27 (lanes 3, 4, 7, and 8) or un-transfected (UT) cells (lanes 1, and 5) were cross-linked with BMH and expression and cross-links were confirmed by western blotting using **A**, V5 specific antibody. **B**, Myc specific antibody. (n = 12).

A repeat was carried out and confirmed similar results (Fig 4.10 lanes, 3- 6).

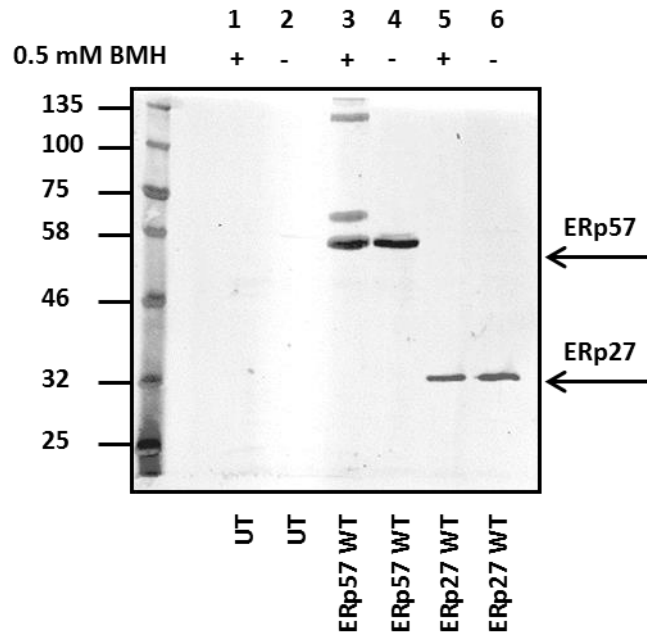


Figure 4.10, The interaction between ERp57 and ERp27 by *in cellular* cross-linking.

HT1080 cells transfected with V5-tagged ERp57 (lanes 3, and 4) and Myc-tagged ERp27 (lanes 5, and 6) or un-transfected (UT) cells (lanes 1, and 2) were cross-linked with BMH and lysed, then expression and cross-links were confirmed with V5 and Myc antibodies. (n = 3).

To avoid co-transfections as this could affect expression efficiency, transient transfection of either V5-tagged ERp57 or Myc-tagged ERp27 constructs was carried out using stable cells expressing either ERp57 or ERp27 to investigate the interaction between ERp57 and ERp27. First, Myc-tagged ERp27 constructs were transfected into V5-ERp57 stable cells, cross-linked, lysed, and then analysed by reducing SDS-PAGE gel (Fig 4.11). Protein expression was verified by anti-V5 and anti-Myc western blots. Protein bands were detected at 57 and 27 kDa but there was no evidence of protein-protein interaction (Fig 4.11, A and B). Non-specific bands were observed at 100 kDa when probed with an anti-Myc-antibody (Fig 4.11B). To confirm the lack of interaction, V5-ERp57 constructs were transiently transfected into Myc-ERp27 stable cells, cross-linked, and lysed, then separated on reducing SDS-PAGE. Expression and cross-links were verified by western blot using V5 and Myc antibodies.

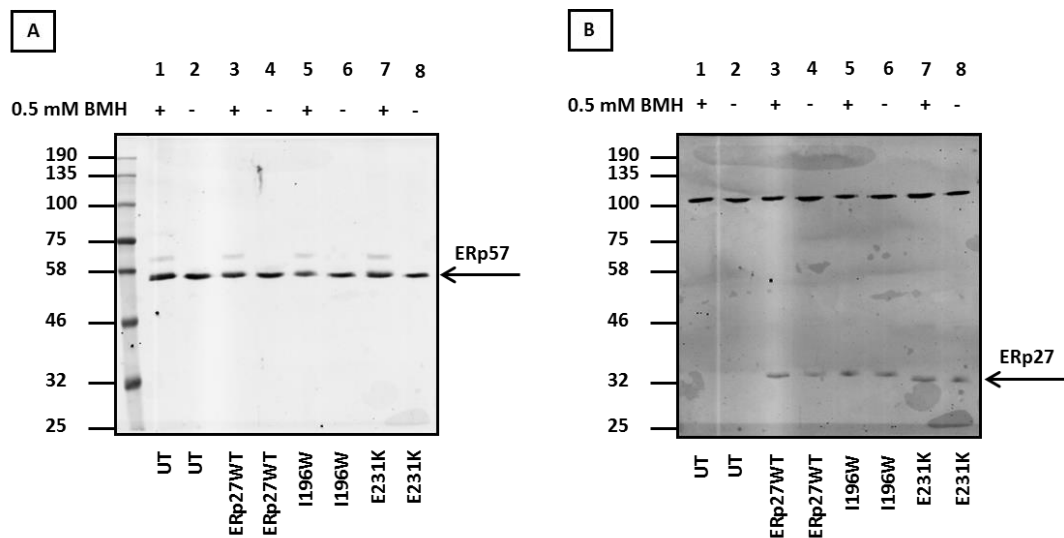


Figure 4.11, The interaction between ERp57 and ERp27 by *in cellular* cross-linking.

ERp57 stable cells expressing V5-tagged ERp57 (lanes 1- 8) and transfected with Myc-tagged ERp27 (lanes 3- 8) were cross-linked with BMH and lysed. Expression and cross-links were confirmed by western blotting using **A**, V5 antibody **B**, Myc antibody.

Protein bands were detected at 57 and 27 kDa (Fig 4.12, A and B) in addition to cross-links with ERp57 only (Fig 4.12A lanes, 3 and 5). Non-specific bands around 100 kDa were picked up again when probed with Myc antibody (Fig. 4.12B).

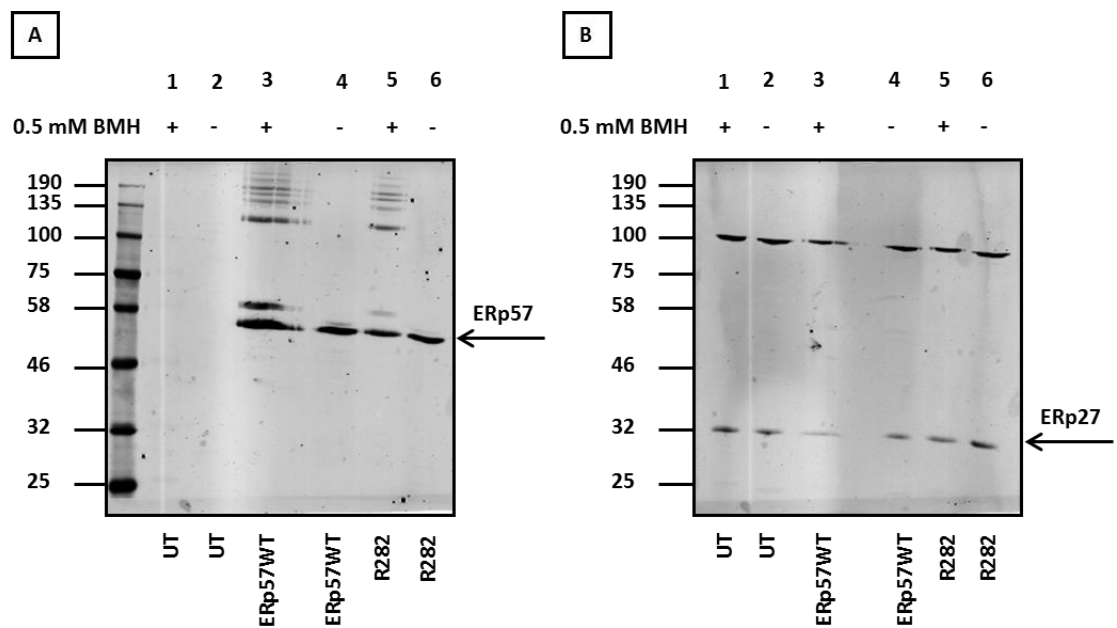


Figure 4.12, The interaction between ERp57 and ERp27 by *in cellular* cross-linking.

A representative western blot of ERp27 stable cells expressing Myc-tagged ERp27 (lanes 1- 6) and transfected with V5-tagged ERp57 (lanes 3- 6) were cross-linked with BMH and lysed. Expression and cross-links were identified by western blotting **A**, V5 antibody and **B**, Myc antibody.

Based on the first batch of the in-cell cross-linking results as ERp27 stable cells were losing expression overtime and since the results obtained using BMH were not conclusive, the cleavable amine-specific cross-linking agent Dithiobis succinimidyl propionate (DSP, Fig 4.13), was used in an ERp57 stable cell-line.

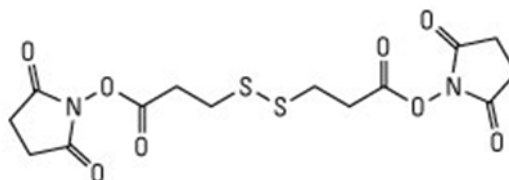


Figure 4.13, The chemical structure of the Dithiobis succinimidyl propionate (DSP) cross-linking agent.

Myc-ERp27 was transiently transfected into cells stably expressing ERp57. Lysates were separated on a non-reducing SDS-PAGE gel followed by western blots using V5 and Myc antibodies (Fig 4.14).

Interestingly, protein bands were detected at 57 kDa (Fig 4.14A lanes 1-4) and 27 kDa (Fig 4.14B lane 4). Cross-links with ERp57 were seen (Fig 4.14A lanes 1 and 3) and ERp27 (Fig 4.14B lane 3). Surprisingly, these cross-links do not correspond to each other as the complexes formed with ERp57 have different patterns and sizes compared to ERp27 complexes. We checked reproducibility under reducing and non-reducing conditions as DSP is a cleavable cross-linking agent and the cross-links could be affected by the addition of reducing agents (Fig 4.15A).

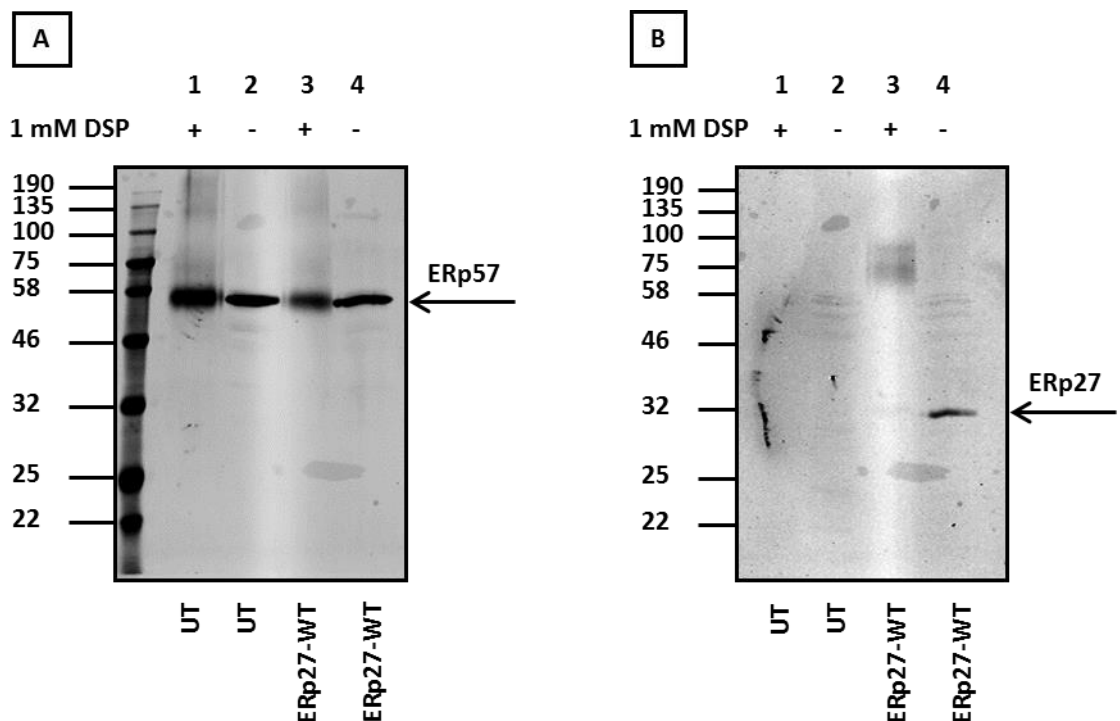


Figure 4.14, The interaction between ERp57 and ERp27 by *in cellular* cross-linking.

A representative western blot of ERp57 stable cells expressing V5-tagged ERp57 (lanes 1, and 4) and transfected with Myc-tagged ERp27 (lanes 3, and 4) were cross-linked with DSP and lysed. Expression and cross-links were identified by western blotting using **A**, V5-antibody and **B**, Myc-antibody. (n = 3).

The cross-links within the non-reduced ERp57 fractions were confirmed (Fig 4.15A lanes, 5 and 7) as well as the non-reduced ERp27 (Fig 4.15B lane, 7). Those cross-links disappeared from the reduced samples (Fig 4.15A lanes, 1 and 3) and (Fig 4.15B lane, 3) suggesting that ERp27 is binding to candidates other than ERp57 in cells.

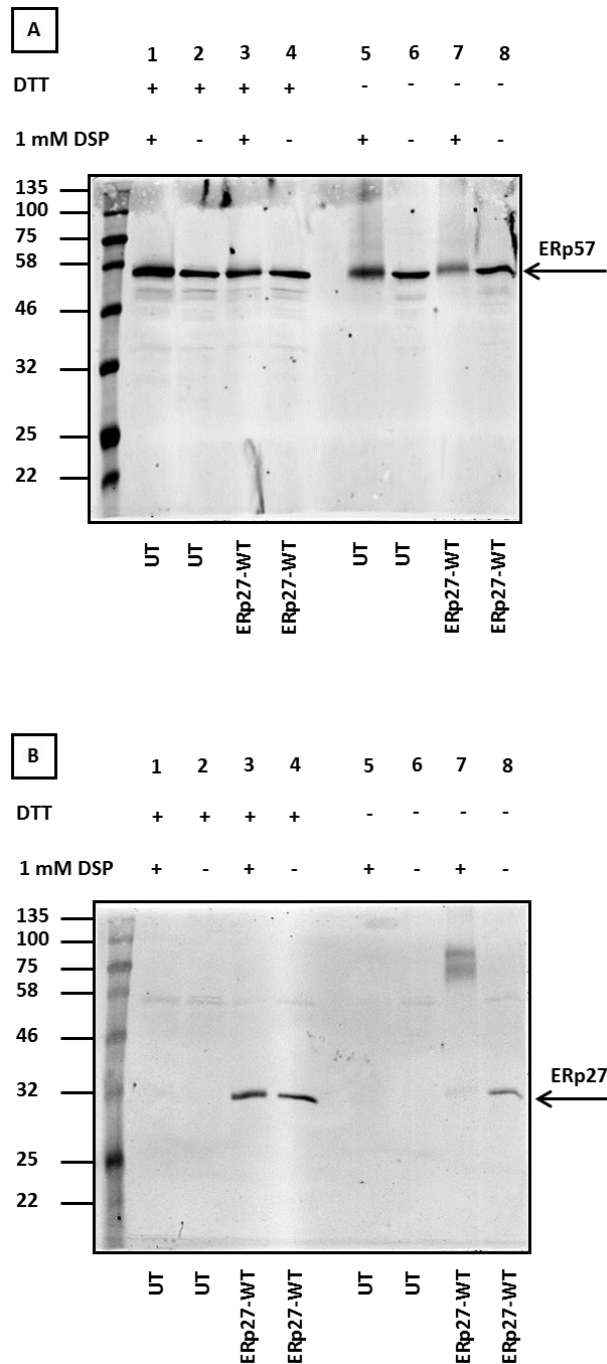


Figure 4.15, The interaction between ERp57 and ERp27 by *in cellular* cross-linking.

ERp57 stable cells expressing V5-tagged ERp57 (lanes 1- 8) and transfected with Myc-tagged ERp27 (lanes 3, 4, 7, and 8) were cross-linked by DSP under reducing and non-reducing conditions then lysed. Expression and cross-links were identified by western blotting using **A**, V5 antibody and **B**, Myc antibody. (n = 3).

As ERp27 showed evidence of interaction to proteins other than ERp57 in cells an experiment was carried out to determine if the cross-links formed are to CRT or CNX as they are the two potential candidates . Myc-tagged ERp27 constructs were transfected into cells stably expressing ERp57. Cells were cross-linked and lysed then lysates were separated on non-reducing SDS-PAGE. Cross-links were visualised by a western blot using CRT and CNX antibodies (Fig 4.16 and 4.17).

ERp27 was detected (Fig 4.16A lanes, 3 and 4) and CRT migrate at 57 kDa (Fig 4.16B lanes, 1- 4). Cross-links to ERp27 were observed (Fig 4.16A lane 3) as well as weak cross-links to CRT (Fig 4.16B lanes 1 and 3). However, these cross-links do not correspond to each other suggesting that CRT does not interact with ERp27.

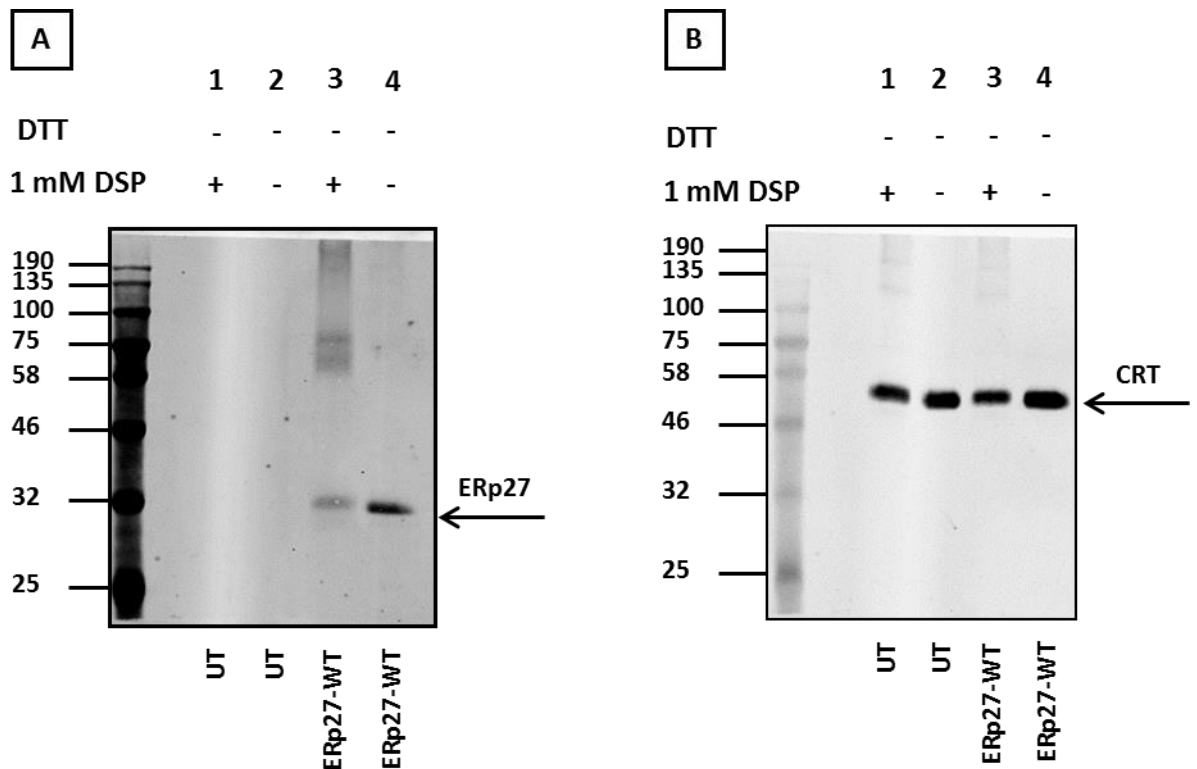


Figure 4.16, The interaction between ERp27 and CRT.

ERp57 stable cells expressing V5-ERp57 and transfected with Myc-tagged ERp27 (lanes 3, and 4) and CRT (lanes 1, and 4) were cross-linked with DSP and lysed. Expression and cross-links were confirmed by western blot using **A**, Myc-antibody. **B**, CRT-antibody. (n = 3).

In addition, the same experiment was repeated using CNX antibody (Fig 4.17). ERp27 was identified at 27 kDa (Fig 4.17A lanes 3 and 4) and CNX migrate around 90 kDa (Fig 4.17B lanes, 1-4). The CNX antibody (Fig 4.17B lanes 1 and 3) did not pick up the same cross-links to ERp27 (Fig 4.17A lane 3). These results strongly suggest that the cross-linked product with ERp27 are not calnexin or calreticulin.

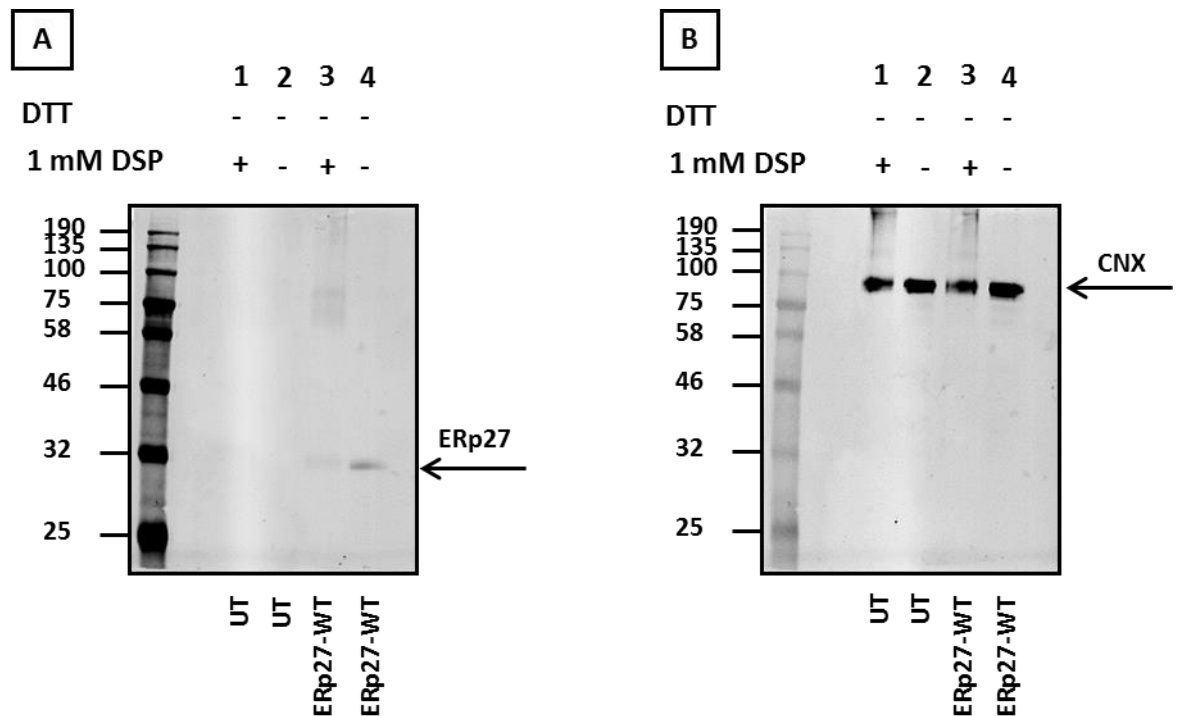


Figure 4.17, The interaction between ERp27 and CNX.

ERp57 stable cells expressing V5-ERp57 and transfected with Myc-tagged ERp27 (lanes 3 and 4) and CNX (lanes 1 and 4) were cross-linked with DSP and lysed. Expression and cross-links were confirmed by western blot using **A**, Myc-antibody. **B**, CNX-antibody. (n = 3).

Since we confirmed that cross-links to ERp27 are not formed with ERp57, CRT, and CNX, samples were prepared after using cross-linking agent and analysed by mass spectrometry to identify interacting proteins. These results will be analysed in the next chapter.

4.3 Discussion

Our results have shown an agreement to some extent with what was established previously by the Ruddock group in terms of the *in vitro* interactions (Alanen et al., 2006). The interactions between the wild type proteins have been proven. The peptide binding mutant of ERp27 verified that ERp27 does not require this site for binding ERp57 and it uses a different binding-site for ERp57.

On the other hand, the E231K mutant that was supposed to prevent the ERp57 binding-site still formed a cross-link with ERp57 in our hands. That suggests that the E231K mutant does not influence the interaction with ERp57. It was assumed that this mutant does not prevent the binding completely but rather reduce it to some extent. However, that does not seem to be the case in the obtained results. That might be due to the variances in the conditions of handling the experiment compared to the Ruddock group (Alanen et al., 2006).

Furthermore, high molecular weight bands formed between ERp57 and ERp27 indicate that multiple ERp27 or ERp57 molecules interact to form heterooligomers at least *in vitro*. Additionally, there was an indication of a competition between ERp27 and CRT for binding to ERp57 when the proteins were combined. That result suggests that ERp27 has an effect on the ERp57 and CRT interaction, as cross-links were formed between ERp57 and CRT as well as ERp57 and ERp27. ERp57 has been thoroughly studied and essentially referred to as a glycoprotein-specific oxidoreductase because of its significant role in the CNX/CRT cycle for glycoproteins folding (Frasconi et al., 2012, Ellgaard and Fricke, 2003, Williams, 2006).

ERp57 was reported to be essential for efficient folding of glycoproteins with mutual structural domains when associated with CNX and CRT (Jessop et al., 2007). ERp57 binds to both CRT and ERp27 using that same binding-site on its b' domain. Consequently, the ERp57/ERp27 interaction and ERp57/CRT interaction should not occur simultaneously (Alanen et al., 2006). Our results imply that the ERp57 and CRT complex is more robust and preferable compared to ERp27. However, ERp27 does compete with CRT for binding ERp57 as cross-links were formed in the protein mixture using ERp27 and ERp57 anti-

bodies. Figures 4.18 and 4.19 are showing the CNX/CRT cycle for glycoprotein folding and two different fates for ERp57.

The interaction between ERp57 and CRT was more prominent when probed with the anti-CRT compared to the His-antibody. That might be due to antibody accessibility and hence the sensitivity of the immunodetection of the His-antibody which makes it for some reason unable to recognise the His-tag on the recombinant protein CRT. Therefore, a specific antibody to CRT would be ideal to use for detection. It was established previously that the immunodetection levels of His-tagged protein markedly varied depending on the His-tag antibody used. Such variability could result in adverse effects on numerous analytical methods (Debeljak et al., 2006).

The aggregation of ERp57 that we noticed within samples that do not contain cross-linking agents may be the result of ERp57 becoming oxidised. This effect could be resolved by adding a reducing agent such as DTT to bring it to the reduced state before using it in an experiment.

The ERp57 *in cellulo* interaction with CRT was repeated as previously described (Jessop et al., 2009a). CRT was co-immunoprecipitated with ERp57. Interestingly, the co-transfection of ERp27 enhanced the immunoprecipitation compared to the wild type or the mutant of ERp57 alone. A non-covalent interaction between ERp57 and CRT was observed as well as the cross-linking complex indicating that the cross-linker was not absolutely required to stabilise the interaction. The increased interaction of CRT and ERp57 in the presence of ERp27 is difficult to explain but could be due to an indirect effect such as the activation of the unfolded protein response.

As co-transfection efficiency could be problematic and affect the expression and cross-linking, the transfection was carried out in stable cells to limit inconsistency. The results from this set of experiments showed that the only cross-links seen were with ERp57 and proteins other than ERp27. This suggests that, at least in cells, ERp57 cannot be cross-linked to ERp27 using a thiol specific cross-linking agent.

The lack of the *in cellulo* interaction between ERp57 and ERp27 when using BMH might be due to the fact that this agent is a sulfhydryl specific cross-linking agent which binds cysteine residues within proteins. Consequently, BMH might not be able to reach cysteines within ERp27 if they are mostly buried away from the surface.

DSP was used as an alternative, it is an amino specific agent with a spacer arm that has a disulphide bond that can be cleaved by the addition of reducing agents such as DTT or TCEP. DSG and DSP both have a similar chemical structure with a slight difference in which DSP has a longer spacer arm that contains a disulphide bond which makes it cleavable unlike DSG.

Strikingly, cross-links were observed with both ERp57 and ERp27 when DSP was used. Yet, it was noticed those cross-links have different patterns when compared to each other. That implies that ERp57 does not interact with ERp27 in living cells, however, ERp27 forms cross-links with other protein candidates which need to be identified. The two potential candidates are calnexin and calreticulin have already been eliminated.

Therefore, further investigation is needed in order to identify possible partners for ERp27 in mammalian cells which will be analysed by mass spectrometry in the next chapter.

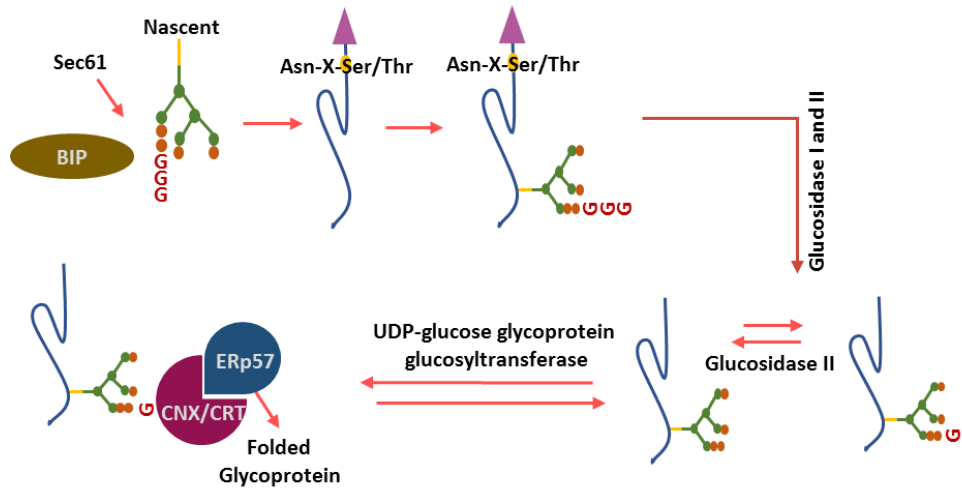


Figure 4.18, The calnexin and calreticulin cycle for glycoprotein folding.

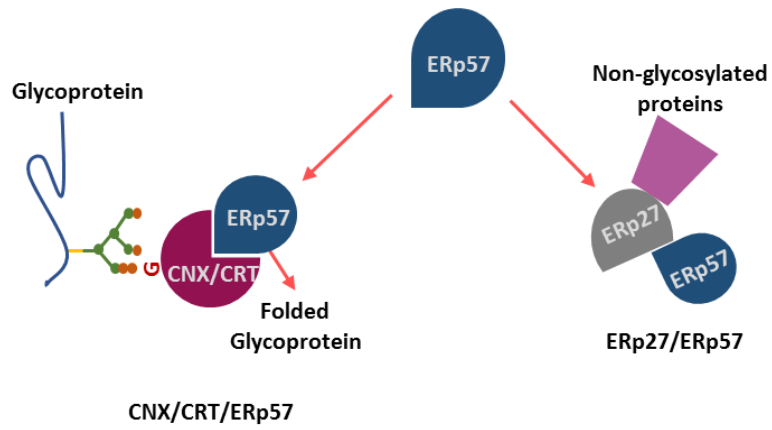


Figure 4.19, The different fates for ERp57. CNX and CRT bring glycoproteins to ERp57 to fold while ERp27 could bring non-glycosylated proteins to ERp57 to fold.

5 *In cellulo* protein-protein interaction by cross-linking assay and mass spectrometry

5.1 Introduction

ERp27 is a non-catalytic member of the PDI family. Its domain structure only contains the two thioredoxin-like domains; b and b' and it lacks both of the CXXC active sites (Alanen et al., 2006). The crystal structure of ERp27 was solved and the C-terminal domain found to be homologous to that of the PDI protein as it has a hydrophobic cleft containing the substrate binding site. Additionally, it contains an ERp57 binding site (Kober et al., 2013).

It was established that ERp27 can bind the peptide Δ -somatostatin by cross-linking (Alanen et al., 2006). Expanding on that result, an ITC experiments have suggested that ERp27 functions as a chaperone as it binds unfolded proteins. However, if the protein is fully folded then ERp27 does not show any evidence for measurable binding affinity (Kober et al., 2013).

ERp27 was found to interact *in vitro* with a well-known PDI family member, ERp57 (Alanen et al., 2006). ERp57 is known as an oxidoreductase that contains redox-active sites and interacts with calnexin (CNX) and calreticulin (CRT) for glycoprotein folding (Ellgaard and Frickel, 2003). However, ERp57 lacks a substrate binding site and interacts with its substrates through the CNX and CRT complex as they work to supply the redox-active site for the suitable substrates (Russell et al., 2004). Based on that model, ERp27 could potentially support ERp57 to interact with a wide variety of other substrates that interact with ERp27 (Alanen et al., 2006, Kober et al., 2013).

Previous research has trapped ERp57 substrates as mixed disulphide complexes which disclosed that CNX and CRT only offer glycoproteins to interact with ERp57. These results imply that under normal cellular conditions the lectins CNX and CRT replace other possible interactions with ERp57 (Jessop et al., 2009a, Kober et al., 2013). Nevertheless, following infection with simian virus 40 (SV40), ERp57 functions independently from the lectins (Schelhaas et al., 2007). This result supported by the fact that the expression of ERp27 increases as a response to unfolded proteins as well as under cellular stress conditions (Kober et al., 2013).

We wanted to study the ERp57 and ERp27 interaction in living cells and investigate if ERp27 would inhibit ERp57 and CRT interaction which has been investigated previously *in*

cellulo (Jessop et al, 2009). Our results revealed that ERp27 co-transfection with ERp57 enhanced the interaction between ERp57 and calreticulin in a way that is not fully understood and might be due to cellular stress conditions (see chapter 4). Interestingly, we also found that ERp27 does not bind to ERp57 *in cellulo* but rather it binds to other candidates which need to be identified. CNX and CRT were two potential candidates that have been eliminated.

To find out the protein candidates that interact with ERp27 in living cells, protein samples were prepared as explained in the previous chapter then after cross-linking they were analysed by mass spectrometry as solid or liquid samples.

Additionally, ERp27 has been reported to be abundant in the pancreatic acinar cells. The expression was confirmed in a personal communication with Professor Kenji Inaba's group in Sendai, Japan.

5.2 Results

5.2.1 Protein sample preparation for Mass Spectrometry

This set of experiments was carried out in order to determine protein partners that interact with ERp27 in living cells. Cells were cross-linked using 1 mM DSP then lysed. The lysate was then separated on SDS-PAGE and samples were sent out to be analysed by mass spectrometry either as solid or liquid samples. Once protein hits were determined, western blotting was carried out to confirm those hits.

To check the transfection expression and cross-links to ERp27-WT and its mutants, HT1080 cells were transfected with ERp27 constructs then cross-linked with DSP (Fig 5.1). Proteins were separated on SDS-PAGE then a western blot was carried out with a myc antibody. Similar patterns of cross-links appeared with ERp27-WT and ERp27-E231K (Fig 5.1 lanes 3 and 7) respectively, however, ERp27-I196W mutant (Fig 5.1 lane 5) gave a slightly different pattern of cross-links.

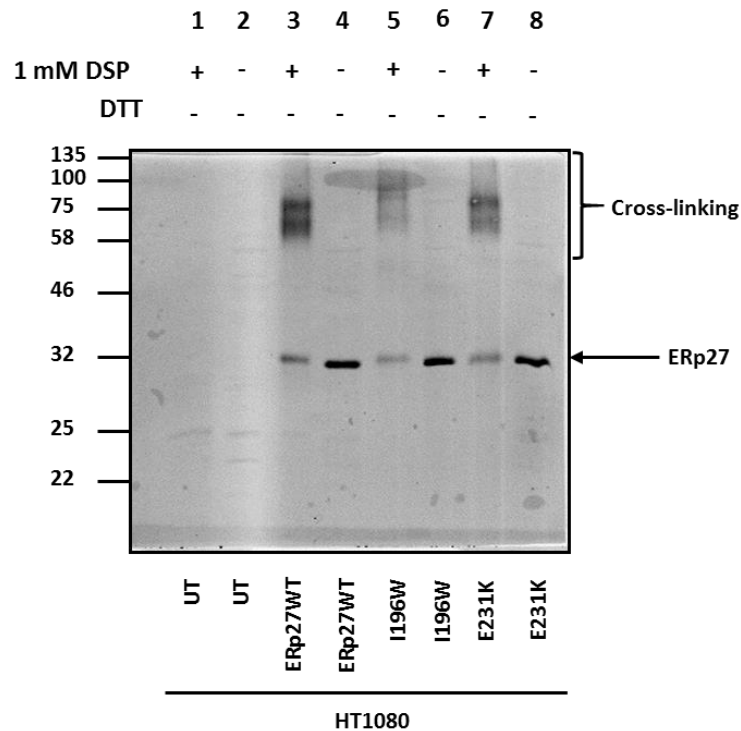


Figure 5.1, *In cellulo* cross-linking of ERp27.

HT1080 cells transfected with myc-tagged ERp27-WT (lanes 3 and 4), ERp27-I196W (lanes 5 and 6), and ERp27-E231K (lanes 7 and 8) or un-transfected (UT) cells (lanes 1 and 2) were cross-linked with 1 mM DSP and lysed. The lysate was separated on SDS-PAGE followed by a western blot using myc specific antibody. (n = 3).

Subsequently, to demonstrate if the additional bands were crosslinked via DSP the experiment was repeated using wild type ERp27 only and the samples separated on SDS-PAGE under reducing and non-reducing conditions followed by a myc western blot (Fig 5.2). Under non-reducing conditions (Fig 5.2 lane 7) a similar pattern of a cross-link to ERp27 appeared as before while the crosslinked product disappeared from the reduced fraction (Fig 5.2 lane 3) as DSP is a cleavable cross-linking agent.

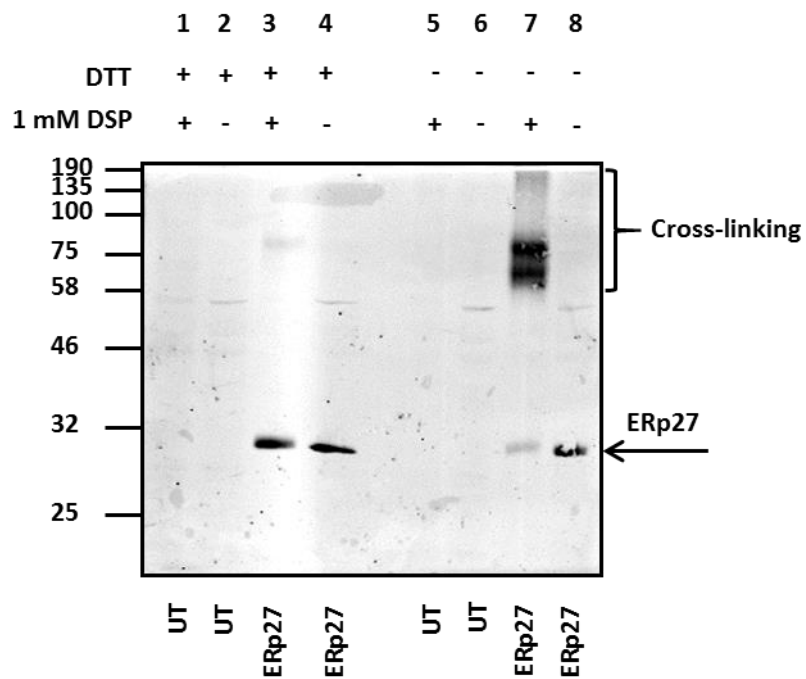


Figure 5.2, *in cellulo* cross-linking of ERp27.

HT1080 cells transfected with myc-tagged ERp27-WT (lanes 3, 4, 7, and 8) or un-transfected (UT) (lanes 1, 2, 5, and 6) were cross-linked with 1 mM DSP and lysed. The lysate was separated on SDS-PAGE and a western blot was carried out using myc specific antibody. (n = 3).

To avoid transfection a comparison between stable cells expressing ERp27-WT and ERp27-E231K mutant was carried out as they gave similar cross-linking results unlike the ERp27-I196W mutant. Cells were cross-linked with DSP and were prepared as described previously. The lysate was separated on SDS-PAGE and then a western blot was carried out using a myc specific antibody. A similar cross-link pattern to that obtained following transient expression was seen with the E231K mutant (Fig 5.3, lane 3). ERp27-WT seemed to lose expression over time (Fig 5.3, lane 2) as shown in the previous chapter.

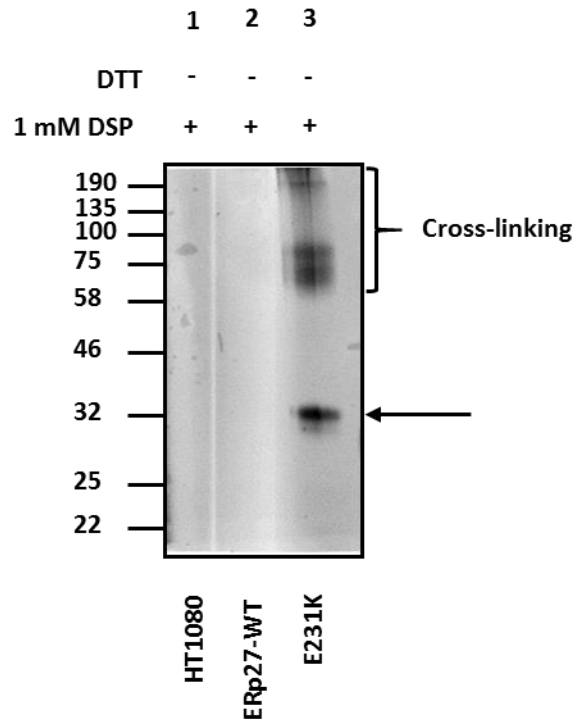


Figure 5.3, *In cellulo* cross-linking of ERp27.

HT1080 (lane 1), ERp27-WT (lane 2), ERp27-E231K (lane 3), cells were cross-linked with 1 mM DSP and lysed. The lysate was then separated on SDS-PAGE and a western blot was carried out using myc specific antibody. (n = 3).

Therefore, E231K was preferred to be used to look at the interaction of ERp27 in cells. A repeat was carried out using the ERp27-E231K stable cells to prepare samples for analysis by mass spectrometry (Fig 5.4). ERp27-E231K cells were cross-linked with DSP and lysed. Then the lysate was separated on SDS-PAGE to check cell expression and cross-linking (Fig 5.4 lanes 1-4).

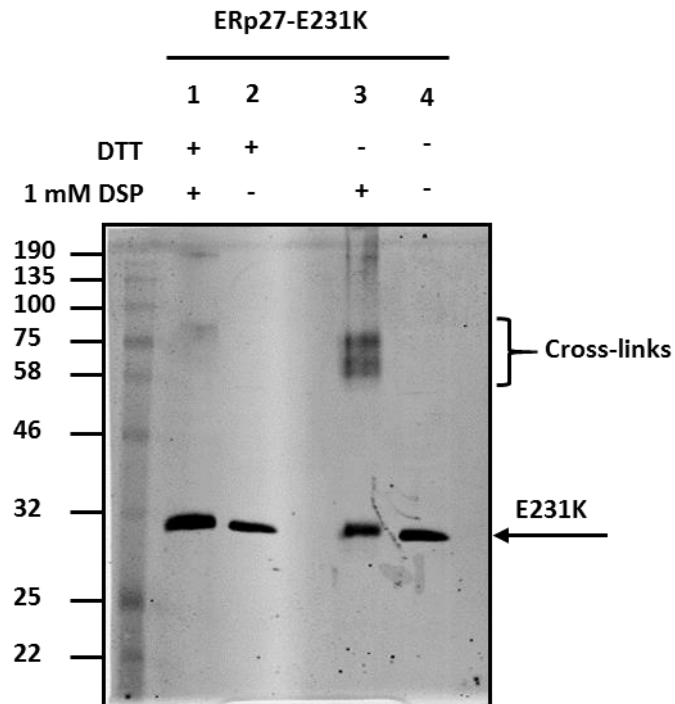


Figure 5.4, *In cellulo* cross-linking of ERp27.

ERp27-E231K stable cells analysed under reducing conditions (lanes 1 and 2) or non-reducing conditions (lanes 3 and 4) were cross-linked with 1mM DSP and lysed. The lysate was then separated on SDS-PAGE and a western blot was carried out using myc specific antibody. (n = 3).

The same procedure was carried out but this time the whole lysate was immunisolated using myc agarose beads and reduced to release the cross-linked materials. The immunisolate was then separated on SDS-PAGE and released proteins visualised by silver-staining (Fig 5.5). The bands of interest were chosen based on the size of the cross-links to ERp27 which run around 75 kDa, and by subtracting 27 kDa out of 75 kDa the output would be 48 kDa, indicated by an asterisk (Fig 5.5 lane 1). The other bands that are indicated by an asterisk were cut out of the gel and sent for analysis to compare with the band of interest (Fig 5.5, lane 1 and 2).

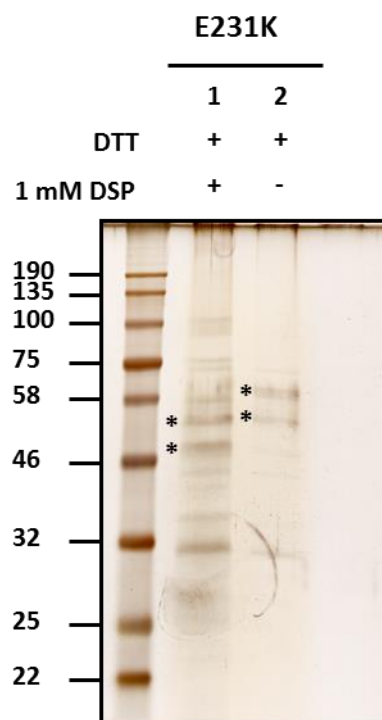


Figure 5.5, *in cellulo* cross-linking of ERp27.

A representative silver-stained gel of cross-linked ERp27 with 1 mM DSP (lanes 1 and 2). The lysate was immunisolated with myc agarose beads and separated on SDS-PAGE then visualised by silver staining. The bands of interest (indicated with asterisks) were sent out for mass spectrometry as solid samples. (n = 3).

The protein digestion was done prior to analysis by mass spectrometry in a different laboratory where in-gel digestion was performed. The in-gel digestion consists of 4 main steps; de-staining, reduction and alkylation, in-gel-digestion with trypsin, and extraction. Gel bands were washed to de-stain the gel from the silver staining. Then the samples went through reduction and alkylation of the cysteines within the protein. Hereby, the disulphide bonds were irreversibly broken up aiding the peptide yield. After that, the in-gel digestion step was carried out in which the serine protease trypsin enzyme is used for

digesting the protein into peptides which are shorter fragments and easy to identify by mass spectrometry. Finally, the gel extraction is carried out to extract the peptides from the gel matrix which can be done in one or several steps.

After analysis by mass spectrometry, the results did not show any protein hits. This experiment has been repeated many times and gave negative results. This may be due to the approach used for protein preparation or to the protein digestion preparations and buffers used for mass spectrometry.

The experiment was then repeated with ERp27-E231K stable cells only with a slight change to the approach. Cells were cross-linked with 1 mM DSP then lysed. The lysate was then split, and a small amount was separated on SDS-PAGE to check the cell expression and cross-linking (Fig 5.6 lane 2). The rest of the lysate was then immunisolated with myc agarose beads then the immunisolated material was washed with the IP buffer then eluted with 10 mM DTT to reduce all disulphide bonds before adding an ammonium bicarbonate buffer, a compatible buffer with the mass spectrometry and sending the proteins in solution for analysis.

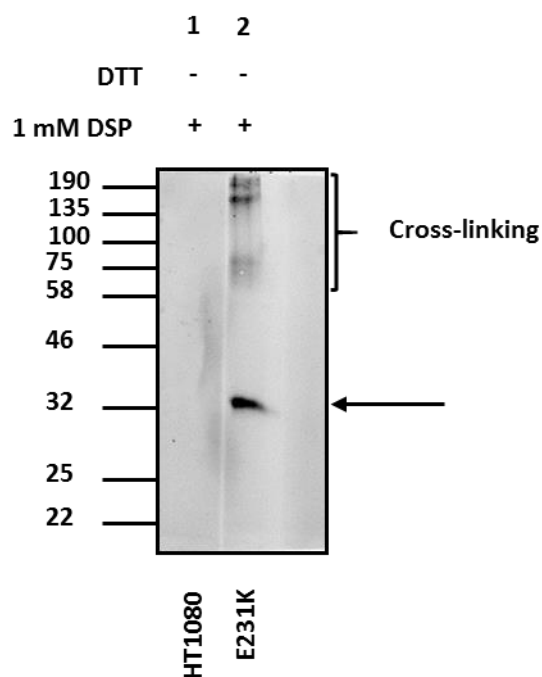


Figure 5.6, *in cellulo* cross-linking of ERp27.

HT1080 and ERp27-E231K cells were cross-linked with 1 mM DSP and lysed. The lysate was then separated on SDS-PAGE and a western blot was carried out using myc antibody to check cells expression and cross-linking. (n = 3).

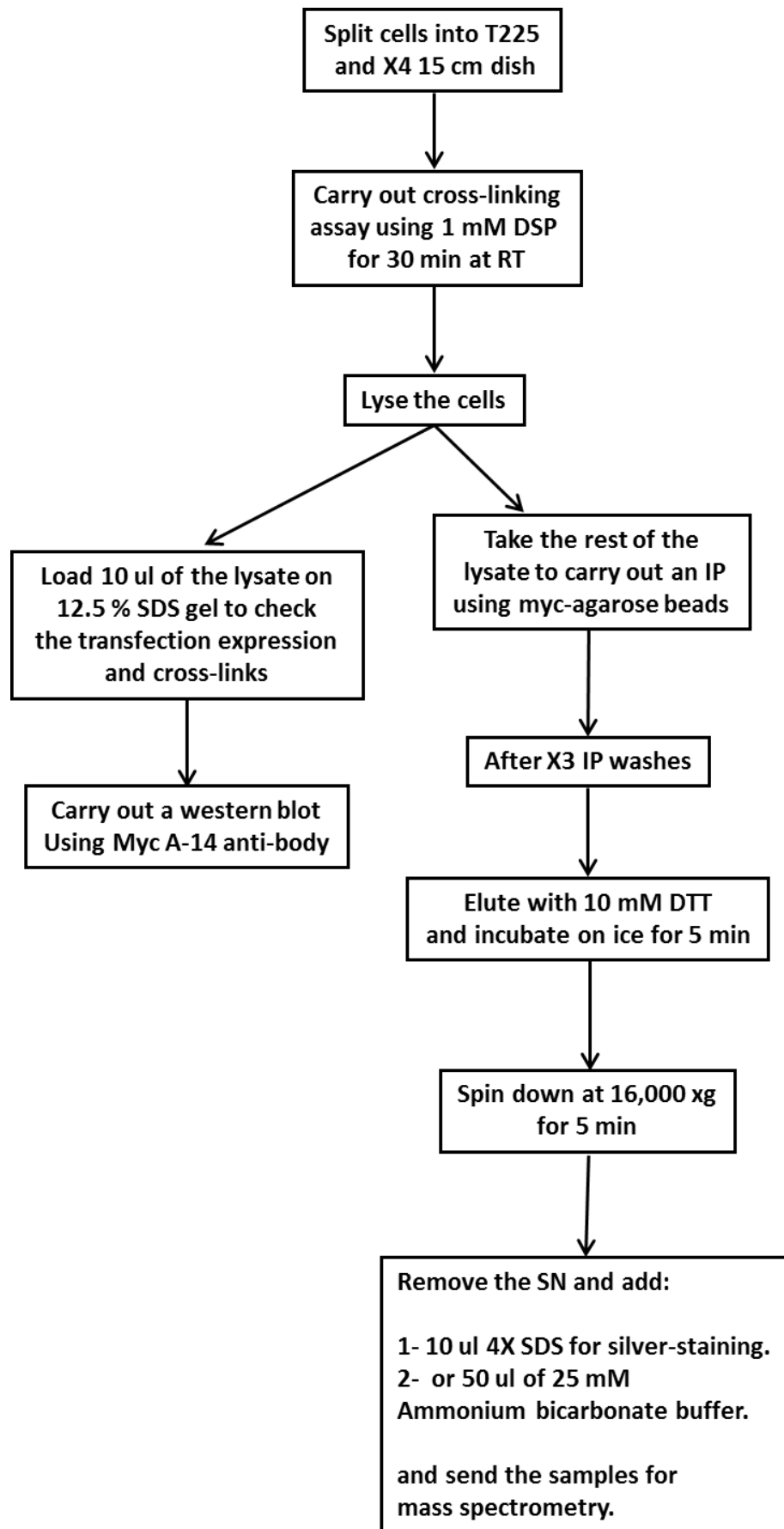


Figure 5.7, A schematic showing the approach of preparing protein samples for mass spectrometry.

The mass spectrometry hits revealed a number of ER proteins as well as other proteins and contaminants such as keratin. This was repeated many times and there were few protein hits that mainly showed up; P5, ERO1, ERp29 and calumenin as indicated in (Table 5.1).

Table 5.1, The protein hits obtained from Mass spectrometry analysis.

The table includes the protein sequence coverage % and the emPAI number.

Number	Protein	Protein sequence coverage %	emPAI
1	P5	31 %	1.26
2	ERO1	12 %	0.23
3	Calumenin	6 %	0.14
4	ERp29	5 %	0.38

After protein hits were identified by mass spectrometry a series of immune western blotting were carried out in order to verify those hits. As indicated in (Fig 5.8), HT1080 (lanes 1 and 2), ERp27-WT (lanes 3 and 4), and ERp27-E231K (lanes 5 and 6) cells were cross-linked with DSP and lysed. A small amount of the lysate was then separated on SDS-PAGE to check the cross-linking and cell expression before proceeding with immuno precipitation. ERp27 was expressed within the E231K cell-line as well as cross-links at 75 kDa. However, ERp27-WT cells have lost expression and therefore no signal was appeared within that cell-line.

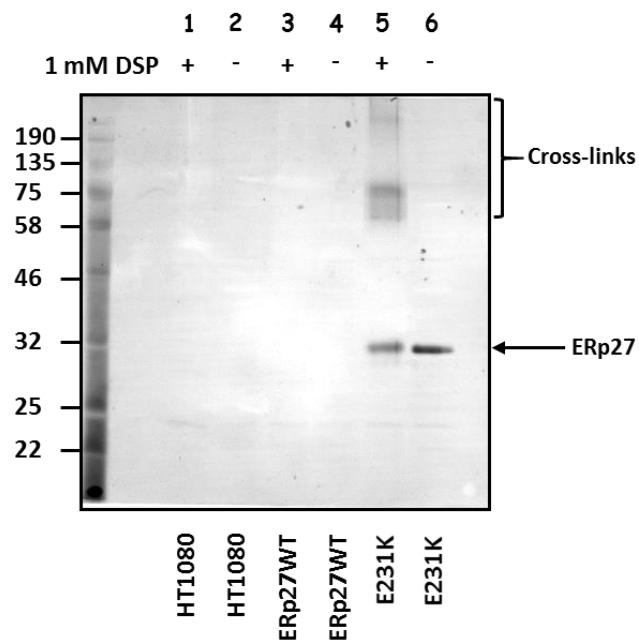


Figure 5.8, *In cellulo* cross-linking of ERp27.

HT1080 (lanes 1 and 2), ERp27-WT (lanes 3 and 4), and E231K (lanes 5 and 6) cell lines were cross-linked with 1 mM DSP and lysed. A small amount of the lysates was then separated on SDS-PAGE followed by western blotting using a specific myc antibody. (n = 3).

Subsequently, to determine what proteins interact with ERp27 in the cross-links, HT1080 and E231K lysates were further analysed by immune precipitation using Myc-Trap agarose beads followed by western blots which were carried out using P5, ERp29, Ero1, and calumenin anti-bodies.

P5 was expressed around 48 kDa within HT1080 cells (Fig 5.9 lane 2) and E231K cells (Fig 5.9 lanes 4). Additionally, in the presence of DSP within E231K cells a cross-linking product higher than 75 kDa appeared (Fig 5.9 lane 3).

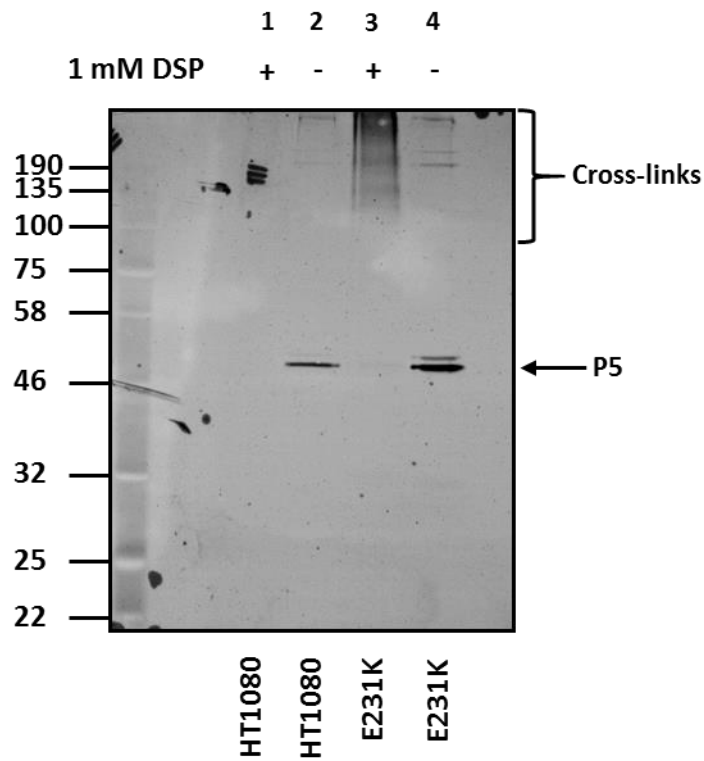


Figure 5.9, *In cellulo* cross-linking of ERp27.

HT1080 (lanes 1 and 2), and E231K (lanes 3 and 4) were cross-linked with 1 mM DSP and lysed. The lysates were then immunoprecipitated using Myc-Trap agarose beads followed by western blot using monoclonal P5 antibody. (n = 3).

Furthermore, Ero1 was identified within the immunisolates from HT1080 cells (Fig 5.10 lane 2) as well as E231K cells (Fig 5.10 lanes 3 and 4) at around 54 kDa. Cross-links were also formed within E231K cells at a higher molecular weight in the presence of the cross-linking reagent (Fig 5.10 lane 3).

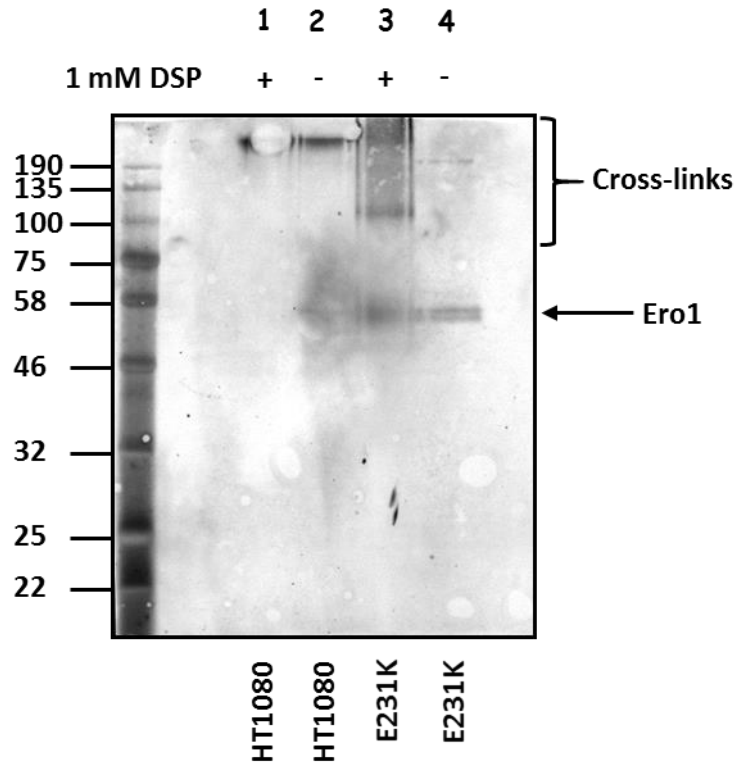


Figure 5.10, *In cellulo* cross-linking of ERp27.

HT1080 cells (lane 1 and 2), and E231K cells (lane 3 and 4) were cross-linked with 1 mM DSP and lysed. The lysates were then immunoprecipitated using Myc-Trap agarose beads followed by western blotting using Ero1 antibody. (n = 3).

However, when the same western blots were probed with ERp29 and calumenin antibodies the results were negative, and no bands were expressed. No conclusive results were obtained and that is maybe due to the antibody being of low affinity and therefore unable to detect a protein signal.

5.2.2 The effect of ERp27 on pancreatic digestive enzymes

ERp27 was reported to be abundant in the pancreas. The PANC-1 and INS-1 cell lines were used to check expression in the pancreatic islet cells which secrete insulin (Fig 5.11A and B). ERp27-WT and E231K stable cells as well as the ERp27 purified protein were used as controls. However, ERp27 does not seem to be expressed in that part of the pancreas (Fig 5.11A). The purified protein ERp27 appeared at 27 kDa and the E231K cell line gave a slightly higher signal around 30 kDa as it is myc-tagged. The rest of the cell lines showed weaker signals around 27 kDa which were initially thought to be ERp27, but they were not evident in the repeat experiment (Fig 5.11B).

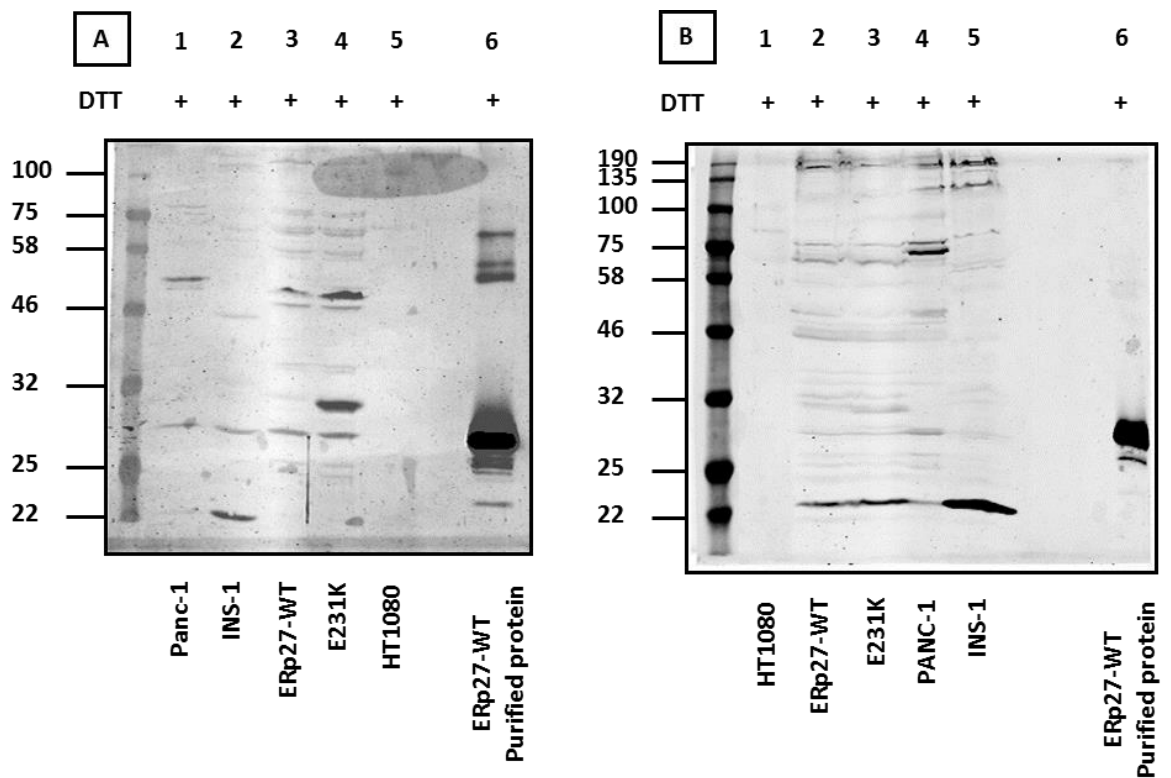


Figure 5.11, The expression of ERp27 in pancreatic islet cells.

A, A representative ERp27 western blot. Pancreatic cell-lines PANC-1 and INS-1 (lanes 1 and 2), as well as ERp27-WT (lane 3), E231K (lane 4), HT1080 (lane 5) cells-lines lysates and purified ERp27 (lane 6) were separated on SDS-PAGE followed by western blot using ERp27 antibody. **B**, A repeat. (n = 3).

Professor Kenji Inaba's group have found that ERp27 is expressed in acinar cells (personal communication). We have repeated the expression in the acinar cells which secrete digestive enzymes. The AR42J (which was provided by Dr Adam Benham, Durham University), 266-6 cell-lines and the pancreas tissue were used to check the expression. The ERp27-WT cell line as well as the purified protein were used as controls. However, the result was not conclusive as ERp27 was detected in the purified protein fraction only (Fig 5.12). The pancreas tissue which was obtained from a mouse that has been starved for 16 h for a behaviour experiment has shown a strong signal lower than 25 kDa which probably does not represent ERp27, but the rest of the samples did not show any obvious bands at the correct size for ERp27.

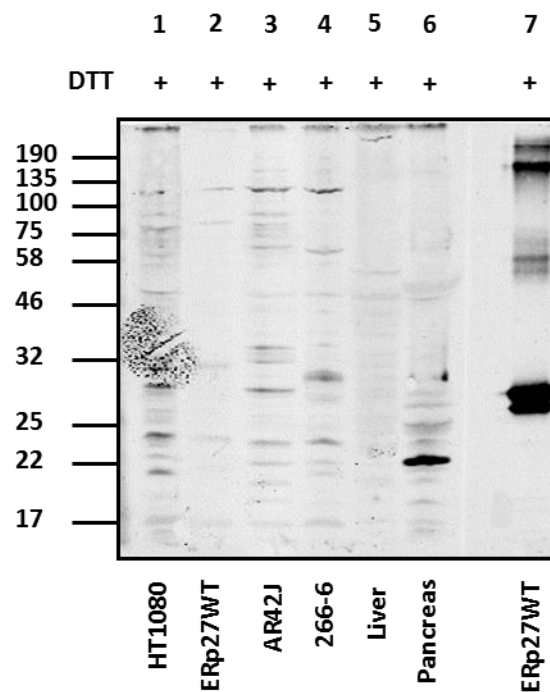


Figure 5.12, The expression of ERp27 in the pancreatic acinar cells.

HT1080 (lane 1), ERp27-WT (lane 2), AR42J (lane 3), 266-6 (lane 4), liver tissue (lane 5), pancreas tissue (lane 6) lysates as well as ERp27 purified protein (lane 7) were separated on SDS-PAGE followed by western blot using ERp27 antibody. (n = 3).

5.3 Discussion

Our results have supported the *in vitro* interaction between ERp27 and ERp57. However, when we tried to identify interactions *in cellulo* we could not detect an interaction. The previous chapter has confirmed that ERp27 does not bind ERp57 *in cellulo*. So, the work that have been done in this chapter was to identify what are the protein candidates that interact with ERp27 in mammalian cells. Our results are summarised in preparing protein samples to be analysed by mass spectrometry.

HT1080, ERp27-WT, and E231K cell-lines were cross-linked using 1 mM DSP and lysed. A small amount of the lysates was then tested for expression and cross-linking by carrying out immune western blot using myc antibody. E231K cells expressed, however, ERp27-WT cells did not, and it lost expression over time as shown in the previous chapter (see chapter 4). Accordingly, we then decided to use HT1080 and E231K cell-lines only. The lysates were then taken further and underwent immunoprecipitation using myc agarose beads followed by silver staining if we are sending the protein as a solid sample for analysis. In other instances, the immunoprecipitation was followed by 10 mM DTT elution if we are sending proteins in solution for mass spectrometry.

Sending our proteins as solid samples have always come back with contaminations and never give any protein hits. The protein digestion step was carried out in a different lab where they used the in-gel technique. Consequently, the negative results may be due to the technique followed or the buffer used for mass analysis. After few trials, we have altered our protocol slightly by eluting the immunoprecipitated materials with 10 mM DTT which helps breaking disulphide bonds within the sample and send our proteins in ammonium bicarbonate buffer which is known to be compatible with mass spectrometry as explained in (Fig 5.7).

After that, the mass spectrometry results have revealed a number of protein hits in which some of them were ER proteins and some were calcium binding proteins or ER chaperones in addition to contaminants such as keratin. After a triplicate, few hits were noticed frequently which are; a protein disulphide isomerase homologue P5 (Kikuchi et al., 2002), Ero1 the major contributor for disulphide bond formation with PDI family

(Cabibbo et al., 2000), calumenin protein (CP) a calcium binding protein (Jung and Kim, 2004), and a non-catalytic PDI member ERp29 (Barak et al., 2009).

To confirm if these hits were real and they are indeed forming cross-links with ERp27 a series of immune western blotting were carried out. Protein samples were prepared as explained earlier using HT1080 and E231K cell-lines only, as cell expression and cross-links were confirmed within these cell-lines. Immunoprecipitation was then carried out using myc agarose beads followed by immune western blot using different anti-bodies.

Our results are novel as there is no research in the literature had shown this interaction of ERp27 *in cellulo*. We have discovered that P5 and Ero1 are indeed forming cross-links with ERp27 in mammalian cells. Both P5 and Ero1 were expressed within HT1080 and E231K cells. However, in the presence of the cross-linking reagent they only formed cross-linking complexes within E231K cells but not with HT1080 cells which make it clear that this interaction is very specific to ERp27. On the other hand, calumenin and ERp29 were not detected in the first place and accordingly did not show any interaction of any kind which might due to the non-efficiency of the antibodies which make them unable to recognise the proteins.

These findings have indeed raised questions about ERp27 functions in mammalian cells. It would have been good to take these findings further and figure out what is the physiological functions of ERp27 and if its interaction with Ero1 may be contribute to disulphide bond formation in mammalian cells. Furthermore, ERp27 interaction with P5 or other possible candidates would reveal other facts about the binding site on ERp27 thioredoxin domains. Additionally, it would be of interest to determine if these interactions are occurring under normal cellular conditions or under ER stress. Under ER stress conditions, ERp27 was found to selectively bind to unfolded proteins *in vitro* which might compete with its interaction with other proteins such as ERp57. However, *in cellulo* this gives room for more investigation to be done.

The other aspect that we wanted to investigate was the expression of ERp27 in pancreatic cells. ERp27 was reported to be abundant in the pancreas so we were aiming to check its expression and then investigate the effect of ERp27 on the expression of digestive enzymes which are secreted by acinar cells. The expression was tested using different pancreatic islet and acinar cell-lines and pancreatic tissue as well as HT1080 and ERp27

stable cells. However, results were not conclusive as the protein was not detected within the cell-lines-tested.

6 Main discussion

The focus of this research project was to investigate if the thiol-inactive PDI family member ERp27 competes with the ER lectins calreticulin and calnexin for binding the thiol-oxidoreductase PDI family member ERp57. We also investigated if ERp27 functions to recruit non-glycosylated protein substrates to ERp57 to fold, just as calreticulin and calnexin bring N-glycosylated proteins to ERp57 to fold correctly during the glycoprotein folding cycle. Therefore, we investigated the protein-protein interaction between the two PDI family members, ERp27 and ERp57 *in vitro* as well as in mammalian cells.

Furthermore, we compared both interactions of ERp57 with ERp27 and calreticulin and calnexin to define whether or not ERp27 competes with the lectins for binding ERp57.

To start the project, a series of protein expressions and purifications were carried out including; WT-ERp27, ERp27-I196W mutation (which prevents peptide binding), ERp27-E231K mutation (which blocks ERp57 binding), and WT-ERp57. ERp57-R282A mutation (which blocks CRT binding) as well as WT-CRT. All proteins were expressed and purified successfully. However, it was noticed that ERp27 has a leaky expression which is undesirable and needed to be solved. Consequently, pLysS cells were used instead of BL21 (DE3) competent cells which is a bacterial strain that is known for enhancing protein expression. However, that did not work. Furthermore, different media was assessed for expression; Lysogeny broth (LB), Terrific broth (TB), and Auto induction (AI). The terrific broth (TB) media was found to support the expression of all the proteins well with BL21 (DE3) competent cells when induced by IPTG compared to AI and LB. Once this matter was solved it was applied for all proteins.

ERp27 and E231K proteins have a tendency to form aggregates when concentrated to high concentrations and appeared as bands at higher molecular weight. These accumulations were formed after a polishing step by gel filtration and it was thought that by diluting these proteins the aggregation would be less severe. As an attempt to remove aggregation, ultra-centrifugation was carried out. However, no remarkable changes were noticed after centrifugation, so we carried out an additional gel filtration column. Despite these problems we purified sufficient protein for further molecular assays.

Our *in vitro* results of protein-protein interaction using ITC experiment confirmed the interaction between calreticulin and ERp57. However, as the concentration of calreticulin was higher than the desired concentration by almost 3.6 fold (i.e. 200 μ M) it was preferable to lower the concentration between 75-100 μ M before repeating the experiment so that the molecules did not reach saturation within the first couple of injections. The experiment was repeated and the K_D was calculated to be 0.26 μ M +/- 0.8 μ M which supports the results obtained previously (Frickel et al., 2002). The ERp57 and calreticulin interaction was carried out by ITC and TROSY NMR, K_D was; 9.1 +/- 3.0 μ M at 8 °C and 18 +/- 5 μ M at 20 °C, respectively (Frickel et al., 2002).

The optimum protein concentration required for ITC is 10-20 μ M for the cell (300 μ l) and 200 μ M for the syringe (100 μ l). Following protein purification and concentration, the protein concentrations obtained were significantly lower than optimal; ERp27 was 29.27 μ M and ERp57 was 7.44 μ M. Regardless of the low protein concentrations the experiment was carried out. Unfortunately, when we titrated ERp27 into ERp57 there was no measurable affinity for their interaction which is most likely due to the low concentration of both proteins. Therefore, further purification and concentration were carried out to achieve the required protein concentration. However, the process was difficult as exceeding certain concentrations caused protein precipitation which may be due to the intrinsic insolubility of both proteins. Hence, the interaction between ERp27 and ERp57 could not be investigated by ITC. However, it cannot be said that there is no interaction taking place, but it could not be detected due to the low concentration of the proteins.

We then investigated the interaction of ERp27 and ERp57 using a chemical cross-linking assay using DSG as carried out previously by the Ruddock group (Alanen et al., 2006). They also demonstrated that this interaction occurred using NMR studies on the purified proteins. Their results showed that ERp27 uses the tip of its b' domain to bind to ERp57. Additionally, the ERp27 b' domain has a sequence motif similar to that found on the P-domain of the ER lectin calreticulin which suggested that both ERp27 and calreticulin bind to the same binding site within ERp57 (Alanen et al., 2006).

Our results are in agreement to some extent with the previous study. The interaction of ERp27 and ERp57 was established as cross-links formed at 84 kDa which is the size of the complex. In addition, the ERp27-I196W mutation (which blocks the peptide binding-site),

confirmed that ERp27 does not require this site for binding to ERp57. However, the ERp27-E231K (which was supposed to prevent the binding to ERp57), did not block the interaction completely as cross-links still formed in our hands which may be due to the differences of handling the experiment compared to the Ruddock group. Moreover, when ERp27, ERp57 and calreticulin were combined to test the competition between ERp27 and calreticulin for binding ERp57, cross-links were formed between ERp57 and calreticulin but not ERp27 when probed with the His antibody. However, the ERp27 western blot showed that cross-links formed between ERp27 and ERp57 within the protein mixture which correspond to the ERp27/ERp57 complexes in the other lanes. Additionally, the ERp57 western blot also showed cross-links between ERp57 and ERp27 as well as calreticulin when combined, suggesting that ERp27 might have an effect on the interaction between ERp57 and calreticulin. Also, since ERp27 cross-links are stronger compared to the calreticulin complex that suggests ERp27 may be stronger and competes with calreticulin for binding to ERp57. The His antibody did not pick up the particular cross-links with ERp27 probably due to inaccessibility of the epitope in these protein samples.

It was noted that the calreticulin signal was weak when the samples were probed with the His antibody. However, when probed with the calreticulin specific antibody the signal was enhanced. This might be due to the accessibility of the His epitope on calreticulin. It was reported previously that the immunodetection levels of different proteins varies depending on the type of the His antibody used. This variation causes diverse effects on a wide range of analytical methods (Debeljak et al., 2006).

To look at the ERp27 and ERp57 interaction in living cells we have repeated the *in cellulo* cross-linking assay as carried out previously where calreticulin was co-immunoprecipitated with ERp57 (Jessop et al., 2009a). Our results showed that ERp27 co-transfection interestingly enhanced the immunoprecipitation compared to ERp57 alone. A non-covalent interaction of ERp57 and calreticulin as well as cross-linking product was observed and indicated that the cross-linking agent is not essential for the stabilisation of this interaction. The increased interaction between ERp57 and calreticulin in the presence of ERp27 is difficult to explain. However, it may be due to the indirect activation of unfolded protein response (UPR).

As the co-transfection could be problematic and have an effect on cell expression as well as the formation of cross-linking products, the transfection was carried out in stable cell-lines to control the inconsistency of transfection. The results showed that the cross-links which formed to ERp57 were different in size compared to the ERp27 crosslinks. These results suggest that ERp57 was not cross-linked to ERp27 at least *in cellulo* using a thiol specific cross-linking agent such as (BMH). Since BMH is a sulfhydryl specific cross-linker that reacts with cysteine residues within proteins, the lack of a crosslink between ERp57 and ERp27 might be due to the cysteines within ERp27 being buried away from the surface. As an alternative DSP was used. It is an amino specific agent with a spacer arm that has a disulphide bond that can be cleaved by the addition of reducing agents such as DTT or TCEP.

Interestingly, when DSP was used, cross-links were seen to both ERp57 and ERp27. However, those cross-links formed adducts with different sizes and patterns which indicated that ERp27 does not cross-link to ERp57 but rather forms cross-links with other proteins. The two potential candidates; calnexin and calreticulin were eliminated from binding ERp27 as they also formed different cross-linking products compared to ERp27.

Following the interesting observation that ERp27 binds other proteins in living cells, it was essential to determine their identity. The crosslinked complexes were prepared by either cutting the bands from SDS-PAGE gels or by eluting them from immunisolates with DTT. The samples were then analysed by mass spectrometry following trypsin digestion. As the ERp27-WT cell-line loses its expression over time, the E231K cell-line was used for this batch of experiments. The E231K mutant formed the same cross-links as the wild-type protein following crosslinking with DSP.

Sending proteins as solid samples for analysis by mass spectrometry did not provide any conclusive results; most of the hits were contaminants such as keratin. After a few attempts, the approach used for protein preparation was slightly modified by carrying out a DTT elution step which breaks the disulphide within the cross linker releasing any interacting protein. The proteins were despatched to the University of Glasgow Polyomics for analysis in ammonium bicarbonate buffer which is compatible with mass spectrometry.

The analysis has revealed a number of protein hits as well as contaminants such as keratin. These proteins were either ER proteins or other proteins. However, a few hits consistently appeared including; P5, Ero1, calumenin, and ERp29 which were investigated by immunoprecipitation and immune western blot.

P5 and Ero1 western blots have identified P5 and Ero1 and protein bands at 48 kDa and 54 kDa, respectively within HT1080 as well as E231K cell-lines. In addition, cross-links were formed with these proteins and ERp27 in the presence of DSP within E231K cells and not HT1080 cells indicating that the formed cross-links are specific to ERp27. These results have also confirmed the mass spectrometry protein hits. The calumenin and ERp29 western blots were negative and did not show any protein expression nor cross-links which is likely due to the antibodies used. Unfortunately, we did not have a positive control to indicate whether these antibodies were at all functional. Hence, it cannot be concluded that calumenin and ERp29 are not interacting with ERp27 in living cells, but merely that we were unable to detect their interactions because of the lack of efficient anti-bodies.

We have investigated the expression of ERp27 in different pancreatic cell-lines including islet cells which secretes insulin; PANC-1 (pancreas/duct) cell-line (provided by Dr. Karen Cosgrove, University of Manchester) and INS-1 cell-line, as well as the acinar cells which secretes digestive enzymes; the AR42J cell-line (provided by Dr. Adam Benham, Durham University), the 266-6 cell-line in addition to pancreas tissue that was obtained from mouse. Unfortunately, ERp27 expression was negative in all tested cell-lines and tissues. ERp27 was reported not to be expressed in islet cells of the pancreas which maybe the reason why we could not see any expression within those cells (Professor Kenji Inaba, personal collaboration). ERp27 was expected to be seen within the pancreatic acinar cells. In a collaboration with Professor Kenji Inaba, the AR42J cell-line was found to be negative. In contrast, mouse pancreatic tissue expressed ERp27. However, when we repeated this experiment ERp27 expression could not be detected within the 266-6 cell-line or pancreatic tissue. This is likely due to the differences in the tissue samples used; however, it is not because of the antibody as the positive control (ERp27 purified protein) was detected.

In summary, we demonstrated competition between ERp27 and calreticulin for binding ERp57 *in vitro*. As ERp27 can bind to unfolded protein substrates it could recruit those

unfolded proteins substrates to ERp57 to be correctly folded before leaving the ER. This pathway might compete with calnexin and calreticulin which brings N-glycoproteins to ERp57 to fold correctly during the glycoprotein folding cycle.

The novel finding of our project was that ERp27 binds other proteins than ERp57 in living cells which suggest more functions for this protein. ERp27 was confirmed to interact with P5 which is protein disulphide isomerase homologue (Kikuchi et al., 2002), which was found to contribute to the regulation of ER stress via IRE1 and PERK. P5 also has a potential role in a number of pathologies associated with protein aggregation such as Alzheimer's disease (Honjo et al., 2014). ERp27 was found to be upregulated during ER stress conditions (Kober et al., 2013, Marselli et al., 2010), which suggest that it might alleviate ER stress by binding unfolded proteins and target them to either ERp57 or P5 for further rounds of folding.

The interaction of ERp27 with Ero1, which is a significant ER oxidoreductase, suggests an involvement in disulphide bond formation. However, ERp27 is a non-catalytic member of the PDI family and lacks a CxxC active site. It remains a possibility that ERp27 might regulate Ero1 activity though this is highly speculative and will require further investigation.

7 Future perspectives

In this thesis we have confirmed the interaction between the two PDI family members ERp27 and ERp57 *in vitro* by the chemical cross-linking assay but we could not detect the same interaction *in cellulo*. However, we still not entirely sure if this interaction does not occur in cells and further investigation is needed to prove for certain that this interaction indeed cannot occur in mammalian cells. One way to do that is by trying different cross-linking reagents in cells. One example is disuccinimidyl tartrate (DST) which is a similar conjugation reagent to DSP as it is primary amine-specific, cleavable by sodium meta-periodate, but the spacer arm is shorter and does not have a disulphide bond, so it is ideal if the cleavability is desired without disturbing protein disulphide bonds.

Regarding the interaction between ERp27 and P5, it is essential to determine the function of such interaction. Similar *in vitro* assays to those carried out for the demonstration of the ERp27 and ERp57 interaction can be carried out for ERp27 and P5. We can express and purify ERp27 and P5 using Nickel agarose affinity and gel filtration chromatography to obtain sufficient amount of proteins to investigate their interaction *in vitro* by the isothermal titration calorimetry (ITC) as well as the chemical cross-linking assays and 2D NMR spectrum. Furthermore, using the wild type ERp27 and the E231K cell-lines to determine ERp27 interaction with P5 *in cellulo* have indicated that ERp27 does not require the ERp57 binding site to interact with P5. Therefore, we need to investigate the peptide binding mutation of ERp27 (I196W) to determine if it is essential for binding P5. This can be studied by the *in cellulo* chemical cross-linking assay. It was noticed that the I196W cell-line gave a slightly different cross-linking pattern compared to ERp27-WT and E231K cell-lines which makes it a possible binding site for P5.

Additionally, P5 has a potential role in the unfolded protein response (UPR) especially in regulating PERK and IRE1 (Groenendyk et al., 2014, Eletto et al., 2014). How the ERp27 interaction with P5 influences these enzymes is to be investigated. Moreover, P5 is known to form non-covalent complexes with BiP and shows specificity towards BiP client proteins (Jessop et al., 2009b). This means that proteins bind to BiP during folding could become substrates for P5. Therefore, P5 interaction with ERp27 could bring ERp27 to this complex and further investigation in mammalian cells should be carried out to determine

if their interaction would have any effect on the UPR. Assays such as the knockout or knockdown of either BiP or P5 can be carried out to see if ERp27 would have any effect on cells undergoing stress when associated with P5.

With regard to the interaction between ERp27 and ERO1 which was investigated in ERp27-WT and E231K cell-lines it was indicated that ERp27 does not need the ERp57 binding site for this interaction. However, we need to further investigate the peptide binding site of ERp27 to determine if it is required for the interaction with ERO1. *In cellulo* or *in vitro* chemical cross-linking assays can be carried out between ERO1 and ERp27-1196W. If these proteins cross-linked, then the peptide binding site of ERp27 is not required for binding ERO1 and other residues should be investigated. However, if cross-links are disrupted that would confirm that the binding site for ERp27 to ERO1 is via the peptide binding site.

The physiological role of ERp27 when interacting with ERO1 still needs to be determined. ERO1 plays a significant role in forming disulphide bonds by binding oxidoreductases of the PDI family which catalyses the formation of disulphide bonds. However, ERp27 is a non-catalytic member and it is highly speculative for ERp27 to have a direct role in disulphide bonds formation, but this does not rule out the possible indirect regulatory function of ERp27. To test that *in vitro* we can mix ERp27 and its mutants with ERO1 and PDI and observe the effect on the folding of RNase.

ER oxidoreductin 1 β (ERO1 β) is a pancreas-specific disulphide oxidase that is known to be upregulated in response to ER stress and to promote protein folding in pancreatic β cells. ERp27 is highly expressed in the pancreas so it would be of interest to investigate if ERp27 interacts with ERO1 β in pancreatic tissue. Overexpression of ERO1 β in β cells results in upregulation of the UPR genes which indicate that ERO1 β overexpression leads to ER stress in β cells (Awazawa et al., 2014). ERp27 was found to be upregulated under the conditions of ER stress (Kober et al., 2013). Whether ERp27 has any impact on ERO1 β during ER stress conditions is to be investigated. We can assay the interaction of ERp27 and ERO1 by *in vitro* and *in vivo* cross-linking experiment or we can knock out or knock down either ERp27 or ERO1 β and monitor what effects that would have on cells undergoing stress.

8 References

- Adachi, Y., Yamamoto, K., Okada, T., Yoshida, H., Harada, A. & Mori, K. 2008. ATF6 Is a Transcription Factor Specializing in the Regulation of Quality Control Proteins in the Endoplasmic Reticulum. *Cell Structure and Function*, 33, 75-89.
- Afshar, N., Black, B. E. & Paschal, B. M. 2005. Retrotranslocation of the chaperone calreticulin from the endoplasmic reticulum lumen to the cytosol. *Molecular and Cellular Biology*, 25, 8844-8853.
- Alanen, H. I., Williamson, R. A., Howard, M. J., Hatahet, F. S., Salo, K. E., Kauppila, A., Kellokumpu, S. & Ruddock, L. W. 2006. ERp27, a new non-catalytic endoplasmic reticulum-located human protein disulfide isomerase family member, interacts with ERp57. *Journal of Biological Chemistry*, 281, 33727-33738.
- Alanen, H. I., Williamson, R. A., Howard, M. J., Lappi, A. K., Jantti, H. P., Rautio, S. M., Kellokumpu, S. & Ruddock, L. W. 2003. Functional characterization of ERp18, a new endoplasmic reticulum-located thioredoxin superfamily member. *Journal of Biological Chemistry*, 278, 28912-28920.
- Alder, N. N., Shen, Y., Brodsky, J. L., Hendershot, L. M. & Johnson, A. E. 2005. The molecular mechanisms underlying BiP-mediated gating of the Sec61 translocon of the endoplasmic reticulum. *Journal of Cell Biology*, 168, 389-399.
- Amin, N. T., Wallis, A. K., Wells, S. A., Rowe, M. L., Williamson, R. A., Howard, M. J. & Freedman, R. B. 2013. High-resolution NMR studies of structure and dynamics of human ERp27 indicate extensive interdomain flexibility. *Biochemical journal*, 450, 321-332.
- Andrin, C., Pinkoski, M. J., Burns, K., Atkinson, E. A., Krahenbuhl, O., Hudig, D., Fraser, S. A., Winkler, U., Tschopp, J., Opas, M., Bleackley, R. C. & Michalak, M. 1998. Interaction between a Ca²⁺-binding protein calreticulin and perforin, a component of the cytotoxic T-Cell granules. *Biochemistry*, 37, 10386-10394.
- Anelli, T., Alessio, M., Bachi, A., Bergamelli, L., Bertoli, G., Camerini, S., Mezghrani, A., Ruffato, E., Simmen, T. & Sitia, R. 2003. Thiol-mediated protein retention in the endoplasmic reticulum: the role of ERp44. *EMBO Journal*, 22, 5015-5022.
- Appenzeller-Herzog, C., Riemer, J., Christensen, B., Sorensen, E. S. & Ellgaard, L. 2008. A novel disulphide switch mechanism in Ero1 alpha balances ER oxidation in human cells. *EMBO Journal*, 27, 2977-2987.
- Appenzeller-Herzog, C. & Ellgaard, L. 2008. The human PDI family: Versatility packed into a single fold. *Biochimica Et Biophysica Acta-Molecular Cell Research*, 1783, 535-548.
- Araki, K. & Nagata, K. 2011. Functional in Vitro Analysis of the ERO1 Protein and Protein-disulfide Isomerase Pathway. *Journal of Biological Chemistry*, 286, 32705-32712.
- Ariyasu, D., Yoshida, H. & Hasegawa, Y. 2017. Endoplasmic Reticulum (ER) Stress and Endocrine Disorders. *International journal of molecular sciences*, 18.
- Arosa, F. A., De Jesus, O., Porto, G., Carmo, A. M. & De Sousa, M. 1999. Calreticulin is expressed on the cell surface of activated human peripheral blood T lymphocytes in association with major histocompatibility complex class I molecules. *Journal of Biological Chemistry*, 274, 16917-16922.
- Atkinson, H. J. & Babbitt, P. C. 2009. An Atlas of the Thioredoxin Fold Class Reveals the Complexity of Function-Enabling Adaptations. *Plos Computational Biology*, 5.
- Awazawa, M., Futami, T., Sakada, M., Kaneko, K., Ohsugi, M., Nakaya, K., Terai, A., Suzuki, R., Koike, M., Uchiyama, Y., Kadowaki, T. & Ueki, K. 2014. Deregulation of Pancreas-Specific Oxidoreductin ERO1 beta in the Pathogenesis of Diabetes Mellitus. *Molecular and Cellular Biology*, 34, 1290-1299.
- B'chir, W., Maurin, A.-C., Carraro, V., Averous, J., Jousse, C., Muranishi, Y., Parry, L., Stepien, G., Fournoux, P. & Bruhat, A. 2013. The eIF2 alpha/ATF4 pathway is essential for stress-induced autophagy gene expression. *Nucleic Acids Research*, 41, 7683-7699.
- Baker, K. M., Chakravarthi, S., Langton, K. P., Sheppard, A. M., Lu, H. & Bulleid, N. J. 2008. Low reduction potential of Ero1 alpha regulatory disulphides ensures tight control of substrate oxidation. *EMBO Journal*, 27, 2988-2997.

Barak, N. N., Neumann, P., Sevana, M., Schutkowski, M., Naumann, K., Malesevic, M., Reichardt, H., Fischer, G., Stubbs, M. T. & Ferrari, D. M. 2009. Crystal Structure and Functional Analysis of the Protein Disulfide Isomerase-Related Protein ERp29. *Journal of Molecular Biology*, 385, 1630-1642.

Bastolla, U. & Demetrius, L. 2005. Stability constraints and protein evolution: the role of chain length, composition and disulfide bonds. *Protein Engineering Design & Selection*, 18, 405-415.

Baumann, O. & Walz, B. 2001. Endoplasmic reticulum of animal cells and its organization into structural and functional domains. *International Review of Cytology - a Survey of Cell Biology*, Vol 205, 205, 149-214.

Belmont, P. J., Chen, W. J., San Pedro, M. N., Thuerlauf, D. J., Lowe, N. G., Gude, N., Hilton, B., Wolkowicz, R., Sussman, M. A. & Glembotski, C. C. 2010. Roles for Endoplasmic Reticulum-Associated Degradation and the Novel Endoplasmic Reticulum Stress Response Gene Derlin-3 in the Ischemic Heart. *Circulation Research*, 106, 307-U35.

Benham, A. M. 2012. Protein Secretion and the Endoplasmic Reticulum. *Cold Spring Harbor Perspectives in Biology*, 4.

Benham, A. M., Van Lith, M., Sitia, R. & Braakman, I. 2013. Ero1-PDI interactions, the response to redox flux and the implications for disulfide bond formation in the mammalian endoplasmic reticulum. *Philosophical Transactions of the Royal Society B-Biological Sciences*, 368.

Berkner, K. L. 2008. Vitamin K-dependent carboxylation. *Vitamin K*, 78, 131-156.

Bertolotti, A., Zhang, Y. H., Hendershot, L. M., Harding, H. P. & Ron, D. 2000. Dynamic interaction of BiP and ER stress transducers in the unfolded-protein response. *Nature Cell Biology*, 2, 326-332.

Black, V. H., Sanjay, A., Van Leyen, K., Luring, B. & Kreibich, G. 2005. Cholesterol and steroid synthesizing smooth endoplasmic reticulum of adrenocortical cells contains high levels of proteins associated with the translocation channel. *Endocrinology*, 146, 4234-4249.

Boyce, M., Bryant, K. F., Jousse, C., Long, K., Harding, H. P., Scheuner, D., Kaufman, R. J., Ma, D. W., Coen, D. M., Ron, D. & Yuan, J. Y. 2005. A selective inhibitor-of eIF2 alpha dephosphorylation protects cells from ER stress. *Science*, 307, 935-939.

Braakman, I. & Bulleid, N. J. 2011. Protein Folding and Modification in the Mammalian Endoplasmic Reticulum. *Annual Review of Biochemistry*, Vol 80, 80, 71-99.

Braakman, I. & Hebert, D. N. 2013. Protein Folding in the Endoplasmic Reticulum. *Cold Spring Harbor Perspectives in Biology*, 5.

Bulleid, N. J. 2012. Disulfide Bond Formation in the Mammalian Endoplasmic Reticulum. *Cold Spring Harbor Perspectives in Biology*, 4.

Bulleid, N. J. & Ellgaard, L. 2011. Multiple ways to make disulfides. *Trends in Biochemical Sciences*, 36, 485-492.

Cabibbo, A., Pagani, M., Fabbri, M., Rocchi, M., Farmery, M. R., Bulleid, N. J. & Sitia, R. 2000. ERO1-L, a human protein that favors disulfide bond formation in the endoplasmic reticulum. *Journal of Biological Chemistry*, 275, 4827-4833.

Cannon, K. S. & Helenius, A. 1999. Trimming and readdition of glucose to N-linked oligosaccharides determines calnexin association of a substrate glycoprotein in living cells. *Journal of Biological Chemistry*, 274, 7537-7544.

Cao, Z., Tavender, T. J., Roszak, A. W., Cogdell, R. J. & Bulleid, N. J. 2011. Crystal Structure of Reduced and of Oxidized Peroxiredoxin IV Enzyme Reveals a Stable Oxidized Decamer and a Non-disulfide-bonded Intermediate in the Catalytic Cycle. *Journal of Biological Chemistry*, 286, 42257-42266.

Capellari, S., Zaidi, S. I. A., Urig, C. B., Perry, G., Smith, M. A. & Petersen, R. B. 1999. Prion protein glycosylation is sensitive to redox change. *Journal of Biological Chemistry*, 274, 34846-34850.

Caramelo, J. J. & Parodi, A. J. 2015. A sweet code for glycoprotein folding. *Febs Letters*, 589, 3379-3387.

Carrara, M., Prischi, F., Nowak, P. R. & Ali, M. M. U. 2015. Crystal structures reveal transient PERK luminal domain tetramerization in endoplasmic reticulum stress signaling. *EMBO Journal*, 34, 1589-1600.

Chakravarthi, S., Jessop, C. E., Willer, M., Stirling, C. J. & Bulleid, N. J. 2007. Intracellular catalysis of disulfide bond formation by the human sulfhydryl oxidase, QSOX1. *Biochemical Journal*, 404, 403-411.

Chambers, J. E., Tavender, T. J., Oka, O. B. V., Warwood, S., Knight, D. & Bulleid, N. J. 2010. The Reduction Potential of the Active Site Disulfides of Human Protein Disulfide Isomerase Limits Oxidation of the Enzyme by Ero1 alpha. *Journal of Biological Chemistry*, 285, 29200-29207.

Chapman, D. C. & Williams, D. B. 2010. ER quality control in the biogenesis of MHC class I molecules. *Seminars in Cell & Developmental Biology*, 21, 512-519.

Chen, J. J., Genereux, J. C. & Wiseman, R. L. 2015. Endoplasmic reticulum quality control and systemic amyloid disease: Impacting protein stability from the inside out. *Iubmb Life*, 67, 404-413.

Chen, X., Shen, J. & Prywes, R. 2002. The luminal domain of ATF6 senses endoplasmic reticulum (ER) stress and causes translocation of ATF6 from the ER to the Golgi. *Journal of Biological Chemistry*, 277, 13045-13052.

Coe, H. & Michalak, M. 2010. ERp57, a multifunctional endoplasmic reticulum resident oxidoreductase. *International Journal of Biochemistry & Cell Biology*, 42, 796-799.

Credle, J. J., Finer-Moore, J. S., Papa, F. R., Stroud, R. M. & Walter, P. 2005. On the mechanism of sensing unfolded protein in the endoplasmic reticulum. *Proceedings of the National Academy of Sciences of the United States of America*, 102, 18773-18784.

Cui, W., Li, J., Ron, D. & Sha, B. 2011. The structure of the PERK kinase domain suggests the mechanism for its activation. *Acta Crystallographica Section D-Biological Crystallography*, 67, 423-428.

Cunnea, P. M., Miranda-Vizueté, A., Bertoli, G., Simmen, T., Damdimopoulos, A. E., Hermann, S., Leinonen, S., Huikko, M. P., Gustafsson, J. A., Sitia, R. & Spyrou, G. 2003. ERdj5, an endoplasmic reticulum (ER)-resident protein containing DnaJ and thioredoxin domains, is expressed in secretory cells or following ER stress. *Journal of Biological Chemistry*, 278, 1059-1066.

Dallner, G., Orrenius, S. & Bergstrand, A. 1963. Isolation and Properties of Rough and Smooth Vesicles from Rat Liver. *Journal of Cell Biology*, 16, 426.

Dandekar, A., Mendez, R. & Zhang, K. 2015. Cross Talk Between ER Stress, Oxidative Stress, and Inflammation in Health and Disease. *Stress Responses: Methods and Protocols*, 1292, 205-214.

Das, I., Krzyzosiak, A., Schneider, K., Wrabetz, L., D'antonio, M., Barry, N., Sigurdardottir, A., Bertolotti, A. 2015. Preventing proteostasis diseases by selective inhibition of a phosphatase regulatory subunit. *Science*, 348, 239-242.

Debeljak, N., Feldman, L., Davis, K. L., Komel, R. & Sytkowski, A. J. 2006. Variability in the immunodetection of His-tagged recombinant proteins. *Analytical Biochemistry*, 359, 216-223.

Dejgaard, K., Theberge, J.-F., Heath-Engel, H., Chevet, E., Tremblay, M. L. & Thomas, D. Y. 2010. Organization of the Sec61 Translocon, Studied by High Resolution Native Electrophoresis. *Journal of Proteome Research*, 9, 1763-1771.

Desilva, M. G., Lu, J., Donadel, G., Modi, W. S., Xie, H., Notkins, A. L. & Lan, M. S. 1996. Characterization and chromosomal localization of a new protein disulfide isomerase, PDIp, highly expressed in human pancreas. *DNA and Cell Biology*, 15, 9-16.

Eletto, D., Eletto, D., Dersh, D., Gidalevitz, T. & Argon, Y. 2014. Protein Disulfide Isomerase A6 Controls the Decay of IRE1 alpha Signaling via Disulfide-Dependent Association. *Molecular Cell*, 53, 562-576.

Ellgaard, L. & Frickel, E. M. 2003. Calnexin, calreticulin, and ERp57 - Teammates in glycoprotein folding. *Cell Biochemistry and Biophysics*, 39, 223-247.

Ellgaard, L. & Helenius, A. 2003. Quality control in the endoplasmic reticulum. *Nature Reviews Molecular Cell Biology*, 4, 181-191.

Ellgaard, L. & Ruddock, L. W. 2005. The human protein disulphide isomerase family: substrate interactions and functional properties. *EMBO Reports*, 6, 28-32.

Elliott, J. G., Oliver, J. D. & High, S. 1997. The thiol-dependent reductase ERp57 interacts specifically with N-glycosylated integral membrane proteins. *Journal of Biological Chemistry*, 272, 13849-13855.

Erickson, R. R., Dunning, L. M., Olson, D. A., Cohen, S. J., Davis, A. T., Wood, W. G., Kratzke, R. A. & Holtzman, J. L. 2005. In cerebrospinal fluid ER chaperones ERp57 and calreticulin bind beta-amyloid. *Biochemical and Biophysical Research Communications*, 332, 50-57.

Fagone, P. & Jackowski, S. 2009. Membrane phospholipid synthesis and endoplasmic reticulum function. *Journal of Lipid Research*, 50, S311-S316.

Feige, M. J. & Hendershot, L. M. 2011. Disulfide bonds in ER protein folding and homeostasis. *Current Opinion in Cell Biology*, 23, 167-175.

Ferrari, D. M. & Soling, H. D. 1999. The protein disulphide-isomerase family: unravelling a string of folds. *Biochemical Journal*, 339, 1-10.

Fliegel, L., Burns, K., Maclennan, D. H., Reithmeier, R. A. F. & Michalak, M. 1989. Molecular-Cloning of the High-Affinity Calcium-Binding Protein (Calreticulin) of Skeletal-Muscle Sarcoplasmic-Reticulum. *Journal of Biological Chemistry*, 264, 21522-21528.

Frاند, A. R. & Kaiser, C. A. 1998. The ERO1 gene of yeast is required for oxidation of protein dithiols in the endoplasmic reticulum. *Molecular Cell*, 1, 161-170.

Frاند, A. R. & Kaiser, C. A. 1999. Ero1p oxidizes protein disulfide isomerase in a pathway for disulfide bond formation in the endoplasmic reticulum. *Molecular Cell*, 4, 469-477.

Frasconi, M., Chichiarelli, S., Gaucchi, E., Mazzei, F., Grillo, C., Chinazzi, A. & Altieri, F. 2012. Interaction of ERp57 with calreticulin: Analysis of complex formation and effects of vancomycin. *Biophysical Chemistry*, 160, 46-53.

Fraser, S. A., Karimi, R., Michalak, M. & Hudig, D. 2000. Perforin lytic activity is controlled by calreticulin. *Journal of Immunology*, 164, 4150-4155.

Frickel, E. M., Frei, P., Bouvier, M., Stafford, W. F., Helenius, A., Glockshuber, R. & Ellgaard, L. 2004. ERp57 is a multifunctional thiol-disulfide oxidoreductase. *Journal of Biological Chemistry*, 279, 18277-18287.

Frickel, E. M., Riek, R., Jelesarov, I., Helenius, A., Wuthrich, K. & Ellgaard, L. 2002. TROSY-NMR reveals interaction between ERp57 and the tip of the calreticulin P-domain. *Proceedings of the National Academy of Sciences of the United States of America*, 99, 1954-1959.

Gao, J., Shi, X., He, H., Zhang, J., Lin, D., Fu, G. & Lai, D. 2017. Assessment of Sarcoplasmic Reticulum Calcium Reserve and Intracellular Diastolic Calcium Removal in Isolated Ventricular Cardiomyocytes. *Journal of visualized experiments : JoVE*.

Gao, J., Zhang, Y., Wang, L., Xia, L., Lu, M., Zhang, B., Chen, Y. & He, L. 2016. Endoplasmic reticulum protein 29 is involved in endoplasmic reticulum stress in islet beta cells. *Molecular Medicine Reports*, 13, 398-402.

Ghiran, I., Klickstein, L. B. & Nicholson-Weller, A. 2003. Calreticulin is at the surface of circulating neutrophils and uses CD59 as an adaptor molecule. *Journal of Biological Chemistry*, 278, 21024-21031.

Gold, L. I., Eggleton, P., Sweetwyne, M. T., Van Duyn, L. B., Greives, M. R., Naylor, S.-M., Michalak, M. & Murphy-Ullrich, J. E. 2010. Calreticulin: non-endoplasmic reticulum functions in physiology and disease. *FASEB Journal*, 24, 665-683.

Groenendyk, J., Peng, Z., Dudek, E., Fan, X., Mizianty, M. J., Dufey, E., Urra, H., Sepulveda, D., Rojas-Rivera, D., Lim, Y., Kim, D. H., Baretta, K., Srikanth, S., Gwack, Y., Ahnn, J., Kaufman, R. J., Lee, S.-K., Hetz, C., Kurgan, L. & Michalak, M. 2014. Interplay Between the Oxidoreductase PDIA6 and microRNA-322 Controls the Response to Disrupted Endoplasmic Reticulum Calcium Homeostasis. *Science Signaling*, 7.

Gross, E., Kastner, D. B., Kaiser, C. A. & Fass, D. 2004. Structure of Ero1p, source of disulfide bonds for oxidative protein folding in the cell. *Cell*, 117, 601-610.

Gross, E., Sevier, C. S., Heldman, N., Vitu, E., Bentzur, M., Kaiser, C. A., Thorpe, C. & Fass, D. 2006. Generating disulfides enzymatically: Reaction products and electron acceptors of the endoplasmic reticulum thiol oxidase Ero1p. *Proceedings of the National Academy of Sciences of the United States of America*, 103, 299-304.

Hacker, G. 2000. The morphology of apoptosis. *Cell and Tissue Research*, 301, 5-17.

Harding, H. P., Zhang, Y. H., Bertolotti, A., Zeng, H. Q. & Ron, D. 2000. Perk is essential for translational regulation and cell survival during the unfolded protein response. *Molecular Cell*, 5, 897-904.

Harding, H. P., Zhang, Y. H. & Ron, D. 1999. Protein translation and folding are coupled by an endoplasmic-reticulum-resident kinase. *Nature*, 397, 271-274.

Harding, H. P., Zhang, Y. H., Zeng, H. Q., Novoa, I., Lu, P. D., Calton, M., Sadri, N., Yun, C., Popko, B., Paules, R., Stojdl, D. F., Bell, J. C., Hettmann, T., Leiden, J. M. & Ron, D. 2003. An integrated

stress response regulates amino acid metabolism and resistance to oxidative stress. *Molecular Cell*, 11, 619-633.

Hartl, F. U. & Hayer-Hartl, M. 2009. Converging concepts of protein folding in vitro and in vivo. *Nature Structural & Molecular Biology*, 16, 574-581.

Hatahet, F. & Ruddock, L. W. 2009. Protein Disulfide Isomerase: A Critical Evaluation of Its Function in Disulfide Bond Formation. *Antioxidants & Redox Signaling*, 11, 2807-2850.

Haze, K., Okada, T., Yoshida, H., Yanagi, H., Yura, T., Negishi, M. & Mori, K. 2001. Identification of the G13 (cAMP-response-element-binding protein-related protein) gene product related to activating transcription factor 6 as a transcriptional activator of the mammalian unfolded protein response. *Biochemical Journal*, 355, 19-28.

Haze, K., Yoshida, H., Yanagi, H., Yura, T. & Mori, K. 1999. Mammalian transcription factor ATF6 is synthesized as a transmembrane protein and activated by proteolysis in response to endoplasmic reticulum stress. *Molecular Biology of the Cell*, 10, 3787-3799.

Hebert, D. N., Foellmer, B. & Helenius, A. 1995. Glucose Trimming and Reglucosylation Determine Glycoprotein Association with Calnexin in the Endoplasmic-Reticulum. *Cell*, 81, 425-433.

Hebert, D. N. & Molinari, M. 2007. In and out of the ER: Protein folding, quality control, degradation, and related human diseases. *Physiological Reviews*, 87, 1377-1408.

Heckler, E. J., Alon, A., Fass, D. & Thorpe, C. 2008. Human quiescin-sulfhydryl oxidase, QSOX1: Probing internal redox steps by mutagenesis. *Biochemistry*, 47, 4955-4963.

Helenius, A., Marquardt, T. & Braakman, I. 1992. The endoplasmic reticulum as a protein-folding compartment. *Trends in Cell Biology*, 2, 227-231.

Helenius, A., Trombetta, E. S., Hebert, D. N. & Simons, J. F. 1997. Calnexin, calreticulin and the folding of glycoproteins. *Trends in Cell Biology*, 7, 193-200.

High, S. 1995. Protein Translocation at the Membrane of the Endoplasmic-Reticulum. *Progress in Biophysics & Molecular Biology*, 63, 233-250.

High, S., Lecomte, F. J. L., Russell, S. J., Abell, B. M. & Oliver, J. D. 2000. Glycoprotein folding in the endoplasmic reticulum: a tale of three chaperones? *FEBS Letters*, 476, 38-41.

Hobman, T. C., Zhao, B. P., Chan, H. N. & Farquhar, M. G. 1998. Immunolocalization and characterization of a subdomain of the endoplasmic reticulum that concentrates proteins involved in COPII vesicle biogenesis. *Molecular Biology of the Cell*, 9, 1265-1278.

Hochstenbach, F., David, V., Watkins, S. & Brenner, M. B. 1992. Endoplasmic-Reticulum Resident Protein of 90 Kilodaltons Associates with the T-Cell and B-Cell Antigen Receptors and Major Histocompatibility Complex Antigens During their Assembly. *Proceedings of the National Academy of Sciences of the United States of America*, 89, 4734-4738.

Hollien, J., Lin, J. H., Li, H., Stevens, N., Walter, P. & Weissman, J. S. 2009. Regulated Ire1-dependent decay of messenger RNAs in mammalian cells. *Journal of Cell Biology*, 186, 323-331.

Hollien, J. & Weissman, J. S. 2006. Decay of endoplasmic reticulum-localized mRNAs during the unfolded protein response. *Science*, 313, 104-107.

Honjo, Y., Ayaki, T., Tomiyama, T., Horibe, T., Ito, H., Mori, H., Takahashi, R. & Kawakami, K. 2017. Decreased levels of PDI and P5 in oligodendrocytes in Alzheimer's disease. *Neuropathology: official journal of the Japanese Society of Neuropathology*.

Honjo, Y., Horibe, T., Torisawa, A., Ito, H., Nakanishi, A., Mori, H., Komiya, T., Takahashi, R. & Kawakami, K. 2014. Protein Disulfide Isomerase P5-Immunopositive Inclusions in Patients with Alzheimer's Disease. *Journal of Alzheimers Disease*, 38, 601-609.

Hosoda, A., Kimata, Y., Tsuru, A. & Kohno, K. 2003. JPDI, a novel endoplasmic reticulum-resident protein containing both a BiP-interacting J-domain and thioredoxin-like motifs. *Journal of Biological Chemistry*, 278, 2669-2676.

Ihara, Y., Cohen-Doyle, M. F., Saito, Y. & Williams, D. B. 1999. Calnexin discriminates between protein conformational states and functions as a molecular chaperone in vitro. *Molecular Cell*, 4, 331-341.

Inaba, K., Masui, S., Iida, H., Vavassori, S., Sitia, R. & Suzuki, M. 2010. Crystal structures of human Ero1 alpha reveal the mechanisms of regulated and targeted oxidation of PDI. *EMBO Journal*, 29, 3330-3343.

Ishizuki, S., Furuhashi, K., Kaneta, S. & Fujihira, E. 1983. Reduced Drug-Metabolism in Isolated Hepatocytes from Adjuvant Arthritic Rats. *Research Communications in Chemical Pathology and Pharmacology*, 39, 261-276.

Jansens, A., Van Duijn, E. & Braakman, I. 2002. Coordinated nonvectorial folding in a newly synthesized multidomain protein. *Science*, 298, 2401-2403.

Jessop, C. E., Chakravarthi, S., Garbi, N., Haemmerling, G. J., Lovell, S. & Bulleid, N. J. 2007. ERp57 is essential for efficient folding of glycoproteins sharing common structural domains. *EMBO Journal*, 26, 28-40.

Jessop, C. E., Tavender, T. J., Watkins, R. H., Chambers, J. E. & Bulleid, N. J. 2009a. Substrate Specificity of the Oxidoreductase ERp57 Is Determined Primarily by Its Interaction with Calnexin and Calreticulin. *Journal of Biological Chemistry*, 284, 2194-2202.

Jessop, C. E., Watkins, R. H., Simmons, J. J., Tasab, M. & Bulleid, N. J. 2009b. Protein disulphide isomerase family members show distinct substrate specificity: P5 is targeted to BiP client proteins. *Journal of Cell Science*, 122, 4287-4295.

Jin, D.-Y., Tie, J.-K. & Stafford, D. W. 2007. The conversion of vitamin K epoxide to vitamin K quinone and vitamin K quinone to vitamin K hydroquinone uses the same active site cysteines. *Biochemistry*, 46, 7279-7283.

Jin, H., Komita, M. & Aoe, T. 2017. The Role of BiP Retrieval by the KDEL Receptor in the Early Secretory Pathway and its Effect on Protein Quality Control and Neurodegeneration. *Frontiers in Molecular Neuroscience*, 10.

Johnson, S., Michalak, M., Opas, M. & Eggleton, P. 2001. The ins and outs of calreticulin: from the ER lumen to the extracellular space. *Trends in Cell Biology*, 11, 122-129.

Jung, D. H. & Kim, D. H. 2004. Characterization of isoforms and genomic organization of mouse calumenin. *Gene*, 327, 185-194.

Kaneko, M., Imaizumi, K., Saito, A., Kanemoto, S., Asada, R., Matsuhisa, K. & Ohtake, Y. 2017. ER Stress and Disease: Toward Prevention and Treatment. *Biological & Pharmaceutical Bulletin*, 40, 1337-1343.

Kapoor, M., Srinivas, H., Kandiah, E., Gemma, E., Ellgaard, L., Oscarson, S., Helenius, A. & Suroliya, A. 2003. Interactions of substrate with calreticulin, an endoplasmic reticulum chaperone. *Journal of Biological Chemistry*, 278, 6194-6200.

Karagoz, G. E., Acosta-Alvear, D., Nguyen, H. T., Lee, C. P., Chu, F. & Walter, P. 2017. An unfolded protein-induced conformational switch activates mammalian IRE1. *ELife*, 6.

Kaufman, R. J. 1999. Stress signaling from the lumen of the endoplasmic reticulum: coordination of gene transcriptional and translational controls. *Genes & Development*, 13, 1211-1233.

Kikuchi, M., Doi, E., Tsujimoto, I., Horibe, T. & Tsujimoto, Y. 2002. Functional analysis of human P5, a protein disulfide isomerase homologue. *Journal of Biochemistry*, 132, 451-455.

Kim, S. J. & Skach, W. R. 2012. Mechanisms of CFTR folding at the endoplasmic reticulum. *Frontiers in Pharmacology*, 3.

Klappa, P., Ruddock, L. W., Darby, N. J. & Freedman, R. B. 1998. The b' domain provides the principal peptide-binding site of protein disulfide isomerase but all domains contribute to binding of misfolded proteins. *EMBO Journal*, 17, 927-935.

Knoblach, B., Keller, B. O., Groenendyk, J., Aldred, S., Zheng, J., Lemire, B. D., Li, L. & Michalak, M. 2003. ERp19 and ERp46, new members of the thioredoxin family of endoplasmic reticulum proteins. *Molecular & Cellular Proteomics*, 2, 1104-1119.

Kober, F.-X., Koelmel, W., Kuper, J., Drechsler, J., Mais, C., Hermanns, H. M. & Schindelin, H. 2013. The crystal structure of the protein-disulfide isomerase family member ERp27 provides insights into its substrate binding capabilities. *Journal of Biological Chemistry*, 288, 2029-2039.

Kodali, V. K. & Thorpe, C. 2010. Oxidative Protein Folding and the Quiescin-Sulfhydryl Oxidase Family of Flavoproteins. *Antioxidants & Redox Signaling*, 13, 1217-1230.

Kosuri, P., Alegre-Cebollada, J., Feng, J., Kaplan, A., Ingles-Prieto, A., Badilla, C. L., Stockwell, B. R., Sanchez-Ruiz, J. M., Holmgren, A. & Fernandez, J. M. 2012. Protein Folding Drives Disulfide Formation. *Cell*, 151, 794-806.

Kozlov, G., Maattanen, P., Schrag, J. D., Pollock, S., Cygler, M., Nagar, B., Thomas, D. Y. & Gehring, K. 2006. Crystal structure of the bb' domains of the protein disulfide isomerase ERp57. *Structure*, 14, 1331-1339.

Kozlov, G., Maeettaenen, P., Thomas, D. Y. & Gehring, K. 2010a. A structural overview of the PDI family of proteins. *FEBS Journal*, 277, 3924-3936.

Kozlov, G., Munoz-Escobar, J., Castro, K. & Gehring, K. 2017. Mapping the ER Interactome: The P Domains of Calnexin and Calreticulin as Plurivalent Adapters for Foldases and Chaperones. *Structure*, 25, 1415-+.

Kozlov, G., Pocanschi, C. L., Rosenauer, A., Bastos-Aristizabal, S., Gorelik, A., Williams, D. B. & Gehring, K. 2010b. Structural Basis of Carbohydrate Recognition by Calreticulin. *Journal of Biological Chemistry*, 285, 38612-38620.

Lash, A. E., Tolstoshev, C. M., Wagner, L., Schuler, G. D., Strausberg, R. L., Riggins, G. J. & Altschul, S. F. 2000. SAGEmap: A public gene expression resource. *Genome Research*, 10, 1051-1060.

Le, A. Q., Steiner, J. L., Ferrell, G. A., Shaker, J. C. & Sifers, R. N. 1994. Association between Calnexin and a Secretion-Incompetent Variant of human Alpha(1)-Antitrypsin. *Journal of Biological Chemistry*, 269, 7514-7519.

Li, J. A., Puceat, M., Perez-Terzic, C., Mery, A., Nakamura, K., Michalak, M., Krause, K. H. & Jaconi, M. E. 2002. Calreticulin reveals a critical Ca²⁺ checkpoint in cardiac myofibrillogenesis. *Journal of Cell Biology*, 158, 103-113.

Li, Y., Bergeron, J., Luo, L. Z., Ou, W. J., Thomas, D. Y. & Kang, C. Y. 1996. Effects of inefficient cleavage of the signal sequence of HIV-1 gp120 on its association with calnexin, folding, and intracellular transport. *Proceedings of the National Academy of Sciences of the United States of America*, 93, 9606-9611.

Liepinsh, E., Baryshev, M., Sharipo, A., Ingelman-Sundberg, M., Otting, G. & Mkrtchian, S. 2001. Thioredoxin fold as homodimerization module in the putative chaperone ERp29: NMR structures of the domains and experimental model of the 51 kDa dimer. *Structure*, 9, 457-471.

Liu, Z., Lv, Y., Zhao, N., Guan, G. & Wang, J. 2015. Protein kinase R-like ER kinase and its role in endoplasmic reticulum stress-decided cell fate. *Cell Death & Disease*, 6.

Loo, M. A., Jensen, T. J., Cui, L. Y., Hou, Y. X., Chang, X. B. & Riordan, J. R. 1998. Perturbation of Hsp90 interaction with nascent CFTR prevents its maturation and accelerates its degradation by the proteasome. *EMBO Journal*, 17, 6879-6887.

Lundstrom, J. & Holmgren, A. 1993. Determination of the Reduction Oxidation Potential of the Thioredoxin-Like Domains of Protein Disulfide-Isomerase from the Equilibrium with Glutathione and Thioredoxin. *Biochemistry*, 32, 6649-6655.

Ma, Q. J., Guo, C. S., Barnewitz, K., Sheldrick, G. M., Soling, H. D., Uson, I. & Ferrari, D. M. 2003. Crystal structure and functional analysis of Drosophila Wind, a protein-disulfide isomerase-related protein. *Journal of Biological Chemistry*, 278, 44600-44607.

Maattanen, P., Kozlov, G., Gehring, K. & Thomas, D. Y. 2006. ERp57 and PDI: multifunctional protein disulfide isomerases with similar domain architectures but differing substrate-partner associations. *Biochemistry and Cell Biology-Biochimie Et Biologie Cellulaire*, 84, 881-889.

Marselli, L., Thorne, J., Dahiya, S., Sgroi, D. C., Sharma, A., Bonner-Weir, S., Marchetti, P. & Weir, G. C. 2010. Gene Expression Profiles of Beta-Cell Enriched Tissue Obtained by Laser Capture Microdissection from Subjects with Type 2 Diabetes. *Plos One*, 5.

Masui, S., Vavassori, S., Fagioli, C., Sitia, R. & Inaba, K. 2011. Molecular Bases of Cyclic and Specific Disulfide Interchange between Human ERO1 alpha Protein and Protein-disulfide Isomerase (PDI). *Journal of Biological Chemistry*, 286.

Matsuo, Y., Akiyama, N., Nakamura, H., Yodoi, J., Noda, M. & Kizaka-Kondoh, S. 2001. Identification of a novel thioredoxin-related transmembrane protein. *Journal of Biological Chemistry*, 276, 10032-10038.

Meldolesi, J. & Pozzan, T. 1998. The endoplasmic reticulum Ca²⁺ store: a view from the lumen. *Trends in Biochemical Sciences*, 23, 10-14.

Meng, X. F., Zhang, C., Chen, J. Z., Peng, S. Y., Cao, Y. Q., Ying, K., Xie, Y. & Mao, Y. M. 2003. Cloning and identification of a novel cDNA coding thioredoxin-related transmembrane protein 2. *Biochemical Genetics*, 41, 99-106.

Merksamer, P. I. & Papa, F. R. 2010. The UPR and cell fate at a glance. *Journal of Cell Science*, 123, 1003-1006.

Mobbs, C. V., Fink, G. & Pfaff, D. W. 1990. HIP-70 - An Isoform of Phosphoinositol-Specific Phospholipase-C-Alpha. *Science*, 249, 566-566.

Murthy, M. S. R. & Pande, S. V. 1994. A Stress-Regulated Protein, GRP58, a Member of Thioredoxin Superfamily, is a Carnitine Palmitoyltransferase Isoenzyme. *Biochemical Journal*, 304, 31-34.

Nadanaka, S., Okada, T., Yoshida, H. & Mori, K. 2007. Role of disulfide bridges formed in the luminal domain of ATF6 in sensing endoplasmic reticulum stress. *Molecular and Cellular Biology*, 27, 1027-1043.

Nakao, H., Seko, A., Ito, Y. & Sakono, M. 2017. PDI family protein ERp29 recognizes P-domain of molecular chaperone calnexin. *Biochemical and Biophysical Research Communications*, 487, 763-767.

Nguyen, V. D., Saaranen, M. J., Karala, A.-R., Lappi, A.-K., Wang, L., Raykhel, I. B., Alanen, H. I., Salo, K. E. H., Wang, C.-C. & Ruddock, L. W. 2011. Two Endoplasmic Reticulum PDI Peroxidases Increase the Efficiency of the Use of Peroxide during Disulfide Bond Formation. *Journal of Molecular Biology*, 406, 503-515.

Nguyen, V. D., Wallis, K., Howard, M. J., Haapalainen, A. M., Salo, K. E. H., Saaranen, M. J., Sidhu, A., Wierenga, R. K., Freedman, R. B., Ruddock, L. W. & Williamson, R. A. 2008. Alternative Conformations of the x Region of Human Protein Disulphide-Isomerase Modulate Exposure of the Substrate Binding b' Domain. *Journal of Molecular Biology*, 383, 1144-1155.

Oka, O. B. V. & Bulleid, N. J. 2013. Forming disulfides in the endoplasmic reticulum. *Biochimica Et Biophysica Acta-Molecular Cell Research*, 1833, 2425-2429.

Okazaki, Y., Ohno, H., Takase, K., Ochiai, T. & Saito, T. 2000. Cell surface expression of calnexin, a molecular chaperone in the endoplasmic reticulum. *Journal of Biological Chemistry*, 275, 35751-35758.

Okumura, M., Kadokura, H. & Inaba, K. 2015. Structures and functions of protein disulfide isomerase family members involved in proteostasis in the endoplasmic reticulum. *Free Radical Biology and Medicine*, 83, 314-322.

Oliver, J. D., Roderick, H. L., Llewellyn, D. H. & High, S. 1999. ERp57 functions as a subunit of specific complexes formed with the ER lectins calreticulin and calnexin. *Molecular Biology of the Cell*, 10, 2573-2582.

Oliver, J. D., Vanderwal, F. J., Bulleid, N. J. & High, S. 1997. Interaction of the thiol-dependent reductase ERp57 with nascent glycoproteins. *Science*, 275, 86-88.

Otteken, A. & Moss, B. 1996. Calreticulin interacts with newly synthesized human immunodeficiency virus type 1 envelope glycoprotein, suggesting a chaperone function similar to that of calnexin. *Journal of Biological Chemistry*, 271, 97-103.

Oyadomari, S. & Mori, M. 2004. Roles of CHOP/GADD153 in endoplasmic reticulum stress. *Cell Death and Differentiation*, 11, 381-389.

Pagani, M., Fabbri, M., Benedetti, C., Fassio, A., Pilati, S., Bulleid, N. J., Cabibbo, A. & Sitia, R. 2000. Endoplasmic reticulum oxidoreductin 1-L beta (ERO1-L beta), a human gene induced in the course of the unfolded protein response. *Journal of Biological Chemistry*, 275, 23685-23692.

Palade, G. 1975. Intracellular Aspects of Process of Protein-Synthesis. *Science*, 189, 347-358.

Palade, G. E. & Siekevitz, P. 1956. Liver Microsomes - an Integrated Morphological and Biochemical Study. *Journal of Biophysical and Biochemical Cytology*, 2, 171-&.

Pincus, D., Chevalier, M. W., Aragon, T., Van Anken, E., Vidal, S. E., El-Samad, H. & Walter, P. 2010. BiP Binding to the ER-Stress Sensor Ire1 Tunes the Homeostatic Behavior of the Unfolded Protein Response. *Plos Biology*, 8.

Pind, S., Riordan, J. R. & Williams, D. B. 1994. Participation of the Endoplasmic-Reticulum Chaperone Calnexin (P88, IP90) in the Biogenesis of the Cystic-Fibrosis Transmembrane Conductance Regulator. *Journal of Biological Chemistry*, 269, 12784-12788.

Pirneskoski, A., Klappa, P., Lobell, M., Williamson, R. A., Byrne, L., Alanen, H. I., Salo, K. E. H., Kivirikko, K. I., Freedman, R. B. & Ruddock, L. W. 2004. Molecular characterization of the principal

substrate binding site of the ubiquitous folding catalyst protein disulfide isomerase. *Journal of Biological Chemistry*, 279, 10374-10381.

Poet, G. J., Oka, O. B. V., Van Lith, M., Cao, Z., Robinson, P. J., Pringle, M. A., Arner, E. S. J. & Bulleid, N. J. 2017. Cytosolic thioredoxin reductase 1 is required for correct disulfide formation in the ER. *EMBO Journal*, 36, 693-702.

Pollard, M. G., Travers, K. J. & Weissman, J. S. 1998. Ero1p: A novel and ubiquitous protein with an essential role in oxidative protein folding in the endoplasmic reticulum. *Molecular Cell*, 1, 171-182.

Prinz, W. A., Grzyb, L., Veenhuis, M., Kahana, J. A., Silver, P. A. & Rapoport, T. A. 2000. Mutants affecting the structure of the cortical endoplasmic reticulum in *Saccharomyces cerevisiae*. *Journal of Cell Biology*, 150, 461-474.

Raghavan, M., Wijeyesakere, S. J., Peters, L. R. & Del Cid, N. 2013. Calreticulin in the immune system: ins and outs. *Trends in Immunology*, 34, 13-21.

Rishavy, M. A., Usabalieva, A., Hallgren, K. W. & Berkner, K. L. 2011. Novel Insight into the Mechanism of the Vitamin K Oxidoreductase (VKOR) Electron Relay Through Cys(43) and Cys(51) Reduces VKOR to allow Vitamin K Reduction and Facilitation of Vitamin K-Dependent Protein Carboxylation. *Journal of Biological Chemistry*, 286, 7267-7278.

Roderick, H. L., Campbell, A. K. & Llewellyn, D. H. 1997. Nuclear localisation of calreticulin in vivo is enhanced by its interaction with glucocorticoid receptors. *FEBS Letters*, 405, 181-185.

Rolls, M. M., Hall, D. H., Victor, M., Stelzer, E. H. K. & Rapoport, T. A. 2002. Targeting of rough endoplasmic reticulum membrane proteins and ribosomes in invertebrate neurons. *Molecular Biology of the Cell*, 13, 1778-1791.

Ron, D. & Walter, P. 2007. Signal integration in the endoplasmic reticulum unfolded protein response. *Nature Reviews Molecular Cell Biology*, 8, 519-529.

Roy, B. & Lee, A. S. 1999. The mammalian endoplasmic reticulum stress response element consists of an evolutionarily conserved tripartite structure and interacts with a novel stress-inducible complex. *Nucleic Acids Research*, 27, 1437-1443.

Rudd, P. M., Wormald, M. R., Wing, D. R., Prusiner, S. B. & Dwek, R. A. 2001. Prion glycoprotein: Structure, dynamics, and roles for the sugars. *Biochemistry*, 40, 3759-3766.

Ruggiano, A., Foresti, O. & Carvalho, P. 2014. ER-associated degradation: Protein quality control and beyond. *Journal of Cell Biology*, 204, 868-878.

Russell, S. J., Ruddock, L. W., Salo, K. E. H., Oliver, J. D., Roebuck, Q. P., Llewellyn, D. H., Roderick, H. L., Koivunen, P., Myllyharju, J. & High, S. 2004. The primary substrate binding site in the b¹ domain of ERp57 is adapted for endoplasmic reticulum lectin association. *Journal of Biological Chemistry*, 279, 18861-18869.

Rutkevich, L. A., Cohen-Doyle, M. F., Brockmeier, U. & Williams, D. B. 2010. Functional Relationship between Protein Disulfide Isomerase Family Members during the Oxidative Folding of Human Secretory Proteins. *Molecular Biology of the Cell*, 21, 3093-3105.

Rutkevich, L. A. & Williams, D. B. 2012. Vitamin K epoxide reductase contributes to protein disulfide formation and redox homeostasis within the endoplasmic reticulum. *Molecular Biology of the Cell*, 23, 2017-2027.

Sadasivan, B., Lehner, P. J., Ortmann, B., Spies, T. & Cresswell, P. 1996. Roles for calreticulin and a novel glycoprotein, tapasin, in the interaction of MHC class I molecules with TAP. *Immunity*, 5, 103-114.

Sakono, M., Seko, A., Takeda, Y. & Ito, Y. 2014. PDI family protein ERp29 forms 1:1 complex with lectin chaperone calreticulin. *Biochemical and Biophysical Research Communications*, 452, 27-31.

Sato, Y., Nadanaka, S., Okada, T., Okawa, K. & Mori, K. 2011. Luminal Domain of ATF6 Alone Is Sufficient for Sensing Endoplasmic Reticulum Stress and Subsequent Transport to the Golgi Apparatus. *Cell Structure and Function*, 36, 35-47.

Schelhaas, M., Malmstrom, J., Pelkmans, L., Haugstetter, J., Ellgaard, L., Gruenewald, K. & Helenius, A. 2007. Simian virus 40 depends on ER protein folding and quality control factors for entry into host cells. *Cell*, 131, 516-529.

Schindler, A. J. & Schekman, R. 2009. In vitro reconstitution of ER-stress induced ATF6 transport in COPII vesicles. *Proceedings of the National Academy of Sciences of the United States of America*, 106, 17775-17780.

Schulman, S., Wang, B., Li, W. & Rapoport, T. A. 2010. Vitamin K epoxide reductase prefers ER membrane-anchored thioredoxin-like redox partners. *Proceedings of the National Academy of Sciences of the United States of America*, 107, 15027-15032.

Sevier, C. S. & Kaiser, C. A. 2006a. Conservation and diversity of the cellular disulfide bond formation pathways. *Antioxidants & Redox Signaling*, 8, 797-811.

Sevier, C. S. & Kaiser, C. A. 2006b. Disulfide transfer between two conserved cysteine pairs imparts selectivity to protein oxidation by Ero1. *Molecular Biology of the Cell*, 17, 2256-2266.

Sha, H., He, Y., Chen, H., Wang, C., Zenno, A., Shi, H., Yang, X., Zhang, X. & Qi, L. 2009. The IRE1 alpha-XBP1 Pathway of the Unfolded Protein Response Is Required for Adipogenesis. *Cell Metabolism*, 9, 556-564.

Simon, S. M. & Blobel, G. 1991. A Protein-Conducting Channel in the Endoplasmic-Reticulum. *Cell*, 65, 371-380.

Sitia, R. & Braakman, I. 2003. Quality control in the endoplasmic reticulum protein factory. *Nature*, 426, 891-894.

Smith, M. J. & Koch, G. L. E. 1989. Multiple Zones in the Sequence of Calreticulin (CRP55, Calregulin, HACBP), A Major Calcium-Binding ER/SR Protein. *EMBO Journal*, 8, 3581-3586.

Solda, T., Galli, C., Kaufman, R. J. & Molinari, M. 2007. Substrate-specific requirements for UGT1-dependent release from calnexin. *Molecular Cell*, 27, 238-249.

Sullivan, D. C., Huminiecki, L., Moore, J. W., Boyle, J. J., Poulos, R., Creamer, D., Barker, J. & Bicknell, R. 2003. EndoPDI, a novel protein-disulfide isomerase-like protein that is preferentially expressed in endothelial cells acts as a stress survival factor. *Journal of Biological Chemistry*, 278, 47079-47088.

Tannous, A., Pisoni, G. B., Hebert, D. N. & Molinari, M. 2015. N-linked sugar-regulated protein folding and quality control in the ER. *Seminars in Cell & Developmental Biology*, 41, 79-89.

Tatu, U., Hammond, C. & Helenius, A. 1995. Folding and Oligomerization of Influenza Hemagglutinin in the ER and the Intermediate Compartment. *EMBO Journal*, 14, 1340-1348.

Tavender, T. J. & Bulleid, N. J. 2010. Peroxiredoxin IV protects cells from oxidative stress by removing H₂O₂ produced during disulphide formation. *Journal of Cell Science*, 123, 2672-2679.

Tavender, T. J., Sheppard, A. M. & Bulleid, N. J. 2008. Peroxiredoxin IV is an endoplasmic reticulum-localized enzyme forming oligomeric complexes in human cells. *Biochemical Journal*, 411, 191-199.

Tavender, T. J., Springate, J. J. & Bulleid, N. J. 2010. Recycling of peroxiredoxin IV provides a novel pathway for disulphide formation in the endoplasmic reticulum. *EMBO Journal*, 29, 4185-4197.

Thuerauf, D. J., Marcinko, M., Belmont, P. J. & Glembotski, C. C. 2007. Effects of the isoform-specific characteristics of ATF6 alpha and ATF6 beta on endoplasmic reticulum stress response gene expression and cell viability. *Journal of Biological Chemistry*, 282, 22865-22878.

Tian, G., Kober, F.-X., Lewandrowski, U., Sickmann, A., Lennarz, W. J. & Schindelin, H. 2008. The Catalytic Activity of Protein-disulfide Isomerase Requires a Conformationally Flexible Molecule. *Journal of Biological Chemistry*, 283, 33630-33640.

Tian, G., Xiang, S., Noiva, R., Lennarz, W. J. & Schindelin, H. 2006. The crystal structure of yeast protein disulfide isomerase suggests cooperativity between its active sites. *Cell*, 124, 61-73.

Tirasophon, W., Lee, K., Callaghan, B., Welihinda, A. & Kaufman, R. J. 2000. The endoribonuclease activity of mammalian IRE1 autoregulates its mRNA and is required for the unfolded protein response. *Genes & Development*, 14, 2725-2736.

Tjoelker, L. W., Seyfried, C. E., Eddy, R. L., Byers, M. G., Shows, T. B., Calderon, J., Schreiber, R. B. & Gray, P. W. 1994. Human, Mouse, and Rat Calnexin cDNA Cloning - Identification of Potential Calcium-Binding Motifs and gene Localization to Human-Chromosome-5. *Biochemistry*, 33, 3229-3236.

Tsai, B., Rodighiero, C., Lencer, W. I. & Rapoport, T. A. 2001. Protein disulfide isomerase acts as a redox-dependent chaperone to unfold cholera toxin. *Cell*, 104, 937-948.

Tsaytler, P., Harding, H. P., Ron, D. & Bertolotti, A. 2011. Selective Inhibition of a Regulatory Subunit of Protein Phosphatase 1 Restores Proteostasis. *Science*, 332, 91-94.

Tu, B. P. & Weissman, J. S. 2002. The FAD- and O₂-dependent reaction cycle of Ero1-mediated oxidative protein folding in the endoplasmic reticulum. *Molecular Cell*, 10, 983-994.

Urade, R. & Kito, M. 1992. Inhibition by acidic Phospholipids of Protein-Degradation by ER-60 Protease, A novel Cysteine Protease, of Endoplasmic-Reticulum. *FEBS Letters*, 312, 83-86.

Van Lith, M., Hartigan, N., Hatch, J. & Benham, A. M. 2005. PDILT, a divergent testis-specific protein disulfide isomerase with a non-classical SXXC motif that engages in disulfide-dependent interactions in the endoplasmic reticulum. *Journal of Biological Chemistry*, 280, 1376-1383.

Vanleeuwen, J. E. M. & Kears, K. P. 1996. Calnexin associates exclusively with individual CD3 delta and T cell antigen receptor (TCR) alpha proteins containing incompletely trimmed glycans that are not assembled into multisubunit TCR complexes. *Journal of Biological Chemistry*, 271, 9660-9665.

Vembar, S. S. & Brodsky, J. L. 2008. One step at a time: endoplasmic reticulum-associated degradation. *Nature Reviews Molecular Cell Biology*, 9, 944-U30.

Vitale, A. & Denecke, J. 1999. The endoplasmic reticulum - Gateway of the secretory pathway. *Plant Cell*, 11, 615-628.

Voeltz, G. K., Rolls, M. M. & Rapoport, T. A. 2002. Structural organization of the endoplasmic reticulum. *EMBO Reports*, 3, 944-950.

Wada, I., Kai, M., Imai, S., Sakane, F. & Kanoh, H. 1997. Promotion of transferrin folding by cyclic interactions with calnexin and calreticulin. *EMBO Journal*, 16, 5420-5432.

Wada, I., Rindress, D., Cameron, P. H., Ou, W. J., Doherty, J. J., Louvard, D., Bell, A. W., Dignard, D., Thomas, D. Y. & Bergeron, J. J. M. 1991. SSR-Alpha and Associated Calnexin are Major Calcium-Binding Proteins of the Endoplasmic-Reticulum Membrane. *Journal of Biological Chemistry*, 266, 19599-19610.

Walter, P. & Ron, D. 2011. The Unfolded Protein Response: From Stress Pathway to Homeostatic Regulation. *Science*, 334, 1081-1086.

Wang, C., Chen, S., Wang, X., Wang, L., Wallis, A. K., Freedman, R. B. & Wang, C.-C. 2010. Plasticity of Human Protein Disulfide Isomerase Evidence for Mobility around the X-Linker Region and its Functional Significance. *Journal of Biological Chemistry*, 285, 26788-26797.

Wang, C. C. & Tsou, C. L. 1993. Protein Disulfide-Isomerase is both an enzyme and a chaperone. *FASEB Journal*, 7, 1515-1517.

Wang, L., Li, S.-J., Sidhu, A., Zhu, L., Liang, Y., Freedman, R. B. & Wang, C.-C. 2009. Reconstitution of Human Ero1-L alpha/Protein-Disulfide Isomerase Oxidative Folding Pathway in Vitro Position-Dependent differences in role between the a and a' domains of Protein-Disulfide Isomerase. *Journal of Biological Chemistry*, 284, 199-206.

Wang, L., Zhang, L., Niu, Y., Sitia, R. & Wang, C.-C. 2014. Glutathione Peroxidase 7 Utilizes Hydrogen Peroxide Generated by Ero1 alpha to Promote Oxidative Protein Folding. *Antioxidants & Redox Signaling*, 20, 545-556.

Ware, F. E., Vassilakos, A., Peterson, P. A., Jackson, M. R., Lehrman, M. A. & Williams, D. B. 1995. The Molecular Chaperone Calnexin binds GLC(1)MAN(9)GLCNAC(2) Oligosaccharide as an Initial step in recognizing unfolded glycoproteins. *Journal of Biological Chemistry*, 270, 4697-4704.

Watson, M. L. 1955. The nuclear envelope - its structure and relation to cytoplasmic membranes. *Journal of Biophysical and Biochemical Cytology*, 1, 257-&.

Wijeyesakere, S. J., Gafni, A. A. & Raghavan, M. 2011. Calreticulin Is a Thermostable Protein with Distinct Structural Responses to Different Divalent Cation Environments. *Journal of Biological Chemistry*, 286, 8771-8785.

Williams, A., Peh, C. A. & Elliott, T. 2002. The cell biology of MHC class I antigen presentation. *Tissue Antigens*, 59, 3-17.

Williams, D. B. 2006. Beyond lectins: the calnexin/calreticulin chaperone system of the endoplasmic reticulum. *Journal of Cell Science*, 119, 615-623.

Yamamoto, K., Sato, T., Matsui, T., Sato, M., Okada, T., Yoshida, H., Harada, A. & Mori, K. 2007. Transcriptional induction of mammalian ER quality control proteins is mediated by single or combined action of ATF6 alpha and XBP1. *Developmental Cell*, 13, 365-376.

Yanagitani, K., Kimata, Y., Kadokura, H. & Kohno, K. 2011. Translational Pausing Ensures Membrane Targeting and Cytoplasmic Splicing of XBP1u mRNA. *Science*, 331, 586-589.

Ye, J., Rawson, R. B., Komuro, R., Chen, X., Dave, U. P., Prywes, R., Brown, M. S. & Goldstein, J. L. 2000. ER stress induces cleavage of membrane-bound ATF6 by the same proteases that process SREBPs. *Molecular Cell*, 6, 1355-1364.

Yoshida, H. 2007. ER stress and diseases. *FEBS Journal*, 274, 630-658.

Yoshida, H., Haze, K., Yanagi, H., Yura, T. & Mori, K. 1998. Identification of the cis-acting endoplasmic reticulum stress response element responsible for transcriptional induction of mammalian glucose-regulated proteins - Involvement of basic leucine zipper transcription factors. *Journal of Biological Chemistry*, 273, 33741-33749.

Yoshida, H., Matsui, T., Yamamoto, A., Okada, T. & Mori, K. 2001. XBP1 mRNA is induced by ATF6 and spliced by IRE1 in response to ER stress to produce a highly active transcription factor. *Cell*, 107, 881-891.

Yoshida, H., Okada, T., Haze, K., Yanagi, H., Yura, T., Negishi, M. & Mori, K. 2000. ATF6 activated by proteolysis binds in the presence of NF-Y (CBF) directly to the cis-acting element responsible for the mammalian unfolded protein response. *Molecular and Cellular Biology*, 20, 6755-6767.

Yoshida, H., Oku, M., Suzuki, M. & Mori, K. 2006. pXBP1(U) encoded in XBP1 pre-mRNA negatively regulates unfolded protein response activator pXBP1(S) in mammalian ER stress response. *Journal of Cell Biology*, 172, 565-575.

Zapun, A., Darby, N. J., Tessier, D. C., Michalak, M., Bergeron, J. J. M. & Thomas, D. Y. 1998. Enhanced catalysis of ribonuclease B folding by the interaction of calnexin or calreticulin with ERp57. *Journal of Biological Chemistry*, 273, 6009-6012.